Title
5.13 Paleointensities

Permalink
https://escholarship.org/uc/item/51w2h3pt

Authors
Tauxe, L
Yamazaki, T

Publication Date
2015

DOI
10.1016/b978-0-444-53802-4.00107-x

Peer reviewed

TREATISE ON GEOPHYSICS, SECOND EDITION - CONTRIBUTORS' INSTRUCTIONS

 PROOFREADING

The text content for your contribution is in final form when you receive proofs. Please read proofs for accuracy and clarity, as well as for typographical errors, but please DO NOT REWRITE.

At the beginning of your article there is a page containing any author queries, keywords, and the authors' full address details.

Please address author queries as necessary. While it is appreciated that some articles will require updating/revising, please try to keep any alterations to a minimum. Excessive alterations may be charged to the contributors.

The shorter version of the address at the beginning of the article will appear under your author/co-author name(s) in the published work and also in a List of Contributors. The longer version shows full contact details and will be used to keep our internal records up-to-date (they will not appear in the published work). For the lead author, this is the address that the honorarium and any offprints will be sent to. Please check that these addresses are correct.

Titles and headings should be checked carefully for spelling and capitalization. Please be sure that the correct typeface and size have been used to indicate the proper level of heading. Review numbered items for proper order – e.g., tables, figures, footnotes, and lists. Proofread the captions and credit lines of illustrations and tables. Ensure that any material requiring permissions has the required credit line, and that the corresponding documentation has been sent to Elsevier.

Note that these proofs may not resemble the image quality of the final printed version of the work, and are for content checking only. Artwork will have been redrawn/relabelled as necessary, and is represented at the final size.

PLEASE KEEP A COPY OF ANY CORRECTIONS YOU MAKE.

DISPATCH OF CORRECTIONS

Proof corrections should be returned in one communication to Gemma Tomalin (TGP2proofs@elsevier.com) by 04-Aug-2014 using one of the following methods:

1. PREFERRED: If corrections are minor they should either be annotated on the pdf of your proof, or can be listed in an e-mail to Gemma Tomalin in the Elsevier MRW Production Department at TGP2proofs@elsevier.com. The e-mail should state the article code number in the subject line. Corrections should be consecutively numbered and should state the paragraph number, line number within that paragraph, and the correction.

2. If corrections are substantial, send the amended hardcopy by courier to the Elsevier MRW Production Department (The Boulevard, Langford Lane, Kidlington, Oxford, OX5 1AJ, UK). If it is not possible to courier your corrections, fax the relevant marked pages to the Elsevier MRW Production Department with a covering note clearly stating the article code number and title. (Fax number: +44 (0)1865 843974). A copy will then be sent to your volume editor.

Note that a delay in the return of proofs could mean a delay in publication. Should we not receive your corrected proofs within 7 days, Elsevier may have to proceed without your corrections.

CHECKLIST

Author queries addressed/answered? ☑

Affiliations, names and addresses checked and verified? ☑

Permissions details checked and completed? ☑

Outstanding permissions letters attached/enclosed? ❏

Figures and tables checked? ☑

If you have any questions regarding these proofs please contact the Elsevier MRW Production Department at: TGP2proofs@elsevier.com.

TGP2: 00107

Non-Print Items

Abstract:

Folgheraiter suggested over a century ago that baked materials could in principle be used to study variations of the Earth's magnetic field intensity in the past although he foresaw great difficulties. Over the last century, enormous progress has been made in laying the theoretical foundations for using archaeological and geologic materials to study variations in the strength of the magnetic field. Along with better theoretical foundations have come improvements in experimental design. Over the last decade, there has been an explosion of papers presenting data concerning variations in paleointensity through time using both igneous and sedimentary records. In this chapter, we will explore the theoretical basis for paleointensity experiments in igneous and sedimentary environments, review the existing data, and highlight current topics of interest.

Keywords: DRM; Geomagnetic field behavior; Paleointensity; TRM

Author and Co-author Contact Information:

Lisa Tauxe
Scripps Institution of Oceanography
University of California San Diego
San Diego
CA 92093-0220
USA

Au9

Toshitsugu Yamazaki
Geological Survey of Japan, AIST
Tsukuba 305-8567
Japan

Atmosphere and Ocean Research Institute
University of Tokyo
Kashiwa
Chiba 277-8564
Japan

TGP2: 00107

AUTHOR QUERY FORM

Book: Treatise on Geophysics (TGP2) **Chapter: 00107**	**Please e-mail your responses and any corrections to:** **E-mail: TGP2proofs@elsevier.com**

Dear Author,

Any queries or remarks that have arisen during the processing of your manuscript are listed below and are highlighted by flags in the proof. (AU indicates author queries; ED indicates editor queries; and TS/TY indicates typesetter queries.) Please check your proof carefully and answer all AU queries. Mark all corrections and query answers at the appropriate place in the proof (e.g., by using on-screen annotation in the PDF file http://www.elsevier.com/book-authors/science-and-technology-book-publishing/overview-of-the-publishing-process) or compile them in a separate list, and tick off below to indicate that you have answered the query.
Please return your input as instructed by the project manager.

Location in Chapter	Query / remark
AU:1, page 4	Please provide complete details for reference Tauxe (2005).
AU:2, page 4	Do figures require permission? If so, please supply relevant details for us to request permission, or any correspondence granting permission, and ensure that any publisher required credit line is added to the caption.
AU:3, page 6	Reference citations in figure legends have been changed per style. Please check if it is ok.
AU:4, page 8	Please provide complete details for reference Yu and Tauxe (2004).
AU:5, page 29	Equation [12] is cited in the text but not given in this chapter. Please check.
AU:6, page 33	References Morimoto et al. (1997), Yoshihara and Hamano (2000), Sumita et al. (2001), Macouin et al. (2003), Bergh (1970), Hale (1987), McElhinny and Evans (1968), Schwartz and Simons (1969), Smirnov and Tarduno (2003), Smirnov et al. (2003, 2005) are cited in the text but not provided in the reference list. Please provide them in the reference list or delete these citations from the text.
AU:7, page 22	Please check "Difference between pTRM at pTRM check step at T" for completeness.
AU:8, page 25	Please provide appropriate reference citation instead of year of publication here and elsewhere in Table 2.
AU:9, page 50	Please check the full affiliations for accuracy. These are for Elsevier's records and will not appear in the printed work.
AU:10, page 2	Please provide appropriate chapter number instead of "separate chapter in this volume".
AU:11, page 6	Please check sentence starting "(Köenigsberg/Thellier–Thellier," for completeness.
AU:12, page 6	Please provide the full form of 'IRM'.
AU:13, page 12	In the reference list Tanaka et al. 1995a and 1995b are mentioned as separate references. Therefore we have changed all citations of Tanaka et al. 1995 to Tanaka et al. 1995a,b. Please amend the citations in the text if necessary.

TGP2: 00107

AU:14, page 12	In the reference list Ben-Yosef et al., 2008a and 2008b are mentioned as separate references. Therefore we have changed all citations of Ben-Yosef et al., 2008 to Ben-Yosef et al., 2008a,b. Please amend the citations in the text if necessary.
AU:15, page 12	Citation "Ben-Yosef et al., 2009" has not been found in the reference list. Please supply full details for this reference.
AU:16, page 12	Citation "Gee et al., 2010" has not been found in the reference list. Please supply full details for this reference.
AU:17, pages 13, 31	Citation "Heller et al., 2002" has not been found in the reference list. Please supply full details for this reference.
AU:18, page 13	Please provide the full form of PSD and MD.
AU:19, page 13	Please check if edit to sentence starting "On the other hand. . ." is okay.
AU:20, page 13	Please check if edits to sentences starting "In order to get. . ." and "In this method. . ." are okay.
AU:21, page 13	The citation "Aitken (1988)" has been changed to match the author name/date in the reference list. Please check here and in subsequent occurrences, and correct if necessary.
AU:22, page 13	Please check if "field–infield step" is okay as edited.
AU:23, page 14	The abbreviation "DRM" has been defined as "depositional remanence" and "'detrital remanence magnetization" in the document. Please check, and correct if necessary.
AU:24, page 15	Citation "Katari and Tauxe, 2000" has not been found in the reference list. Please supply full details for this reference.
AU:25, page 16	Please check if edit to sentence starting "Taking a given. . ." is okay.
AU:26, page 19	Please provide the full form of ODP, PSV, and DSDP.
AU:27, page 20	Please check if edit to sentence starting "As a result. . ." is okay.
AU:28, page 20	Please check if edit to sentence starting "However, in stable. . ." is okay.
AU:29, page 21	Citation "Yamazaki, 2012" has not been found in the reference list. Please supply full details for this reference.
AU:30, page 21	Citation "Kissel et al., 2004" has not been found in the reference list. Please supply full details for this reference.
AU:31, page 22	The citation "Biggin et al., 2010" has been changed to match the author name/date in the reference list. Please check here and in subsequent occurrences, and correct if necessary.
AU:32, page 28	The citation "Barbetti et al., 1977" has been changed to match the author name/date in the reference list. Please check here and in subsequent occurrences, and correct if necessary.
AU:33, page 31	The citation "Juarez et al. 2000" has been changed to match the author name/date in the reference list. Please check here and in subsequent occurrences, and correct if necessary.
AU:34, page 33	Citation "Meynadier et al., 1995" has not been found in the reference list. Please supply full details for this reference.
AU:35, page 33	The citation "Westphal and Munschy (1999)" has been changed to match the author name/date in the reference list. Please check here and in subsequent occurrences, and correct if necessary.

TGP2: 00107

AU:36, page 33	Please check if "Southeast Indian Ridge" is okay as edited.
AU:37, page 34	Citation "Meynadier and Valet (2000)" has not been found in the reference list. Please supply full details for this reference.
AU:38, page 35	Citation "Valet et al. (2000)" has not been found in the reference list. Please supply full details for this reference.
AU:39, page 35	Please check if "B/M boundary" should be changed to "M/B boundary."
AU:40, page 35	Citation "Ziegler and Constable (2011)" has not been found in the reference list. Please supply full details for this reference.
AU:41, page 36	Please provide appropriate figure citation in place of 'fig:padmVanom'.
AU:42, page 3	Please provide appropriate chapter numbers instead of Chapters 5.9, 5.10, and 13.4.4.
AU:43, page 38	Please check if edit to sentence starting "By using the Monte Carlo . . ." is okay.
AU:44, page 38	Citation "Hughen et al. (2002)" has not been found in the reference list. Please supply full details for this reference.
AU:45, page 39	The citation "Tauxe and Shackleton (1997)" has been changed to match the author name/date in the reference list. Please check here and in subsequent occurrences, and correct if necessary.
AU:46, page 41	Citation "Kok (1999)" has not been found in the reference list. Please supply full details for this reference.
AU:47, page 42	References that occur in the reference list but are not cited in the text. Please position each reference in the text or delete it from the reference list. Ben Yosef et al., 2009, Gee and Bowles, 2010, Heller and Peterson, 1982, Imbrie et al., 1984, McElhinny, 1973, Meynadier and Valet, 1995, Paterson et al., 2012, Tauxe and Love, 2003.
AU:48, pages 8, 19	Please provide better quality artwork for figures 7 and 15.

TGP2: 00107

a0010

107 Paleointensities

L Tauxe, University of California San Diego, San Diego, CA, USA
T Yamazaki, Geological Survey of Japan, AIST, Tsukuba, Japan; University of Tokyo, Chiba, Japan

107.1   Introduction

The geomagnetic field acts both as an umbrella, shielding us from cosmic radiation, and as a window, offering one of the few glimpses of the inner workings of the Earth. Ancient records of the geomagnetic field can inform us about the geodynamics of the early Earth and changes in boundary conditions through time. Thanks to its essentially dipolar nature, the geomagnetic field has acted as a guide, pointing to the axis of rotation, thereby providing latitudinal information for both explorers and geologists. A complete understanding of the geomagnetic field requires not only a description of the direction of field lines over the surface of the Earth but also information about its strength. While directional information is relatively straightforward to obtain, intensity variations are much more difficult and are the subject of this chapter.

In his treatise, De Magnete, published in 1600, William Gilbert described variations in field strength with latitude based on the sluggishness or rapidity with which a compass settled on the magnetic direction. Magnetic intensity was first measured quantitatively in the late 1700s by French scientist Robert de Paul, although all records were lost in a shipwreck. Systematic measurement of the geomagnetic field intensity began in 1830 (see, e.g., Stern, 2003 for a review). Despite studies of the geomagnetic field that included some mention of its strength, stretching back to at least the time of Gilbert, basic questions such as what is the average field strength and whether there are any predictable trends remain subject to debate. To study field intensity in the past requires us to use 'accidental' records; we rely on geologic or archaeological materials, which can reveal much about the behavior of the Earth's magnetic field in ancient times.

There have been several fine reviews of the field of paleointensity (see, e.g., Valet, 2003) and the subject is developing very rapidly. Paleointensity data derived from archaeological materials will be considered elsewhere (Chapter 103). This chapter will review the theoretical basis for paleointensity experiments in igneous and sedimentary environments especially with regard to experimental design. We will then turn to new and updated existing databases. Finally, we will highlight current topics of interest.

107.2   Theory of Paleointensity

In principle, it is possible to determine the intensity of ancient magnetic fields because the primary mechanisms by which rocks become magnetized (e.g., thermal, chemical, and detrital remanent magnetizations or TRM, CRM, and DRM, respectively) can be approximately linearly related to the ambient field for low fields such as the Earth's. Thus, we have by assumption

$$M_{\mathrm{NRM}} \simeq \alpha_{\mathrm{anc}} H_{\mathrm{anc}}$$

and

$$M_{\mathrm{lab}} \simeq \alpha_{\mathrm{lab}} H_{\mathrm{lab}} \qquad [1]$$

where α_{lab} and α_{anc} are dimensionless constants of proportionality, M_{NRM} and M_{lab} are natural and laboratory remanent magnetizations, respectively, and H_{anc} and H_{lab} are the

magnitudes of the ancient and laboratory fields, respectively. If α_{lab} and α_{anc} are the same, we can divide the two equations and rearrange terms to get

$$H_{\mathrm{anc}} = \frac{M_{\mathrm{NRM}}}{M_{\mathrm{lab}}} H_{\mathrm{lab}}$$

In other words, if the laboratory remanence has the same proportionality constant with respect to the applied field as the ancient one, the remanences are linearly related to the applied field, and the natural remanence (NRM) is composed solely of a single component, all one needs to do to get the ancient field is to measure M_{NRM}, give the specimen a laboratory proxy remanence M_{lab}, and multiply the ratio by H_{lab}.

In practice, paleointensity is not so simple. The remanence acquired in the laboratory may not have the same proportionality constant as the original remanence (e.g., the specimen has altered its capacity to acquire remanence or was acquired by a mechanism not reproduced in the laboratory). The assumption of linearity between the remanence and the applied field may not hold true. Or the NRM may have multiple components acquired at different times with different constants of proportionality.

In Sections 107.3 and 107.4, we will discuss the assumptions behind paleointensity estimates and outline various approaches for getting paleointensity data. We will start by considering thermal remanences and then address depositional ones. (To our knowledge, no one has deliberately attempted paleointensity using other remanence types such as chemical or viscous remanences.) In Section 107.5, we will briefly consider ways in which these remanences can be compromised by remagnetization processes. Section 107.6 considers how paleointensity data can be evaluated as to their reliability and Section 107.7 reviews the published data and database initiatives. We concentrate here on data prior to the Holocene as the Holocene is the subject of a separate chapter in this volume. Finally, Section 107.8 highlights some of the major issues posed by the paleointensity data.

107.3   Paleointensity with Thermal Remanence

It appears that Folgheraiter (1899) was the first to propose that normalized thermal remanences of pottery be used to study the ancient magnetic field, although Königsberger and/or Thellier is most often given credit. Königsberger (1936) described an experimental protocol for estimating the ratio of NRM to a laboratory-acquired TRM (Figure 1(a)) and assembled data from igneous and metamorphic rocks that spanned from the Precambrian to the present (Figure 1(b)). He noted that with few exceptions, the ratio $M_{\mathrm{NRM}}/M_{\mathrm{lab}}$ decreased with increasing age and discussed various possible explanations for the trend, including changing geomagnetic field strength and shaking by earthquakes. His preferred reason for the trend in normalized remanence, however, was that magnetized bodies lose their magnetism over time, a phenomenon we now recognize as magnetic viscosity. In fact, Königsberger believed that the trend in normalized remanence could be used to date rocks (see also Koenigsberger, 1938a,b). It was Thellier (1938) who argued strongly for the use of the thermal remanences of
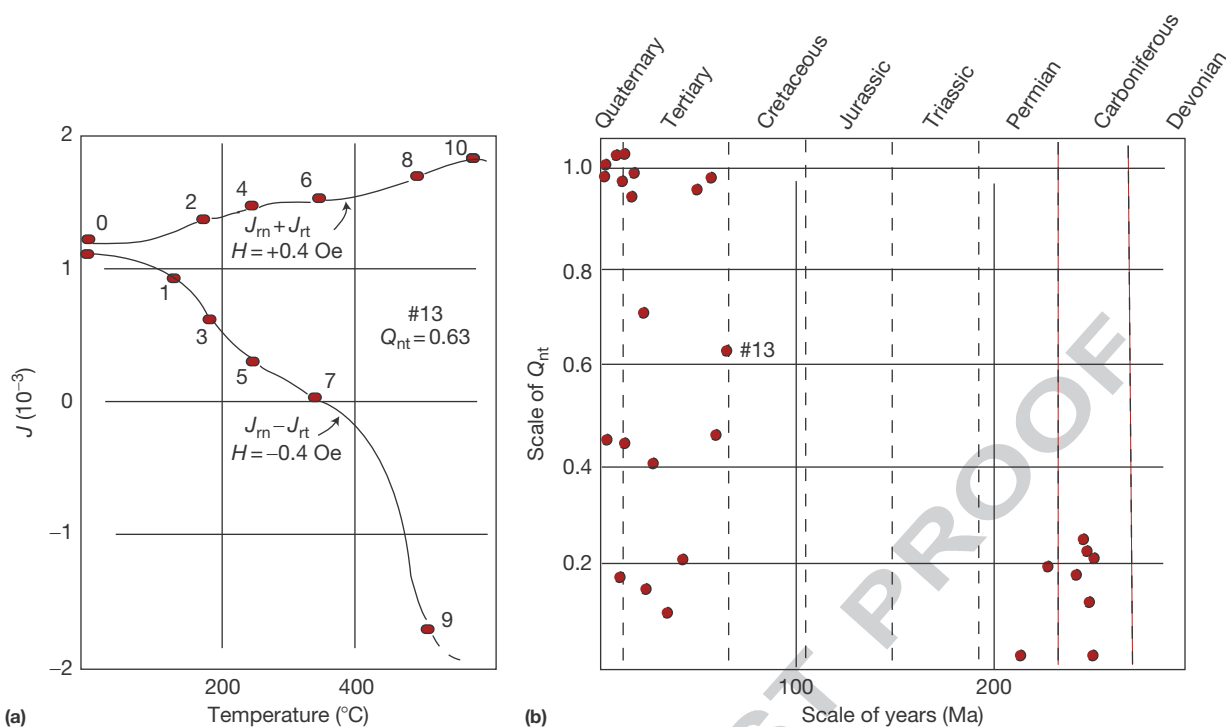
f0010 **Figure 1** (a) Example of thermal normalization experiment of Koenigsberger (1938a,b). A specimen is heated to given temperature and cooled in a field of +0.4 Oe (40 μT) (e.g., step #1). Then, the specimen is heated to same temperature and cooled in field of −0.4 Oe (e.g., step #2). The two curves can be decomposed to give M_{nrm} and M_{lab}, the ratio of which was termed Q_{nt} by Königsberger. (b) Q_{nt} data for a number of specimens compiled by Königsberger (1938b). The specimen from (a) is labeled #13. These data were interpreted by Königsberger to reflect the decay of magnetic remanence with time.

archaeological artifacts normalized by laboratory TRMs for studying the past magnetic fields.

p0055 Königsberger's approach was largely empirical; he knew that TRMs were proportional to the magnetic fields in which they cooled and that remanences tended to decay over time and he was well aware of the relationship between coercivity and thermal blocking. Nonetheless, he had very few tools at his disposal to discriminate among the myriad possible explanations for his observed trend that the NRM/TRM ratio appeared to decay with increasing age. For example, he did not call on apparent polar wander to explain deviant directions, relying instead on the idea that parts of lava flows tend to cool below their Curie temperatures before they stop moving.

p0060 The theoretical basis for how ancient magnetic fields might be preserved was clarified with the work of Nobel Prize winner (Néel, 1949, 1955). Modern theory of TRM is discussed in detail in **Chapter 102** (see also Tauxe et al., 2010 and a recent review by Valet, 2003), but we review the essential ideas here.

p0065 Briefly, a magnetized rod in the absence of a magnetic field will tend to be magnetized in one of several (often two) 'easy' directions. In order to overcome the intervening energy barrier and get from one easy direction to another, a magnetic particle must have energy sufficient to leap through some intervening 'hard' direction. According to the Boltzmann distribution law, the probability of a given particle having an energy ε is proportional to $e^{-\varepsilon/kT}$ where k is the Boltzmann constant and T is the temperature in kelvin (yielding thermal energy for the product kT). Therefore, it may be that at a certain time, the magnetic moment may have enough thermal energy to flip the sense of magnetization from one easy axis to another.

p0070 If we had a collection of magnetized particles with some initial statistical alignment of moments giving a net remanence M_o, the random flipping of magnetic moments from one easy axis to another over time will eventually lead to the case where there is no preferred direction and the net remanence will have decayed to zero. The rate of approach to magnetic equilibrium is determined by the 'relaxation time,' which describes the frequency of moments flipping from one easy axis to another.

p0075 Relaxation time according to the Néel theory is given by

$$\tau = \frac{1}{C}\exp\frac{[\text{anisotropy energy}]}{[\text{thermal energy}]} = \frac{1}{C}\exp\frac{[Kv]}{[kT]} \qquad [2]$$

where C is a frequency factor with a value of something like $10^{10}\,\text{s}^{-1}$, v is volume, and K is an 'anisotropy constant.' Equation [2] is sometimes called the Néel equation.

p0080 The energy barrier for magnetic particles to flip through a 'hard direction' into the direction of the applied field H (the anisotropy energy) requires less energy than to flip the other way, so relaxation time must be a function of the applied field. The more general equation for relaxation time is given by

$$\tau = \frac{1}{C}\exp\frac{[Kv]}{[kT]}\left[1 - \frac{H}{H_c}\right]^2 \qquad [3]$$

where H and H_c are the applied field and the field required to overcome the anisotropy energy and change the moment of the particle (known as the 'coercivity').

p0085   From eqn [2], we know that τ is a strong function of temperature. As described by Néel (1955), there is a very sharply defined range of temperatures over which τ increases from geologically short to geologically long timescales (see Dunlop and Özdemir (1997) and Tauxe et al. (2010) for more details). Taking reasonable values for magnetite, the most common magnetic mineral, we can calculate the variation of relaxation time as a function of temperature for a cubic grain of width $= 25$ nm as shown in Figure 2. At room temperature, such a particle has a relaxation time of longer than the age of the Earth, while at a few hundred degrees centigrade, the grain has a relaxation time that allows the magnetization to flip frequently between easy axes and can maintain an equilibrium with the external field. Such populations will have a slight statistical preference for the direction of the applied field because of the small difference in relaxation time between directions closer to the applied field direction from eqn [3].

p0090   The temperature at which τ is equal to about 10^2–10^3 s is defined as the blocking temperature, T_b. At or above the blocking temperature, but below the Curie temperature (the temperature at which all spontaneous magnetization is lost), a population of these grains is in equilibrium with the applied

field and is called 'superparamagnetic.' Further cooling increases the relaxation time such that the magnetization is effectively blocked and the rock acquires a thermal remanence.

p0095   Consider a lava flow that has just been extruded (see Figure 3). First, the molten lava solidifies into rock. While the rock is above the Curie temperature, there is no remanent magnetization; thermal energy dominates the system. As the rock cools through the Curie temperature of its magnetic phase(s), exchange energy (the energy that encourages electronic spins to align with each other) becomes more important and the rock acquires a magnetization. The magnetization, however, is free to track the prevailing magnetic field because anisotropy energy is still less important than the energy encouraging alignment with the magnetic field (the magnetostatic energy). At this high temperature, the magnetic moments in the lava flow are superparamagnetic and tend to flop from one easy direction to another, with a slight statistical bias toward the direction with the minimum angle to the applied field (Figure 3(c)). The equilibrium magnetization of superparamagnetic grains is only slightly aligned, and the degree of alignment is a quasilinear function of the applied field for low fields like the Earth's. The magnetization approaches saturation at higher fields, depending on the details of the controls on anisotropy energy like shape, size, and mineralogy.

107.3.1   Linearity Assumption   s0025

p0100   From theory, we expect thermal remanences of small single domain particles to be approximately linearly related to the applied field for low fields like the Earth's. However, as particle size increases, TRMs can become quite nonlinear even at relatively low fields (see Figure 4). Predicted TRM curves with respect to the applied field for randomly oriented populations of single domain particles ranging in size from 20 to 100 nm widths are plotted in Figure 4(a). We calculated these curves assuming quasi-equidimensional grains (1.5:1) and highly elongate grains (10:1). For the elongate grains, the TRM is predicted to be distinctly nonlinear even for the 80 nm particles. (The approximate range of the present Earth's field is shown as the shaded box.) Particles of magnetite larger than about 90 nm will have more complicated remanent states (flower, vortex, and multidomain) and will not necessarily

f0015   **Figure 2**   Variation of relaxation time versus temperature for a 25 nm
Au1 Au2   width cube of magnetite. Reproduced from Tauxe (2005).
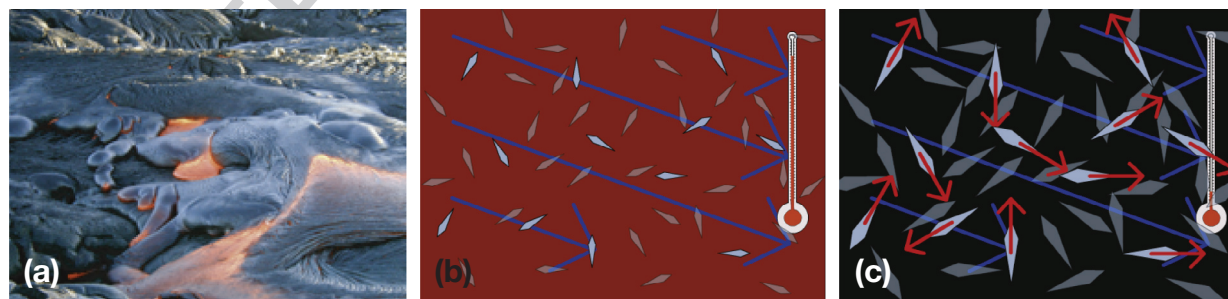
f0020   **Figure 3**   (a) Picture of lava flow courtesy of Daniel Staudigel. (b) While the lava is still well above the Curie temperature, crystals start to form but are nonmagnetic. (c) Below the Curie temperature but above the blocking temperature, certain minerals become magnetic, but their moments continually flip among the easy axes with a statistical preference for the applied magnetic field. As the lava cools down, the moments become fixed, preserving a thermal remanence. (b and c) Modified from animation of Genevieve Tauxe available at http://magician.ucsd.edu/Lab_tour/movs/TRM.mov. Reproduced from Tauxe (2005).

TGP2: 00107
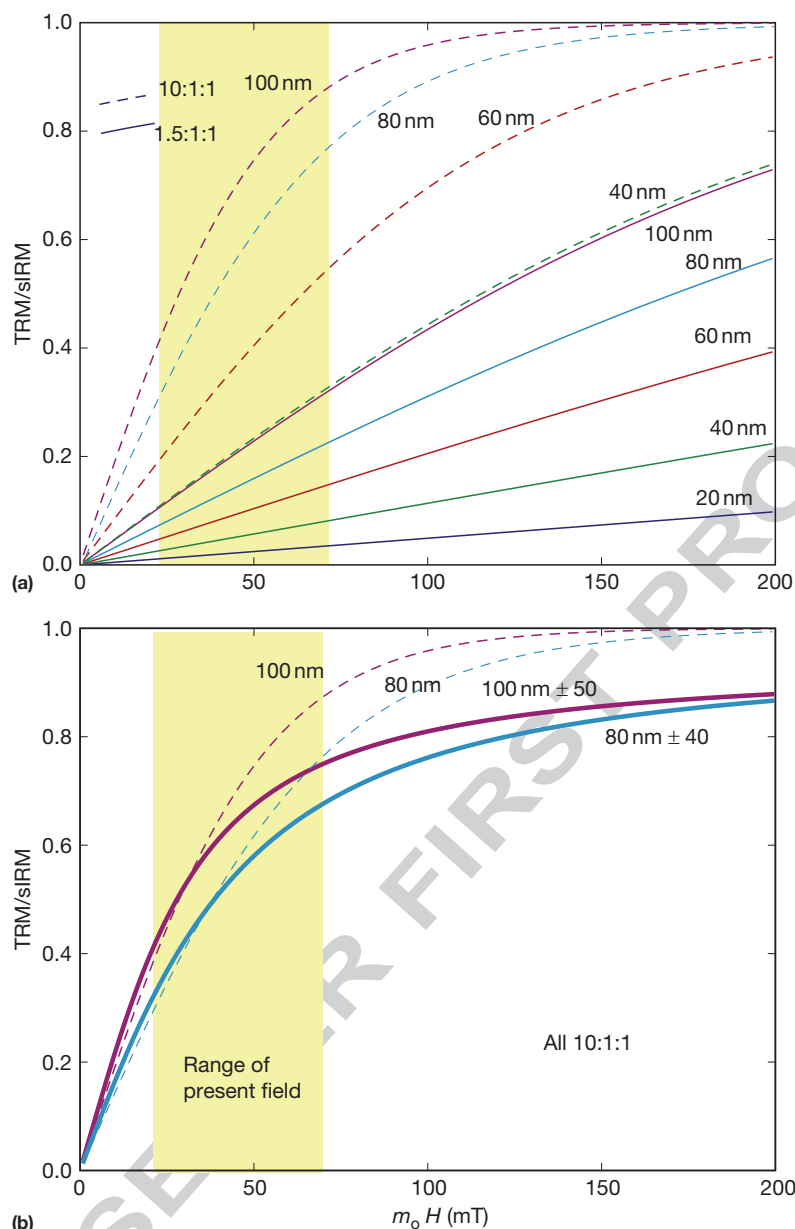
f0025 **Figure 4** Predicted thermal remanent magnetization (TRM) expressed as a fraction of saturation for various particle sizes and distributions of magnetite. Note the nick point for which the linearity assumption fails is a strong function of particle size, but linearity holds true for equant particles in fields less than a hundred µT. Strongly elongate particles will behave in a more nonlinear fashion.

follow the predicted curves, which are based on single domain theory.

p0105 We note in passing that Kletetschka et al. (2006) had postulated that multidomain particles have TRMs that are highly nonlinear at fields below some threshold value with linear behavior at higher field values. This behavior was observed using a Schonstedt oven, which has very poor field control, and we were unable to reproduce the observations in the SIO laboratory, which has excellent field control; linear behavior was observed in fields as low as 10 nT (Yongjae Yu, personal communication).

p0110 Figure 4(b) shows the effect of having a distribution of grain sizes. We calculated curves for populations with normally distributed particle widths (all with 10:1 elongation) with mean widths of 80 and 100, respectively. The effect of the distribution of particle sizes is depression of the TRM below that for a uniform distribution because smaller particles have much lower TRMs at a given field strength that the effect is asymmetrical. (The difference between 80 and 100 nm widths at, say, 100 µT is much less than the difference between 60 and 80 nm at the same field. Note also that grains smaller than about 20 nm are superparamagnetic at room temperature and do not contribute to the TRM at all, so distributions that include small particles will have suppressed TRMs relative to their theoretical saturation remanences.)

p0115 Dunlop and Argyle (1997) discovered strongly nonlinear TRM acquisition behavior in synthetic specimens with mean

TGP2: 00107

grain sizes in the single domain grain range. Although their lab fields were mostly much higher than those of the Earth's field (up to 9 mT!), the results should give practitioners of paleointensity pause. Moreover, Selkin et al. (2007) had found nonlinear TRM behavior in natural specimens with single domain behavior, and the nonlinearity is distinct in fields as low as 50 μT.

p0120   The modeling exercises shown **Figure 4** and the experimental results of Dunlop and Argyle (1997) and Selkin et al. (2007) suggest that it would be a wise practice to incorporate a test of TRM linearity into paleointensity experiments as a matter of routine. If the relationship between TRM and applied field is known empirically, then biased results can be corrected to the true ancient intensity.

s0030   107.3.2   Alteration During Heating

p0125   The second assumption for absolute paleointensity determinations is that the laboratory and ancient proportionality constants are the same (i.e., $\alpha_{lab} = \alpha_{anc}$ in eqn [1]). Simply measuring the NRM and giving the specimen a total TRM does nothing to test this assumption. For example, alteration of the specimen during heating could change the capacity to acquire thermal remanence and give erroneous results with no way of assessing their validity.

p0130   There are several ways of checking the ability of the specimen to acquire thermal remanence in paleointensity experiments. The most commonly used are experiments that employ stepwise replacement of the NRM with a laboratory thermal remanence (Köenigsberg/Thellier–Thellier, or KTT family of experiments) and those that compare anhysteretic remanence before and after heating ('Shaw' family of experiments). Other approaches attempt to prevent the alteration from occurring, for example, by heating in controlled atmospheres or vacuum or by using microwaves to heat just the magnetic phases, leaving the rest of the specimen cool. Another approach is to find materials that are particularly resistant to alteration (e.g., submarine basaltic glass or single plagioclase crystals). Finally, some methods attempt to normalize the remanence with IRM and avoid heating altogether. We will briefly describe each of these in turn, beginning with the KTT family of experiments.

s0035   107.3.2.1   KTT family of experiments

p0135   Detection of changes in the proportionality constant caused by alteration of the magnetic phases in the rock during heating has been a goal in paleointensity experiments since the earliest days. As we have already seen (**Figure 1(a)**), Koenigsberger (1936, 1938a,b) heated specimens up in stages, progressively replacing the NRM with partial thermal remanences (pTRMs), an experiment that was elaborated on by Thellier (1938) and Thellier and Thellier (1959). The so-called KTT approach is particularly powerful when lower-temperature steps are repeated, to verify directly that the ability to acquire a thermal remanence has not changed.

p0140   The stepwise approach relies on the assumption that pTRMs acquired by cooling between any two temperature steps (e.g., 500 and 400 °C in **Figure 5**) are independent of those acquired between any other two temperature steps. This assumption is called the 'law of independence' of pTRMs. The approach also assumes that the total TRM is the sum of all the independent
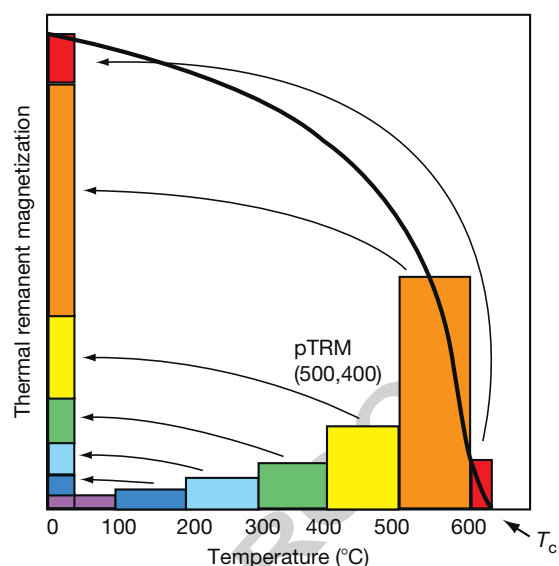
Figure 5   Laws of independence and additivity. Partial thermal remanences (pTRMs) acquired by cooling between two temperature steps are independent from one another and sum together to form the total TRM. Reproduced from McElhinny MW (1973) *Paleomagnetism and Plate Tectonics*. Cambridge: Cambridge University Press.

pTRMs (see **Figure 5**), an assumption called the 'law of additivity.'

p0145   There are several possible ways to progressively replace the NRM with a pTRM in the laboratory. In the original KTT method (see, e.g., **Figure 1(a)**), the specimen is heated to some temperature (T_1) and cooled in the laboratory field B_{lab}. After measurement of the combined remanence, what is left of the NRM plus the new laboratory pTRM is

$$M_1 = M_{NRM} + M_{pTRM}$$

p0150   Then, the specimen is heated a second time and cooled upside down (in field $-B_{lab}$). The second remanence is therefore

$$M_2 = M_{NRM} - M_{pTRM}$$

p0155   Simple vector subtraction allows the determination of the NRM remaining at each temperature step and the pTRM gained (see **Figure 6(a)**). These are nowadays plotted against each other in what is usually called an 'Arai plot' (Nagata et al., 1963) as in **Figure 6(b)**. The KTT method implicitly assumes that a magnetization acquired by cooling from a given temperature is entirely replaced by reheating to the same temperature (i.e., $T_b = T_{ub}$), an assumption known as the 'law of reciprocity.'

p0160   As magnetic shielding improved, more sophisticated approaches were developed. In the most popular paleointensity technique (usually attributed to Coe, 1967), we substitute cooling in zero field for the first heating step. This allows the direct measurement of the NRM remaining at each step. The two equations now are

$$M_1 = M_{NRM}$$

and

$$M_2 = M_{NRM} + M_{pTRM}$$

TGP2: 00107
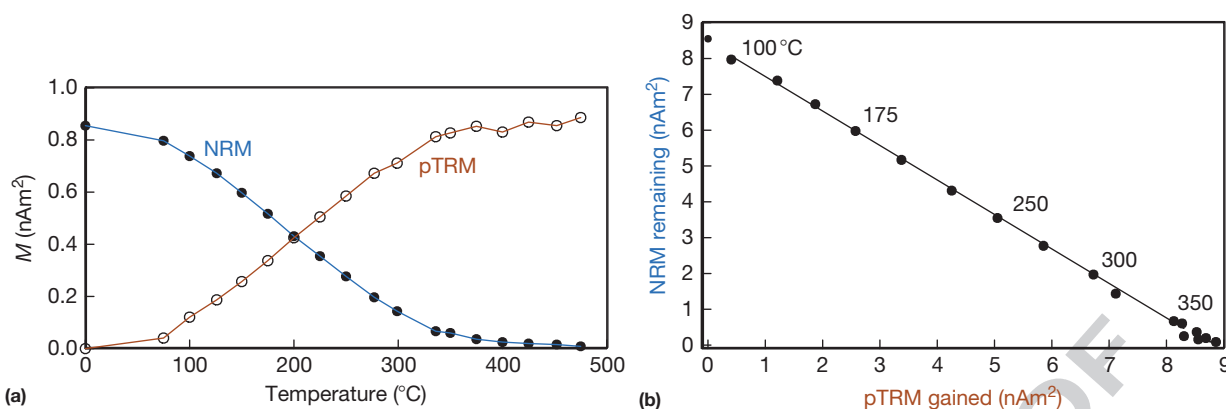
f0035   **Figure 6**   Illustration of the KTT method for determining absolute paleointensity. (a) Thermal demagnetization of NRM shown as filled circles and the laboratory-acquired pTRM shown as open symbols and (b) plot of NRM component remaining versus pTRM acquired for each temperature step. Reproduced from Tauxe (2005).

p0165   The laboratory M_{pTRM} in this 'zero-field/infield' (or ZI) method is calculated by vector subtraction. Alternatively, the first heating and cooling can be done in the laboratory field and the second in zero field (Aitken et al., 1988; see also Valet et al., 1998), here called the 'infield/zero-field' or (IZ) method.

p0170   In all three of these protocols, lower-temperature infield cooling steps can be repeated to determine whether the remanence carrying capacity of the specimen has changed. These steps are called 'pTRM checks.' Differences between the first and second M_{pTRM}s at a given temperature indicate a change in capacity for acquiring thermal remanences and are grounds for suspicion or rejection of the data after the onset of such a change. Some have proposed that paleointensity data can be 'fixed' even if the pTRM checks show significant alteration (e.g., McClelland and Briden, 1996; Valet et al., 1996). The argument is that if pTRM checks can be brought back in accordance with the original pTRM measurements using a correction factor, then if that same correction factor is applied to all subsequent pTRM measurements, the effect of the alteration has been accounted for and the data can be considered 'reliable.' We consider this correction to carry some risk and 'corrected' data should be clearly marked as such.

p0175   Despite its huge popularity and wide spread use, the approach of progressively replacing the NRM with a thermal remanence has several drawbacks. Alteration of the ability to acquire a pTRM is not the only cause for failure of the assumption of equality of α_{lab} and α_{anc}. Both experiment (Bol'shakov and Shcherbakova, 1979; Shcherbakova et al., 2000) and theory (e.g., Dunlop and Xu, 1994; Xu and Dunlop, 1994) suggest that the essential assumption of equivalence of blocking and unblocking temperatures may break down for larger particles.

p0180   Micromagnetic modeling of hysteresis behavior can shed some light on what might be going on. In simulated hysteresis experiments, particles can be subjected to a large DC applied magnetic field, sufficient to completely saturate them. As the field is lowered, certain particles form vortex structures at some applied field strength (see Figure 7). These vortex structures are destroyed again as the field is ramped back up to saturation. However, the field at which the vortex is destroyed is higher than the field at which it formed. This is the phenomenon

responsible for 'transient hysteresis' (see Fabian, 2003; Yu and Tauxe, 2005).

p0185   One can imagine that something similar to transient hysteresis could occur if we cooled a particle from its Curie temperature and then heated it back up again. Just below the Curie temperature, the particle would be in a saturated state (because the magnetization is quite low and the vortex structure is just an attempt by the particle to reduce its external field). As the specimen cools down, the magnetization grows. At some temperature, a vortex structure may form. As the specimen is heated back up again, the vortex may well remain stable to higher temperatures than its formation temperature by analogy to the behavior in the simulated hysteresis experiment.

p0190   If the particle is large enough to have domain walls in its remanent state, then the scenario is somewhat different and not easily tractable by theory (see Chapter 102). At just below its Curie temperature, the particle is at saturation. As the particle cools, domain walls will begin to form at some temperature. The remanent state will have some net moment because the domain walls are distributed such that there is incomplete cancelation leaving a small net remanence, proportional to the applied field for moderate field strengths. As the temperature ramps up again, the walls 'walk around' within the particle seeking to minimize the magnetostatic energy and are not destroyed until temperatures very near the Curie temperature.

p0195   The fact that blocking and unblocking of remanence occur at different temperatures in some particles means that a pTRM blocked at a given temperature will remain stable to higher temperatures; the unblocking temperature is not equal to the blocking temperature. This means that $\alpha_{lab} \neq \alpha_{anc}$ and the key assumptions of the KTT-type methods are not met. The Arai plots may be curved (see Dunlop and Özdemir, 1997, for a more complete discussion), and if any portion of the NRM/TRM data are used instead of the entire temperature spectrum, the result could be biased. For example, the lower-temperature portion might be selected on the grounds that the higher-temperature portion is affected by alteration or the higher-temperature portion might be selected on the grounds that the lower-temperature portion is affected by viscous remanence. Both of these interpretations would be wrong.

Au48
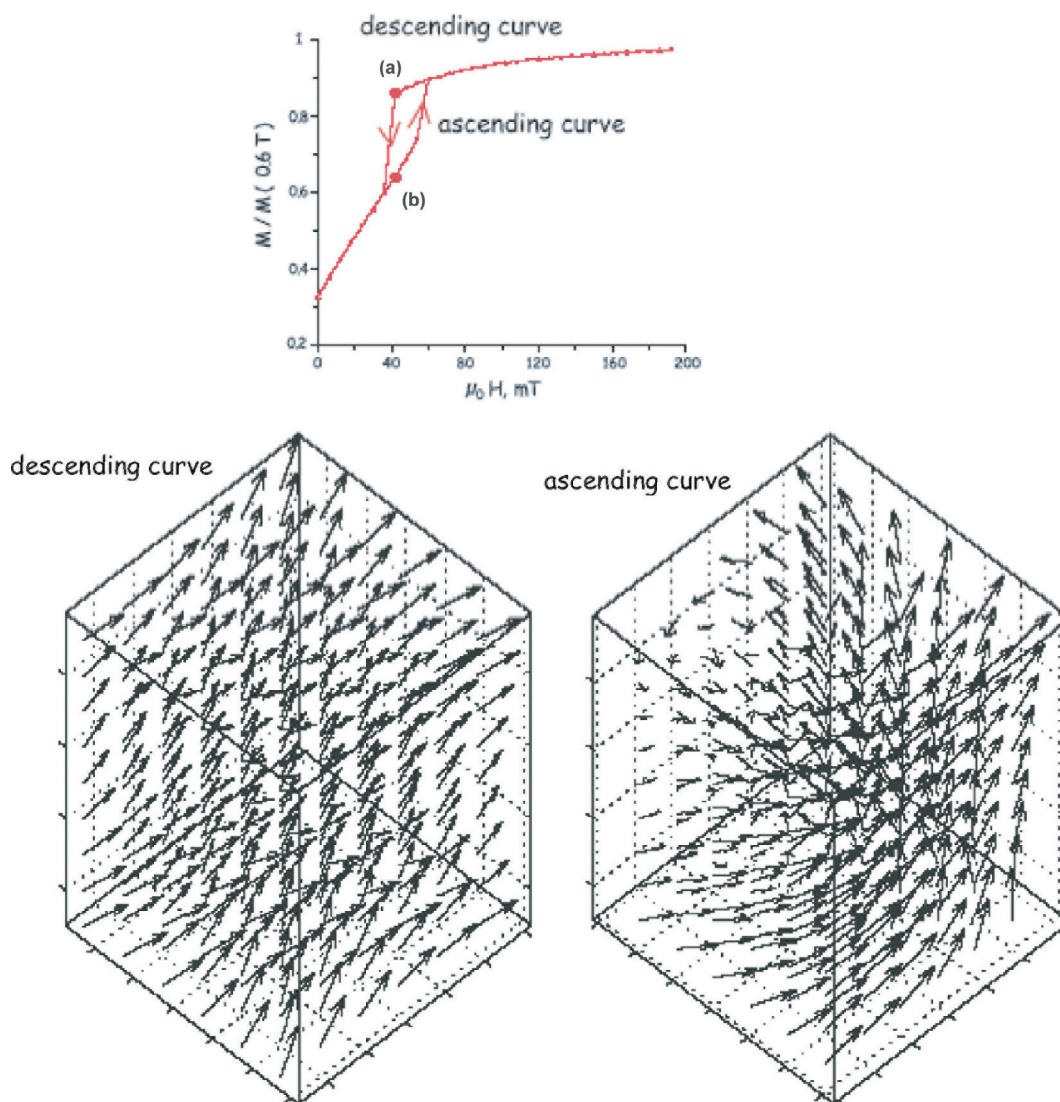
f0040   **Figure 7**   Example of irreversible behavior when particle is brought from a saturated state at high field to zero fields and back up again. A vortex structure forms on the descending curve in the simulated hysteresis loop at the sharp drop in magnetization at about 40 μT (labeled '(a)'). A snapshot of the micromagnetic state is shown to the lower left. This feature intensifies as the field drops to zero, resulting in a loss of magnetization. When the field ramps back up again, the vortex remains stable well past its formation field (labeled '(b)'). A snapshot of the micromagnetic state on the ascending curve is shown in the lower right. The vortex is not destroyed until a higher field, when the loop is closed. Reproduced from Yu and Tauxe (2004).

Au4

p0200   In order to detect inequality of blocking and unblocking and the presence of unremoved portions of the pTRM known as 'high-temperature pTRM tails,' several embellishments to the KTT-type experiment have been proposed and more are on the way. In one modification, a second zero-field step is inserted after the infield step in the ZI method. This so-called pTRM tail check (e.g., Riisager and Riisager, 2001) assesses whether the pTRM gained in the laboratory at a given temperature is completely removed by reheating to the same temperature. If not, the specimen is said to have a 'pTRM tail,' a consequence of an inequality of the unblocking temperature T_{ub} and the original blocking temperature T_b in violation of the law of reciprocity and grounds for rejection. A second modification is to alternate between the IZ and ZI procedures (the so-called 'IZZI' method first conceived with AgNés Genevey and described by Yu et al., 2004). The IZZI method is also extremely sensitive to the presence of pTRM tails and may obviate the need for the pTRM tail check step. An example of a complete IZZI experiment is shown in Figure 8.

p0205   There are several other violations of the fundamental assumptions that require additional tests and/or corrections in the paleointensity experiment besides alteration or failure of the law of reciprocity. For example, if the specimen is anisotropic with respect to the acquisition of thermal remanence, the anisotropy tensor must be determined and the intensity corrected (e.g., Fox and Aitken, 1980). The detection and correction for anisotropy can be very important in certain paleomagnetic (and archaeomagnetic) materials. The correction involves determining the TRM (or the anhysteretic remanence (ARM) proxy) anisotropy tensor and matrix multiplication to recover the original magnetic vector (see Selkin et al., 2000, for a more complete discussion). Moreover, because the approach
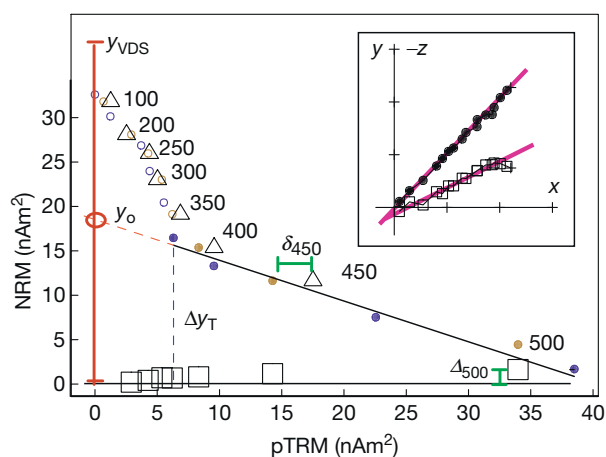
f0045 **Figure 8** Data from an IZZI experiment. Circles are the pTRM gained at a particular temperature step versus the NRM remaining. Solid symbols are those included in the slope calculation. Blue (darker) symbols are the infield–zero-field steps (IZ) and the brown (lighter) symbols are the zero-field–infield steps (ZI). The triangles are the pTRM checks and the squares are the pTRM tail checks. The difference between the pTRM check and the original measurement is δ_i as shown by the horizontal bar labeled δ_{450}. The difference between the first NRM measurement and the repeated one (the pTRM tail check) is shown by the vertical bar labeled Δ_{500}. The vector difference sum (VDS) is the sum of all the NRM components (tall vertical bar labeled VDS). The NRM fraction is shown by the vertical dashed bar. The insets are the vector components (x, y, z) of the zero-field steps. The solid symbols are (x, y) pairs and the open symbols are (x, z) pairs. The specimen was unoriented with respect to geographic coordinates. The laboratory field was applied along the z-axis in the infield steps. Redrawn from Tauxe L and Staudigel H (2004) Strength of the geomagnetic field in the Cretaceous Normal Superchron: New data from submarine basaltic glass of the Troodos Ophiolite. *Geochemistry*, *Geophysics*, *Geosystems* 5(2): Q02H06. http://dx.doi.org/10.1029/2003GC000635.

to equilibrium is a function of time, slower cooling results in a larger TRM; hence, differences in cooling rate between the original remanence acquisition and that acquired in the laboratory will lead to erroneous results (e.g., Halgedahl et al., 1980). Compensating for differences in cooling rate is relatively straight forward if the original cooling rate is known and the specimens behave according to single domain theory. Alternatively, one could take an empirical approach in which the rock is allowed to acquire a pTRM under varying cooling rates (e.g., Genevey and Gallet, 2003), an approach useful for cooling rates of up to a day or two.

s0040 **107.3.2.2 Shaw family of experiments**

p0210 The previous section was devoted to experiments in which detection of nonideal behavior is done by repeating various temperature steps. In this section, we will consider an alternative approach, long in use in paleointensity studies, which employs the laboratory proxy ARM. The so-called Shaw method (e.g., Shaw, 1974) is based on ideas first explored by van Zijl et al. (1962a,b). In its simplest form, we measure the NRM and then progressively demagnetize the NRM with alternating fields (AFs) to establish the coercivity spectrum of the specimen prior to heating. The specimen is then given an ARM (M_{ARM_1}) by subjecting the specimen to progressively higher

peak AFs, which decay in the presence of a small bias field. The use of ARM has been justified because it is in many ways analogous to the original TRM (see Chapter 102). M_{ARM_1} is then progressively demagnetized to establish the original relationship between the coercivity spectrum of the M_{NRM} (presumed to be a thermal remanence) and ARM prior to any laboratory heating.

p0215 As with the KTT-type methods, M_{NRM} is normalized by a laboratory thermal remanence. But in the case of the Shaw-type methods, the specimen is given a total TRM, (M_{TRM_1}), which is AF demagnetized as well. Finally, the specimen is given a second ARM (M_{ARM_2}) and demagnetized for the last time.

p0220 The general experiment is shown in Figure 9(a) and 9(b). If the first and second ARMs do not have the same coercivity spectrum as in Figure 9(b), the coercivity of the specimen has change and the NRM/TRM ratio is suspect.

p0225 Rolph and Shaw (1985) suggested that the ratio M_{ARM_1}/M_{ARM_2} at each demagnetizing step be used to 'correct' for the alteration bias of M_{TRM_1} by

$$M_{TRM_1^*} = M_{TRM_1} \frac{M_{ARM_1}}{M_{ARM_2}}$$

p0230 So doing can in some cases restore linearity between NRM and TRM as shown in Figure 9(c).

p0235 Valet and Herrero-Bervera (2000) argued that only data requiring no correction and utilizing the entire coercivity spectrum should be used. They further pointed out that many specimens are required to lend credibility to a paleointensity experiment. As the former requirement generally leaves very few specimens, Valet and Herrero-Bervera reasoned that a quicker experimental procedure would ultimately result in more acceptable data, hence a better overall outcome, even if the results from many experiments are discarded. To speed up the measurement process, they employed a truncated Shaw method in which no ARMs are imparted, but both the NRM and the laboratory TRM are completely demagnetized using AFs. Linearity of the two when plotted as in Figure 9(a) is taken as the sole criterion for acceptance.

p0240 Tsunakawa and Shaw (1994) suggested that a tendency for chemical alteration could also be detected if the specimen is heated to above the Curie temperature twice, each followed by AF demagnetization (see Figure 9(d)–9(f)). During the second heating step, the specimen is left at high temperature for a longer period of time than the first heating step to encourage alteration to continue so that it may be detected by the method. If the slope $M_{TRM_1}/M_{TRM_2^*}$ differs by more than experimental error, the experimental results are rejected.

p0245 The issue of contamination of the remanence by multidomain particles has also been considered in the Shaw-type methods. It has long been known (Ozima et al., 1964) that specimens can lose much of their remanence by cooling to temperatures below about $-160\,^{\circ}$C and warming in zero field. This behavior is generally attributed to magnetocrystalline-dominated remanences cycling through the so-called Verwey transition at which the axis of magnetocrystalline anisotropy changes, erasing the magnetic memory of these particles (see, e.g., Dunlop and Özdemir, 1997). This behavior is frequently assumed to occur most readily in multidomain particles; hence, their contribution could be minimized if specimens are pretreated to low temperatures (low-temperature demagnetization,
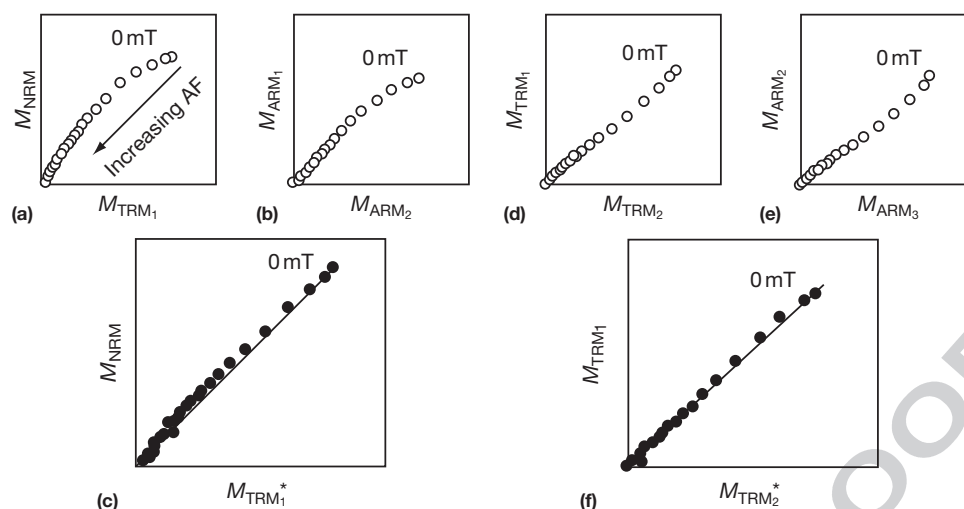
f0050   **Figure 9**   Shaw family of methods (see text). (a) Plot of pairs of NRM and the first TRM for each AF demagnetization step. (b) Plot of pairs of the first ARM and the second ARM for each AF demagnetization step. (c) Plot of pairs of NRM and TRM adjusted by the ratio of ARM_1/ARM_2 for that AF step from (b) TRM_1^*. (d) Same as (a) but for the first and second TRMs. (e) Same as (a) but for the second and third ARMs. (f) Same as (c) but for first and second TRM where TRM_2^* is adjusted using ARM_2/ARM_3 ratio from (e). Redrawn from Yamamoto Y, Tsunakawa H, and Shibuya H (2003) Palaeointensity study of the Hawaiian 1960 lava: Implications for possible causes of erroneously high intensities. *Geophysical Journal International* 153(1): 263–276.

or LTD) prior to measurement. Yamamoto et al. (2003) and Yamamoto and Tsunakawa (2005) argued that one of the major causes of failure in paleointensity experiments is the effect of multidomain particles, which violate the essential assumption that the original blocking temperature is the same as the laboratory unblocking temperature. They therefore treat specimens to LTD prior to AF demagnetization of each remanence. This 'LTD-DHT Shaw' method gave improved results for the otherwise disappointingly difficult Hawaiian 1960 lava flow (see, e.g., Tanaka and Kono, 1991; Valet, 2003; Valet and Herrero-Bervera, 2000).

p0250   The LTD-DHT Shaw experiment assumes that mainly, the multidomain particles are affected by the LTD step. However, Carter-Stiglitz et al. (2002, 2003) found that single domain magnetites can and do lose substantial remanence by LTD as well. This behavior means that LTD treatment may demagnetize part of the desired as well as the undesired NRM. It is possible that the SD remanence removed by LTD may be the low coercivity contribution and unimportant to the paleointensity.

p0255   The primary reasons stated for using the Shaw method are that (1) it is faster and (2) because the specimen is only heated once (albeit to a high temperature), alteration is minimized. The first rationale is no longer persuasive because modern thermal ovens have high capacities and the KTT method is certainly not slower than the Shaw method on a per specimen basis. This is particularly true for the LTD-DHT Shaw method as this experiment takes approximately 8 h to complete per specimen. The second rationale may have some validity. The key features of any good experiment are the built-in tests of the important assumptions.

s0045   **107.3.3   Methods That Minimize Alteration**

p0260   Several alternative approaches have been proposed in which instead of detecting nonideal behavior such as alteration, they

attempt to minimize it. These methods include reducing the number of heating steps required (as in the Shaw methods), heating specimens in controlled atmospheres, reducing the time at temperature by, for example, measuring the specimens at elevated temperature, and using microwaves to excite spin moments as opposed to direct thermal heating. Finally, there has been some effort put into finding materials that resist alteration during the heating experiments.

107.3.3.1   Reduced number of heating steps   s0050

Kono and Ueno (1977) described in detail a single heating per   p0265 temperature step method suggested by Kono (1974) whereby the specimen is heated in a laboratory field applied perpendicular to the NRM. M_{pTRM} is obtained by vector subtraction. Reducing the number of heatings can reduce the alteration to some extent. However, this method has only rarely been applied because it can only be used for strictly univectorial NRMs (an assumption that is difficult to test with the data generated by this method) and requires rather delicate positioning of specimens in the furnace or fancy coil systems that generally have a limited region of uniform field, reducing the number of specimens that can be analyzed in a single batch. While pTRM checks are possible with this method, they necessitate additional heating steps and are not generally performed.

A second strategy for reducing the number of heating steps   p0270 was proposed by Hoffman et al. (1989) and modified by Hoffman and Biggin (2005) (see also Dekkers and Böhnel, 2006). In the Hoffman–Biggin version, at least five specimens from a given cooling unit are sliced into four specimens each, one of which is dedicated to rock magnetic analysis. The remaining specimens (at least 15) are heated a total of five times giving remanence measurements $\mathbf{M_1} - \mathbf{M_5}$. (Please note that bold face parameters are vectors, while normal text variables are scalars, in this case the magnitudes.) In the first three heating steps, the specimens are treated to increasingly high temperatures (T_0, T_1, and T_2) and cooled in zero field. The first

TGP2: 00107

heating step ostensibly removes any secondary overprint (e.g., a VRM, viscous remanent magnetization) and M_1 serves as the baseline for normalizing all subsequent steps so that data from different specimens can be combined. After the three zero-field heating steps, the specimens are heated again to T_2 and cooled with the laboratory field switched on between T_2 and T_0 after which it is switched off. This treatment step gives the pTRM acquired between T_2 and T_0 by vector subtraction of $\mathbf{M_4 - M_3}$. The fifth heating step is to T_1 followed by a zero-field cooling. This final step serves to supply both the pTRM acquired between T_2 and T_1 by vector subtraction of $\mathbf{M_4 - M_5}$ and a kind of 'pseudo pTRM check' step as explained later.

p0275   In interpreting results, there are two data points from each specimen with estimates for NRM remaining versus pTRM gained, denoted T_1 and T_2. The NRM remaining part of T_1 and T_2 are ratios M_2/M_1 and M_3/M_1, respectively. The pTRMs gained at T_1 and T_2 are $|\mathbf{M_5 - M_4}|/M_1$ and $|\mathbf{M_4 - M_3}|/M_1$. Because all remanences are normalized by the NRM remaining after zero-field cooling from T_0 (M_1) measured for each specimen, we can combine data from the different specimens together on a single Arai-like plot (see **Figure 10**).

p0280   Hoffman and Biggin (2005) had several criteria that help screen out 'unreliable' data. First, they require that the directions of the zero-field steps trend to the origin on an orthogonal plot and have low scatter. This helps eliminate data for which the characteristic remanence has not been isolated (although three zero-field steps are not generally considered sufficient for this purpose). Second, they require the γ-intercept to be between 0.97 and 1.03 and that the correlation coefficient must be ≥ 0.97. If the T_1 data are displaced from the line connecting the T_2 point and a γ-intercept of 1.0, then the specimen may have altered during laboratory heating (e.g., open symbols in **Figure 10**) and can be rejected.

p0285   Noting that the results of the multispecimen procedure when applied to the 1971 Hawaiian flow (shown in **Figure 10**) were significantly different than the known field (37 μT),
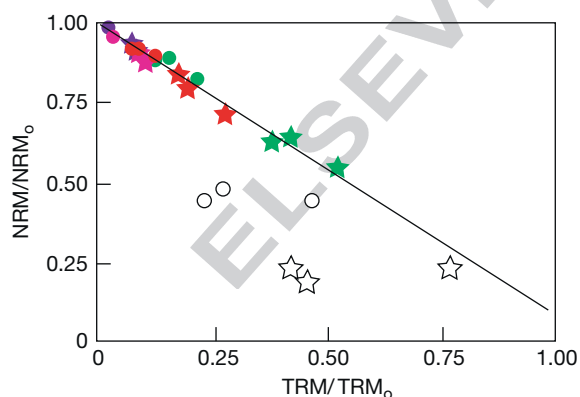
f0055   **Figure 10**   Illustration of multispecimen approach for specimens from the 1971 Hawaiian lava flow. Different colors represent data from different specimens. Different symbols are different heating steps. Open symbols are from specimen that failed initial selection criteria. The best-fit line represents a slope that predicts a 'paleo' field of 33 μT, whereas the actual field was 37 μT. Redrawn from Hoffman KA and Biggin AJ (2005) A rapid multi-sample approach to the determination of absolute paleointensity. *Journal of Geophysical Research* 110: B12108. http://dx.doi.org/10.1029/2005JB003646.

Hoffman and Biggin (2005) suggested that the data, which are heavily influenced by data from a single, low blocking temperature specimen (green symbols in **Figure 10**), could be reweighted to remove the bias. Furthermore, they proposed averaging all the data by accepted specimen and including the γ-intercept in the calculation. These modifications yielded a concordant result with the known field within error. Finally, they redefined many of the parameters typically used in paleointensity experiments (see **Section 107.6**) for use with the multispecimen method.

p0290   The primary advantage of the multispecimen approach put forward by Hoffman and Biggin (2005) is the speed with which measurements can be made, allowing many more specimens to be analyzed. While the method may be fast, it loses multiple pTRM checks and any ability to assess the equivalence of blocking and unblocking. Moreover, the method strongly emphasizes the lower blocking temperature portion of the blocking temperature spectrum (especially in the moment corrected version). This means that the remanence is contaminated by viscous or multidomain remanences leading to a concave downward curve in the Arai plot; the multispecimen result will overestimate the true value of the paleointensity. Finally, it is experimentally very difficult to turn the laboratory field off precisely when the specimen's internal temperature is T_0 because only the oven temperature is known and the specimen temperature lags behind that of the oven by variable and unknown amounts, depending on the exact disposition of the specimens in the oven. This bias will lead to scatter and contribute to a systematic bias (the field will always be turned off at too high a temperature, thereby underestimating the pTRM gained).

p0295   On the positive side, the presentation of all specimen data on a single Arai diagram (also proposed by Chauvin et al., 2005) is an interesting modification of the traditional Arai diagram. Plotting all the KTT data from specimens from a given cooling unit on a single Arai diagram allows instant assessment of the reproducibility of data and of course can be done with traditional experimental results.

107.3.3.2   *Use of controlled atmospheres to reduce alteration*   s0055

p0300   Alteration during heating is caused by oxidation (or reduction) of the magnetic minerals in the specimen. There have been several strategies to reduce this effect with varying degrees of success. Thellier (1938) tried using vacuum and nitrogen atmospheres. Taylor (1979) developed a technique for paleointensity determination that encapsulated specimens in silica glass. By placing an oxygen 'getter' such as titanium in the evacuated glass tube along with the specimen, he suggested that oxygen fugacity could be maintained and alteration would be reduced. This technique was tested by Sugiura et al. (1979) who claimed some improvement in experimental results on lunar glass specimens. Valet et al. (1998) performed paleointensity experiments by heating in argon atmospheres and cooling in nitrogen atmospheres. They reported a significant improvement in their argon results over those performed in air. More recently, Kissel and Laj (2004) also used a furnace with a controlled argon atmosphere to minimize alteration, and Mochizuki et al. (2004) incorporated heating in a vacuum to the LTD-DHT Shaw experiments, a practice that has been

TGP2: 00107

adopted as routine for this method in subsequent investigations and successfully recovered the historical field for samples from the 1986 Oshima lava flow in Japan. The difficulties of heating and cooling in vacuum and controlled atmospheres are (1) difficulty in achieving a uniform and reproducible temperature in the oven and (2) unintended oxidation or reduction reactions. It appears that reduction in alteration can be achieved using these techniques, although the overwhelming majority of paleointensity experiments are done in air.

s0060 107.3.3.3   Measurement at elevated temperature

p0305 Boyd (1986) suggested that measurements could be made more rapidly if they were measured at elevated temperatures instead of cooling back to room temperature for measurement. The idea was that alteration could be detected immediately and the experiment aborted, before wasting time finishing the entire measurement sequence. A variant of the method using an infield–infield approach was applied to the 1960 Hawaiian lava flow and the 2.2 ka Kotaki pyroclastic flow by Tanaka et al. (1995a,b). In the case of the historical flow where the 'ancient' field is known (36 μT), the method overestimated the true field by 13%. The idea of measuring at elevated temperatures was warmed up by Le Goff and Gallet (2004) who developed a vibrating sample magnetometer equipped with magnetic field coils, which allow the specimen to be measured at temperature and in controlled fields, greatly speeding up the measurement process and, one hopes, reducing the effects of cooling rate and specimen alteration. This method has been applied in archaeomagnetic studies with great success (e.g., Gallet and Le Goff, 2006).

s0065 107.3.3.4   Use of microwaves for thermal excitation

p0310 Until now, we have not concerned ourselves with HOW the magnetic moment of a particular grain flips its moment. Earlier, we mentioned 'thermal energy' and left it at that. But how does thermal energy do the trick?

p0315 An external magnetic field generates a torque on the electronic spins, and in isolation, a magnetic moment will respond to the torque in a manner similar in some respects to the way a spinning top responds to gravity: the magnetic moment will precess about the applied field direction, spiraling in and come to a rest parallel to it. Because of the strong exchange or superexchange coupling in magnetic phases, spins tend to be aligned parallel (or antiparallel) to one another, and the spiraling is done in a coordinated fashion, with neighboring spins as parallel as possible to one another. This phenomenon is known as a 'spin wave.'

p0320 Raising the temperature of a body transmits energy (via 'phonons') to the electronic spins, increasing the amplitude of the spin waves. This magnetic energy is quantized in 'magnons.' In the traditional KTT experiment, the entire specimen is heated, and the spin waves are excited to the point that some may flip their moments as described in Section 107.3.

p0325 As in most kitchens, there are two ways of heating things up: the conventional oven and the microwave oven. In the microwave oven, molecules with certain vibrational frequencies (e.g., water) are excited by microwaves. These heat up, passing their heat on to the rest of the pizza (or whatever). If the right microwave frequency is chosen, ferromagnetic particles can also be excited directly, inviting the possibility of heating only the magnetic phases, leaving the matrix alone (e.g., Walton et al., 1993). The rationale for developing this method is to reduce the degree of alteration experienced by the specimen because the matrix often remains relatively cool, while the ferromagnetic particles themselves get hot. (The magnons get converted to phonons, thereby transferring the heat from the magnetic particle to the matrix encouraging alteration, but there may be ways of reducing this tendency (see Walton, 2004).)

p0330 The same issues of nonlinearity, alteration, reciprocity, anisotropy, cooling rate differences, etc. arise in the microwave approach as in the thermal approach. Ideally, the same experimental protocol could be carried out with microwave ovens as with thermal ovens. In practice, however, it has proved quite difficult to repeat the same internal temperature, making double (or even quadruple) heatings problematic although progress toward this end may have been made (e.g., Böhnel et al., 2003). It is likely that the issues of reciprocity of blocking and unblocking in the original (thermally blocked) and the laboratory (microwave unblocked) and differences in the rate of blocking and unblocking will remain a problem for some time as they have for thermally blocked remanences.

p0335 Concerns were raised by Valet (2003) and Le Goff and Gallet (2004) that the theoretical equivalence between thermal unblocking and microwave unblocking has not yet been explained. In fact, Walton (2005) pointed out that resonance within the magnetic particles is wavelength-dependent. This raises the possibility that unblocking may occur in an entirely different manner in microwave processes than in thermal ones (by chords instead of scales to use a musical metaphor) leading to serious questions about the applicability of the method for recovery of paleointensity estimates.

p0340 With improvements in the ability to repeat internal temperature steps, the microwave method has been adapted to a variety of experimental protocols without a loss in experimental quality (e.g., Biggin et al., 2007; Hill et al., 2002; Yamamoto and Shaw, 2008). The results of Yamamoto and Shaw (2008) provide further encouragement as their investigations recovered the laboratory field and only slightly overestimated the historical field value of the Hawaiian 1970 lava flow using a microwave version of the LTD-DHT Shaw protocol.

107.3.3.5   Using materials resistant to alteration   s0070

p0345 Another very important approach to the paleointensity problem has been to find and exploit materials that are themselves resistant to alteration. There are an increasing variety of promising materials, ranging from quenched materials, to single crystals extracted from otherwise alteration-prone rocks, to very slowly cooled plutonic rocks (e.g., layered intrusions). Quenched materials include volcanic glasses (e.g., Pick and Tauxe, 1993, 1994), metallurgical slag (e.g., Ben-Yosef et al., 2008a,b, 2009; Shaar et al., 2010, 2011a,b), and welded tuffs (Gee et al., 2010). Single crystals of plagioclase or other silicates extracted from igneous rocks (Tarduno et al., 2006, 2007, 2010) can yield excellent results, while the lava flows themselves may be prone to alteration or other nonideal behavior. Parts of layered intrusions (e.g., Selkin et al., 2000) can also perform extremely well during the paleointensity experiment.

TGP2: 00107

p0350
Au17
While some articles have called the reliability of submarine basaltic glass results into question (e.g., Heller et al., 2002), Tauxe and Staudigel (2004), Bowles et al. (2005), Bowles et al. (2011), and Tauxe et al. (2013) addressed these concerns in great detail, and the reader is referred to those papers and the references therein for a thorough treatment of the subject. There is no basis in experiment or theory for questioning the origin of remanence of submarine basaltic glass.

s0075 **107.3.4 Methods for Non-Single Domain Remanences**

p0355
We have already noted several approaches intended to detect and/or remove the effect of pTRM tails (e.g., the pTRM tail check of Riisager and Riisager, 2001, the IZZI method of Yu et al., 2004, and the LTD-DHT Shaw method of Yamamoto et al., 2003). Dekkers and Böhnel (2006) argued that their multispecimen procedure ('multispecimen parallel differential pTRM method'), which employs a single heating/cooling step with the laboratory field oriented parallel to the NRM, can be used on specimens of any domain state. The fundamental assumption of this method is the assumed linearity of pTRM with applied field, which the authors claim is independent of domain state. As already discussed, this may not be true, particularly for multidomain grains. Fabian and Leonhardt (2010) experimentally showed that the original protocol of Dekkers and Böhnel overestimates paleointensity for intermediate PSD and MD grain sizes, and they proposed a modified protocol for correcting potential domain state-dependent effects including pTRM tail. On the other hand, de Groot et al. (2012) observed underestimates of paleointensity even when the modified protocol was used, for which they considered that changes in magnetic domain due to heating are responsible.
Au18
Au19

p0360
Another approach for eliminating the effect of pTRM tails is to compare unblocking temperature of the original NRM with unblocking temperature of a laboratory-induced TRM. This method was tried first by Wilson (1961) and was recently rediscovered by Muxworthy (2010). The so-called Wilson method compares continuous measurement of the NRM while demagnetizing by heating with that of a full TRM induced in a known field. In order to get around the problem of pTRM tails, which persist to blocking temperatures higher than the temperature at which they were acquired (high-temperature tails) or, more insidiously, become demagnetized at temperatures lower than they were acquired (low-temperature tails), the Wilson method first demagnetizes the NRM and then demagnetizes a laboratory remanence and compares the two unblocking spectra. In this method, the measurements are done as a continuous thermal demagnetization (measuring the remanence at high temperature), and so this method is faster than the standard Thellier-type methods in which the samples must first be cooled and measured at room temperature. The problem with this method is that alteration of the sample may occur in the first demagnetization and can never be detected.
Au20

p0365
Sbarbori et al. (2009) took a different approach. They first completed a set of IZZI experiments on a suite of samples from Isla Socorro, Mexico. Some specimens had curved Arai plots but passed all the alteration checks and had magnetizations that trended straight to the origin. They interpreted these as having multidomain magnetic carriers and thought to circumvent the problem by imparting a second TRM and repeating the IZZI experiment in order to plot unblocking temperature against unblocking temperature. However, the second experiment yielded straight Arai plots and the initial curved behavior could not be reproduced. Although there was no evidence for chemical alteration (all pTRM checks passed), the domain state of the specimen had clearly changed. Nonetheless, this type of approach may be useful in some cases in which the curved Arai plots can be reproduced. If there is a straight line between the natural and laboratory remanence unblocking spectra, pTRM checks pass in both experiments, and the NRM trends directly to the origin, there may be a way to determine paleointensity from multidomain remanences that are unbiased. Worryingly, Shaar et al. (2011b) found that multidomain remanences tend to underestimate the ancient field strength even if the total NRM is used, implying that the NRM decayed in a manner not predicted by the Néel theory (Néel, 1949) and that no paleointensity method can recover the ancient field strength for MD remanences.

p0370
Wang and Kent (2013) embellished the method of direct comparison of unblocking of the NRM with unblocking of the laboratory TRM in a protocol they call 'back-zero-forth' or BZF. In this protocol, the NRM of the specimens is first treated to infield cooling along one axis (B), followed by zero-field cooling (Z) and then by a second infield cooling step with the field applied along the opposite direction (F). This mimics the traditional infield–infield method of Königsberger (1936) and embeds the IZ approach of Aitken et al. (1988) and a ZI similar to the Coe (1967) approach (except for the presence of pTRM tails generated by the field–infield step). After the initial BZF treatment, the specimens are given a total TRM in a laboratory field and the BZF experiment is repeated. The unblocking of the NRM is plotted against the unblocking of the laboratory TRM, similar to the Sbarbori et al. (2009) and Muxworthy (2010) approaches. This new BZF protocol enables comparison of the II, IZ, and ZI protocols. As in the much less labor-intensive IZZI protocol, the influence of MD grains may be detected and the second BZF experiment may allow the MD effect to be corrected.
Au21
Au22

s0080 **107.3.5 Use of IRM Normalization**

p0375
Sometimes, it is difficult or impossible to heat specimens because they will alter in the atmosphere of the lab or the material is too precious to be subjected to heating experiments (e.g., lunar samples and some archaeological artifacts). Looking again at Figure 4 suggests an alternative for order of magnitude guesstimates for paleointensity without heating at all. TRM normalized by a saturation remanence (IRM) is quasilinearly related to the applied field up to some value depending on mineralogy and grain-size population.

p0380
Several investigators (e.g., Cisowski and Fuller, 1986; Gattacceca and Rochette, 2004; Kletetschka et al., 2004) have advocated the use of IRM normalization of the NRMs of lunar and meteorite samples to estimate paleointensity. Cisowski and Fuller (1986) argued that, especially when both remanences were partially demagnetized using AF demagnetization, the NRM:IRM ratio gave order of magnitude constraints on absolute paleointensity and reasonable relative paleointensity estimates. Their argument is based on monomineralic suites of

rocks with uniform grain size. They further argued optimistically that multidomain contributions can be eliminated by the AF demagnetization.

p0385   As can be seen by examining **Figure 4**, at best, only order of magnitude estimates for absolute paleointensity are possible. The monomineralic and uniform grain-size constraints make even this unlikely. Finally, multidomain TRMs and IRMs do not behave similarly under AF demagnetization, the former being much more stable than the latter. Nonetheless, if magnetic uniformity can be established, it may in fact be useful for establishing relative paleointensity estimates as is done routinely in sedimentary paleointensity studies (see **Section 107.6**). The caveats concerning single component remanences are still valid, and perhaps, complete AF demagnetization of the NRM would be better than a single 'blanket' demagnetization step. Moreover, we should bear in mind that for larger particles, TRM can be strongly nonlinear with applied field at even relatively low fields (30 µT) according to the experimental results of Dunlop and Argyle (1997) (see also **Figure 1(a)** of Kletetschka et al., 2006). The problem with the IRM normalization approach is that domain state, linearity of TRM, and nature of the NRM cannot be assessed. The results are therefore difficult to interpret in terms of ancient fields.

s0085   107.4   Paleointensity with Depositional Remanences

p0390   Sediments become magnetized in quite a different manner than igneous bodies. Detrital grains are already magnetized, unlike igneous rocks, which crystallize above their Curie temperatures. Magnetic particles that can rotate freely will turn into the direction of the applied field, which can result in a DRM. Sediments are also subject to postdepositional modification through the action of organisms, compaction, diagenesis, and the acquisition of VRM, all of which will affect the magnetization and our ability to tease out the geomagnetic signal. In the following, we will consider the syndepositional processes of physical alignment of magnetic particles in viscous fluids (giving rise to the primary DRM) and then touch on the postdepositional processes important to paleointensity in sedimentary systems.

s0090   107.4.1   Physical Alignment of Magnetic Moments in Viscous Fluids

p0395   The theoretical and experimental foundation for using DRM for paleointensities is far less complete than for TRM. Tauxe (1993) reviewed the literature available through 1992 thoroughly and the reader is referred to that paper for background (see also Valet, 2003). In the last decade, there have been important contributions to both theory and experiment and we will outline our current understanding here.

p0400   Placing a magnetic moment **m** in an applied field **B** results in a torque Γ on the particle $\mathbf{\Gamma} = \mathbf{m} \times \mathbf{B}$. The magnitude of the torque is given by $\Gamma = mB \sin\theta$, where θ is the angle between the moment and the magnetic field vector. This torque is what causes compasses to align themselves with the magnetic field. The torque is opposed by the viscous drag and inertia and the equation of motion governing the approach to alignment is

$$I\frac{d^2\theta}{dt^2} = -\lambda\frac{d\theta}{dt} - mB\sin\theta \qquad [4]$$

where λ is the viscosity coefficient opposing the motion of the particle through the fluid and I is the moment of inertia. Nagata (1961) solved this equation by neglecting the inertial term (which is orders of magnitude less important that the other terms) as

$$\tan\frac{\theta}{2} = \tan\frac{\theta_o}{2}e^{(-mBt/\lambda)} \qquad [5]$$

where θ_o is the initial angle between **m** and **B**. He further showed that by setting $\lambda = 8\pi r^3\eta$ where r is the particle radius and η is the viscosity of water ($\sim 10^{-3}$ kg m^{-1} s^{-1}), the time constant γ of eqn [5] over which an initial θ_o is reduced to $1/e$ of its value is

$$\gamma = \frac{\lambda}{mB} = \frac{6\eta}{MB} \qquad [6]$$

where M is the volume normalized magnetization.

p0405   Now we must choose values η, M, and B. As noted by many authors since Nagata himself (see discussion by Tauxe et al., 2006), plugging in reasonable values for η, M, and B and assuming isolated magnetic particles, the time constant is extremely short (µs). The simple theory of unconstrained rotation of magnetic particles in water, therefore, predicts that sediments with isolated magnetic particles should have magnetic moments that are fully aligned and insensitive to changes in magnetic field strength. Yet even from the earliest days of laboratory redeposition experiments (e.g., Johnson et al., 1948; see **Figure 11(a)**), we have known that depositional remanence (DRM) can have a strong field dependence and that DRMs are generally far less than saturation magnetizations ($\sim 0.1\%$). Much of the research on DRM has focused on explaining the strong field dependence observed for laboratory redepositional DRM.

p0410   The observation that DRM is usually orders of magnitude less than saturation and that it appears to be sensitive to changing geomagnetic field strengths implies that the time constant of alignment is much longer than predicted by eqn [6]. To increase γ, one can either increase viscosity or decrease magnetization.

p0415   One can increase γ by using the viscosity in the sediment column (e.g., Denham and Chave, 1982) instead of the water column. However, something must act to first disrupt the alignment of particles prior to burial, so calling on changes in viscosity is at best an incomplete explanation.

p0420   There are several ways of increasing γ by reducing the value of M hence inhibiting the alignment in the first place. For example, one could use values for M much lower than the saturation magnetizations of common magnetic minerals (e.g., Collinson, 1965; Stacey, 1972). However, even using the magnetization of hematite, which is two orders of magnitude lower than magnetite, results in a time constant of alignment that is still less than a second.

p0425   There are two mechanisms by which the time constant of alignment can be reduced, which account for experimental results of laboratory redeposition experiments: Brownian motion and flocculation. Collinson (1965) called on Brownian motion to disrupt the magnetic moments by analogy to

TGP2: 00107
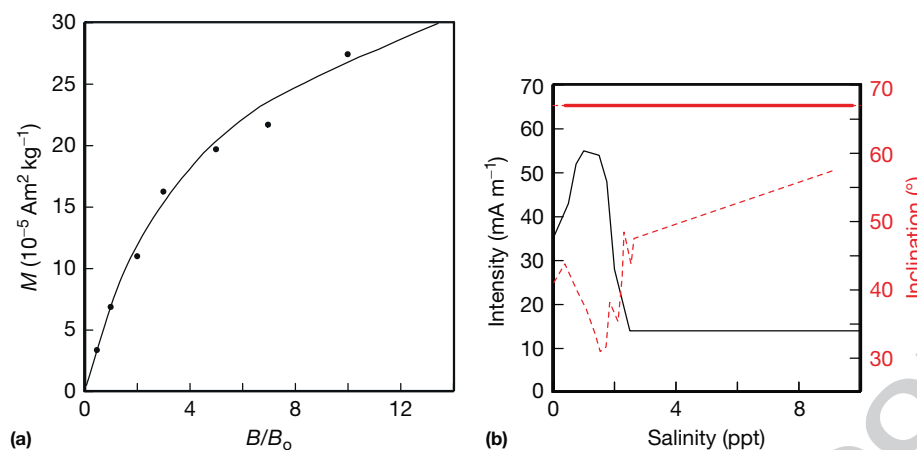
f0060   **Figure 11**   (a) Depositional remanence versus applied field for redeposited glacial varves. B_o was the field in the lab. Data from Johnson et al. (1948). Reproduced from Tauxe L (1993) Sedimentary records of relative paleointensity of the geomagnetic field: Theory and practice. *Reviews of Geophysics* 31: 319–354. (b) Relationship of detrital remanent magnetization (DRM) intensity and salinity for synthetic sediment composed of a mixture of kaolinite and maghemite. Data of Van Vreumingen (1993b). Reproduced from Roberts AP, Tauxe L, and Heslop D (2013) Magnetic paleointensity stratigraphy and high resolution Quaternary geochronology: Successes and future challenges. *Quaternary Science Reviews* 61: 1–16.

paramagnetic gases. Reasonable parameter assumptions suggest that particles smaller than about 100 nm will be affected by Brownian motion suggesting a possible role in DRM of isolated magnetite grains free to rotate in water. Furthermore, Yoshida and Katsura (1985) presented experiments on the magnetization of suspensions in response to applied fields that were entirely consistent with a Brownian motion model. Flocculation was fingered by Shcherbakov and Shcherbakova (1983) (see also Katari and Bloxham, 2001) who noted that in saline environments, sedimentary particles tend to flocculate and that isolated magnetic particles would be highly unlikely. When magnetic moments are attached to nonmagnetic 'fluff,' it is the net magnetization of the floc that must be used in eqn [6], that is, much smaller than the magnetization of the magnetic mineral alone.

p0430   The role of water chemistry (e.g., pH and salinity) has been

Au24   investigated by several authors since the early 1990s (Katari and Tauxe, 2000; Lu et al., 1990; Tauxe et al., 2006; van Vreumingen, 1993a,b). In **Figure 11(b)**, we replot data from one of the van Vreumingen experiments. The data were obtained by depositing a synthetic mixture of kaolinite, illite, and maghemite under various conditions of salinity. There is an intriguing increase in intensity with small amounts of NaCl followed by a dramatic decrease in intensity, which stabilizes for salinities greater than about 4 ppt.

p0435   Both the increase and the decrease in intensity (solid line) can be explained in terms of Brownian motion and flocculation, which is encouraged by increasing salinity. The initial increase in intensity with small amounts of NaCl could be the result of the maghemite particles adhering to the clay particles, increasing viscous drag, hence reducing the effect of Brownian motion. The subsequent decrease in intensity with higher salinities could be caused by building composite flocs with decreased net moments, hence lowering the time constant of alignment. The decrease in net moment with increasing flocculation was also supported by the redeposition experiments of Lu et al. (1990), Katari and Tauxe (2000), and Tauxe et al. (2006).

p0440   There are therefore two completely different systems when discussing DRM: ones in which magnetic particles remain

isolated (e.g., freshwater lakes; see **Figure 12(a)**) and ones in which flocculation plays a role (e.g., marine environments; see **Figure 12(b)**). For the case of magnetite in freshwater, Brownian motion may well be the dominant control on DRM efficiency. In saline waters, the most important control on DRM is the size of the flocs in which the magnetic particles are embedded. In the following, we briefly explore these two very different environments.

107.4.1.1 *Nonflocculating environments*   s0095

In freshwater, we expect to have isolated magnetic particles   p0445 whose magnetic moments would presumably be a saturation remanence. The overwhelming majority of laboratory redeposition experiments have been done in deionized water (e.g., Kent, 1973; Lovlie, 1974) and hence are in the nonflocculating regime. However, only a few studies have attempted to model DRM using a quantitative theory based on Brownian motion (e.g., Collinson, 1965; King and Rees, 1966; Stacey, 1972; Yoshida and Katsura, 1985). Here, we outline the theory to investigate the behavior of DRM that would be expected from a Brownian motion mechanism (henceforth a Brownian remanent magnetization or BRM).

To estimate the size of particles affected by Brownian   p0450 motion, Collinson used the equation

$$\frac{1}{2}mB\phi^2 = \frac{1}{2}kT \qquad [7]$$

where ϕ is the Brownian deflection about the applied field direction (in radians), k is the Boltzmann constant $(1.38 \times 10^{-23}\ \mathrm{J\ K^{-1}})$, and T is the temperature in kelvin. The effect of viscous drag on particles may also be important when the magnetic moments of the particles are low (see Coffey et al. (1996) for a complete derivation), for which we have

$$\frac{\phi^2}{\delta} = \frac{kT}{4\pi\eta r^3}$$

where δ is the time span of observation (say, 1 s). According to this relationship, weakly magnetized particles smaller than
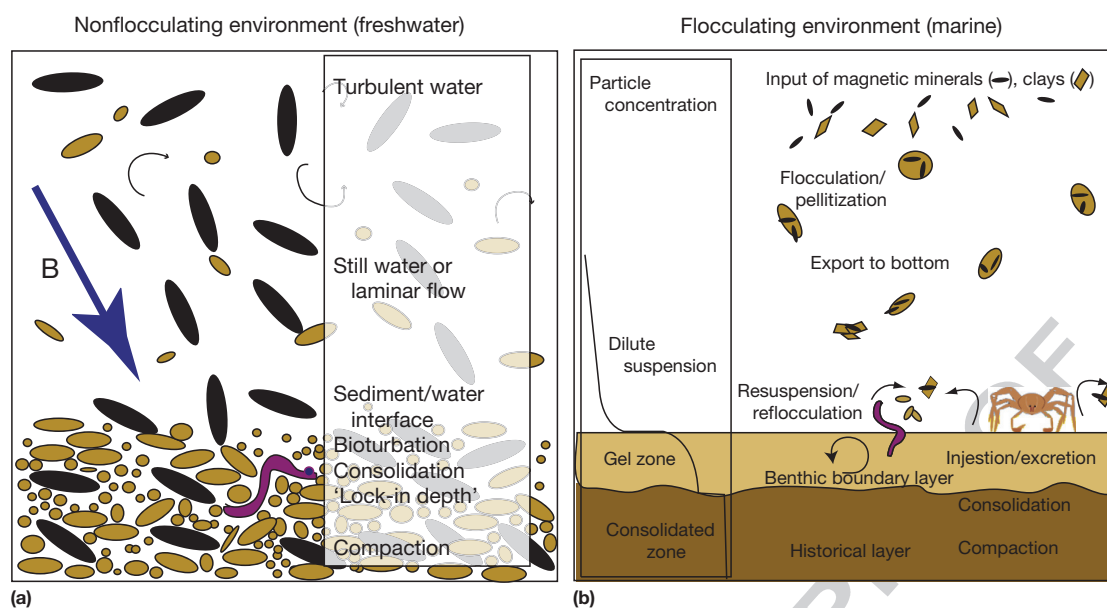
Figure 12   (a) Schematic drawing of traditional view of the journey of magnetic particles from the water column to burial in a nonflocculating (freshwater) environment. Magnetic particles are black. Redrawn from Tauxe L (1993) Sedimentary records of relative paleointensity of the geomagnetic field: Theory and practice. *Reviews of Geophysics* 31: 319–354. (b) View of depositional remanence in a flocculating (marine) environment. Redrawn from Tauxe L, Steindorf J, and Harris A (2006) Depositional remanent magnetization: Toward an improved theoretical and experimental foundation. *Earth and Planetary Science Letters* 244: 515–529.

about a micron will be strongly affected by Brownian motion. Particles that have a substantial magnetic moment, however, will be partially stabilized (according to eqn [7]) and might remain unaffected by Brownian motion to smaller particle sizes (e.g., 0.1 μm). In the case of isolated particles of magnetite, therefore, we should use eqn [7] and BRM should follow the Langevin equation for paramagnetic gases, that is,

$$\frac{BRM}{sIRM} = \coth\left(\frac{mB}{kT}\right) - \frac{kT}{mB} \qquad [8]$$

p0455   To get an idea of how BRMs would behave, we first find m from M_r (here, we use the results from micromagnetic modeling of Tauxe et al. (2002)). Then, we evaluate eqn [8] as a function of B for a given particle size (see **Figure 13(a)**). We can also assume any distribution of particle sizes (e.g., that shown as the inset to **Figure 13(b)**) and predict BRM/sIRM for the distribution (blue line in **Figure 13(b)**). It is interesting to note that BRMs are almost never linear with the applied field unless the particle sizes are very small.

p0460   BRMs would be fixed when the particles are no longer free to move. The fixing of this magnetization presumably occurs during consolidation, at a depth (known as the lock-in depth) where the porosity of the sediment reduces to the point that the particles are pinned (see **Figure 12(a)**). Below that, the magnetization may be further affected by compaction (e.g., Deamer and Kodama, 1990) and diagenesis (e.g., Roberts, 1995).

s0100   ### 107.4.1.2   Flocculating environments
p0465   DRM in flocculating environments (saline waters) has been studied in the laboratory by Lu et al. (1990), van Vreumingen (1993a,b), Katari and Tauxe (2000), and Tauxe et al. (2006) and theoretically by Shcherbakov and Shcherbakova (1983),

Katari and Bloxham (2001), and Tauxe et al. (2006). We summarize the current state of the theory in the following.

Katari and Bloxham (2001) rearranged eqn [5] by replacing   p0470
time with settling distance l, a parameter that is more easily measurable in the laboratory using the empirical relationship of settling velocity to radius of Gibbs (1985). They got

$$\tan\frac{\theta}{2} = \tan\frac{\theta_o}{2}\exp\left(-mBl/8.8\pi\eta r^{3.78}\right) \qquad [9]$$

As in Nagata (1961), a magnetic moment **m** making an   p0475
initial angle θ_o with the applied field **B** will begin to turn toward the direction of the magnetic field. After time t (or equivalently, settling distance, l), the moment will make an angle θ with the field. Tauxe et al. (2006) showed that the new coordinates of **m** (x', y', z') are related to the initial values (x_o, y_o, z_o) by

$$x' = \cos\theta, \quad y' = \sqrt{\frac{1 - x_o^2}{1 + (z_o^2/y_o^2)}}, \quad \text{and} \quad z' = y'\frac{z_o}{y_o} \qquad [10]$$

From the preceding, we can make a simple numerical model   p0480
to predict the DRM for an initially randomly oriented assemblage of magnetic moments, after settling through l. For an initial set of simulations, Tauxe et al. (2006) followed Katari and Bloxham, using the viscosity of water, m of 5 fAm^2 (where femto (f) $= 10^{-15}$), and a settling length l of 0.2 m. In **Figure 14(a)** and **14(b)**, we show the predicted DRM curves as a function of magnetic field and radius. We see that particles, in general, are either nearly aligned with the magnetic field or nearly random with only a narrow band of radii in between the two states for a given value of B. Increasing B increases the size for which particles can rotate into the field, giving rise to the dependence of DRM intensity on applied field strength. Taking a given particle   Au25

TGP2: 00107
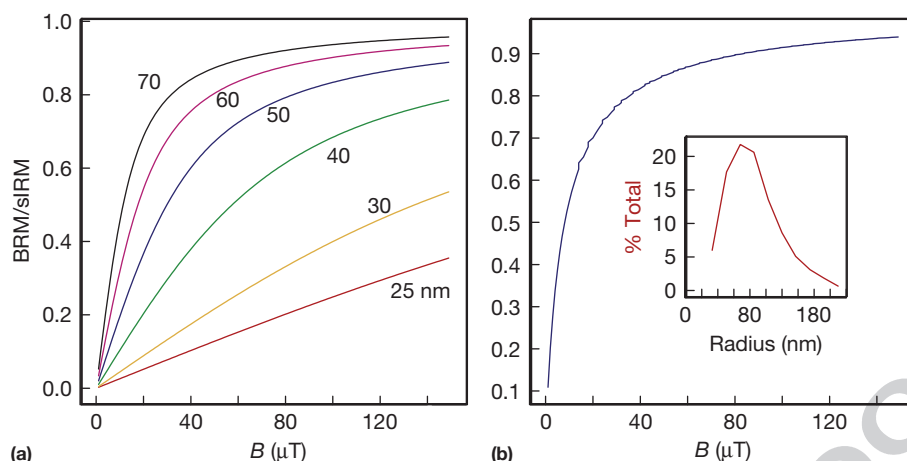
f0070   **Figure 13**   (a) Numerical simulations of Brownian remanent magnetization (BRM) for various sizes of magnetite. (b) BRM simulated for distribution of particle sizes of magnetite shown in inset.
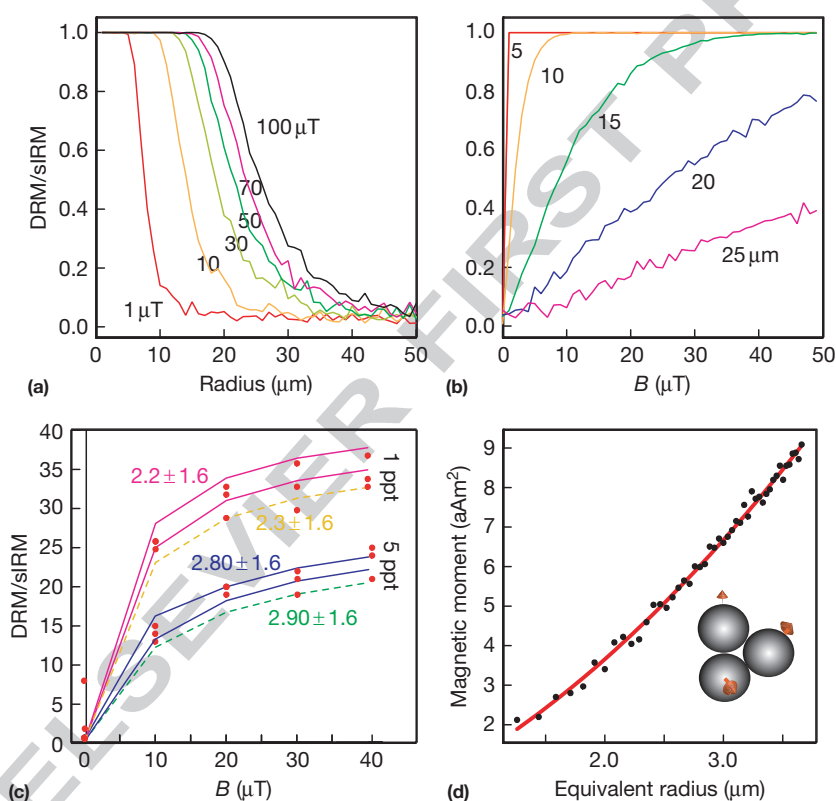
f0075   **Figure 14**   (a) Results of numerical experiments of the flocculation model using the parameters: $l = 0.2$ m and the viscosity of water. M/M_o is the DRM expressed as a fraction of saturation, holding $\overline{m}$ constant and varying B. For a given field strength, particles are either at saturation or randomly oriented, except for within a very narrow size range. (b) Same as (a) but plotted versus applied field (B). (c) Results of settling experiments as a function of field (B) in a flocculating environment. The assumed mean and standard deviations of truncated log-normal distributions for floc radii are shown in the legends and are indicated using the different line styles in the figure. (d) m versus equivalent radius for composite flocs as in inset. Line given by polynomial fit $m = ar^2 + br + c$ where $a = 3.61 \times 10^{-7}$, $b = 1.2 \times 10^{-12}$, $c = -2.1 \times 10^{-19}$ is based on a fundamental floc of 1 μm with a measured saturation remanence. Redrawn from Tauxe L, Steindorf J, and Harris A (2006) Depositional remanent magnetization: Toward an improved theoretical and experimental foundation. *Earth and Planetary Science Letters* 244: 515–529.

size and predicting DRM as a function of the applied field (Figure 14(b)) determines the opposite behavior for DRM than the Brownian motion theory (Figure 13) in that the larger the floc size, the weaker the DRM and also the more linear with respect to the applied field. The theories of Brownian motion, which predicts low DRM efficiency for the smallest particles increasing to near saturation values for particles around 0.1 μm and composite flocs theory, which predicts decreased

TGP2: 00107

DRM efficiency for larger floc sizes, can therefore explain the experimental data of van Vreumingen (1993a,b) shown in **Figure 11(b)**.

p0485   The flocculation model of DRM makes specific predictions that can in principle be tested if the model parameters can be estimated or controlled. Tauxe et al. (2006) tested the theory by dispersing natural sediments in settling tubes to which varying amounts of NaCl had been introduced. Prior to dispersal, each specimen of mud was given a saturation IRM. They measured DRM as a function of floc size (increasing salinity enhanced floc size) and the applied field (see **Figure 14(c)**). In general, their results suggest the following: (1) The higher the NaCl concentration, the lower the net moment (confirming previously published efforts); (2) the higher the salinity, the faster the particles settled (a well-known phenomenon in coastal environments; see, e.g., Winterwerp and Kestern, 2004); (3) the higher the applied field, the higher the DRM, although a saturation DRM (sDRM) appears to be nearly achieved in the 1 ppt NaCl set of tubes by 30 μT (**Figure 14(c)**); and (4) the relationship of DRM to B was far from linear with applied field in all cases. Moreover, in the Katari and Bloxham (2001) model of DRM, a single magnetic particle is assumed to be embedded in each floc; hence, the magnetization of the flocs is independent of floc size. In this view, the sDRM should equal the sum of all the individual flocs, that is, sIRM in the case of these experiments. sDRM was well below sIRM in all experiments (see, e.g., **Figure 14(c)**) and no Katari–Bloxham-type model can account for the results.

p0490   Tauxe et al. (2006) modified the simple theory of Katari and Bloxham (2001) by incorporating the understanding of flocculation from the extensive literature on the subject. In nature, flocs are formed by coalescing of 'fundamental flocs' into composite flocs. Each fundamental floc would have tiny magnetic particles adhering to them and would have the sIRM imparted prior to settling. As the composite flocs grow by chance encounters with other flocs, the net moment of the composite floc will be the vector sum of the moments of the fundamental flocs (see, e.g., inset to **Figure 14(d)**). They modeled the magnetization of flocs as a function of floc radius (assuming a quasispherical shape) through Monte Carlo simulation, an example of which is shown in **Figure 14(d)**. By choosing reasonable log-normal distributions of flocs for settling tube, their model predicts the curves shown in **Figure 14 (c)**, in excellent agreement with the redeposition data.

p0495   A critical aspect of the work of Van Vreumingen (1993a,b) remained unexplained by the theoretical work of Tauxe et al. (2006) and that was the dependence of the inclination on the salinity (dashed line in **Figure 11**). To explain this, Mitra and Tauxe (2009) reprised the idea of 'plates and spheres' of King (1955) and incorporated it into the model of Tauxe et al. (2006) using the numerical approximation of Heslop (2007). Instead of using plates and spheres, however, Mitra and Tauxe (2009) assumed a population of slightly elongate flocs with a continuous size distribution (**Figure 15**). They separated the sizes into two groups: one was small enough to respond mainly to magnetic torques (group M) with a net moment essentially parallel to the applied field and the other was controlled by hydrodynamic torques (group H attaining hydrodynamic stability while settling (with long axes on average

horizontal)). Group H magnetic moments attempt to align with the field, but the net moment is biased shallow. When the flocs become too large to maintain equilibrium with the field, their net magnetization is essentially zero. Therefore, the net magnetic declination of group H flocs tracks the field azimuth, but the net inclination is near zero (**Figure 15**). The net magnetic moments of both groups of flocs contribute to the observed DRM (**Figure 15**). In reality, a floc is not expected to behave according to the simple scheme of particles aligning through action of a magnetic torque, as envisaged in the model, but it would instead follow a complicated trajectory under the simultaneous influence of magnetic and hydrodynamic torques (Heslop, 2007). However, the average behavior of an ensemble of flocs can be approximated by this simple conceptual model. Mitra and Tauxe (2009) used this model to successfully simulate the laboratory results shown in **Figure 11(b)**.

107.4.2   Postdepositional Processes   s0105

It appears that by combining the effects of Brownian motion   p0500 for nonflocculating environments and a composite floc model for flocculating environments, we are on the verge of a quantitative physical theory that can account for the acquisition of depositional remanence near the sediment/water interface. At some point after deposition, this DRM will be fixed because no further physical rotation of the magnetic particles in response to the geomagnetic field is possible. The depth at which moments are pinned is called the lock-in depth. If lock-in depth is selective and some magnetic particles would be fixed while others remain free, there will be some depth (time) interval over which remanence is fixed, resulting in some temporal smoothing of the geomagnetic signal. Physical rotation of particles in response to compaction can also change the magnetic remanence. Other processes not involving postdepositional physical rotation of magnetic particles including 'viscous' (in the sense of magnetic viscosity) remagnetization and diagenetic alteration resulting in a chemical remanence may also modify the DRM. All of these processes influence the intensity of remanence and hamper our efforts to decipher the original geomagnetic signal. We will briefly discuss the effects specific to sediments in the following; chemical alteration and viscous remagnetization effect both TRMs and DRMs and will be addressed in **Section 107.5**.

The 'standard model' of depositional remanence (DRM)   p0505 acquisition was articulated, for example, by Verosub (1977) and Tauxe (1993). In this view, detrital remanence is acquired by locking in different grains over a range of depths. This phased lock-in leads to both significant smoothing and an offset between the sediment/water interface and the fixing of the DRM. Many practitioners of paleomagnetism still adhere to this concept of DRM, which stems from the early laboratory redeposition experiments, which were carried out under nonflocculating conditions (see **Section 107.4.1**). Several studies on natural marine sediments (e.g., deMenocal et al., 1990; Kent and Schneider, 1995; Lund and Keigwin, 1994; see also Channell et al., 2004) are frequently cited, which suggest a high degree of mobility of magnetic particles after deposition resulting in sedimentary smoothing and delayed remanence acquisition.
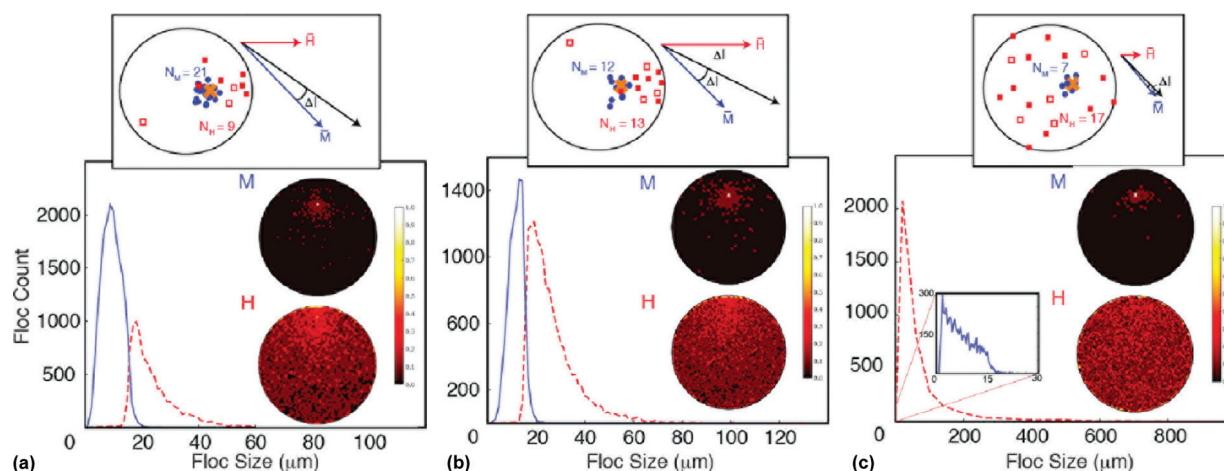
TGP2: 00107

f0080 **Figure 15** Numerical simulation of how paleomagnetic intensity and inclination in sediments are affected by floc size. Lower: the solid blue and red dashed lines represent floc distributions in simulated M and H groups, respectively, where M represents flocs that respond to magnetic torques and H represents flocs that are dominated by hydrodynamic torques. A northward-directed applied field with 45° inclination and 45 mT intensity was used for the simulations. In equal area projections of floc moments for the M (upper) and H (lower) groups, no distinction is made between hemispheres; the lower plots are normalized by the maximum concentration of flocs. High and low concentrations are indicated by darker and lighter shading, respectively, and homogeneity (or lack of alignment) of moment direction is indicated by midtone shading over the entire stereographic projection (as in (c)). For the M group, small dark areas indicate that the majority of moments are well aligned with the applied field. Upper insets: schematic representations of three cases. Left: blue dots and red squares in stereographic projections represent individual floc directions from the M and H groups, respectively. The orange cross is the applied field direction. Right: blue and red arrows represent the recorded paleomagnetic inclinations for the M and H groups. The black arrow is the resultant, and Δ*I* is the inclination flattening. (a) For small floc sizes, most flocs are in group M; few flocs are in group H, and Δ*I* is small. (b) For larger floc sizes, more flocs are in group H and Δ*I* increases. (c) For the largest floc sizes, most flocs are in group H and are so large that they are oriented randomly with respect to the field. The small number of group M flocs is sufficient for Δ*I* to become small. The net magnetic moment decreases from (a) to (c) because of the less efficient alignment of increasingly larger flocs. Adapted from Roberts AP, Chang L, Heslop D, Florindo F, and Larrasoaña J (2012) Searching for single domain magnetite in the "pseudo-single-domain" sedimentary haystack: Implications of biogenic magnetite preservation for sediment magnetism and relative paleointensity determinations. *Journal of Geophysical Research* 117: B08104; Mitra R and Tauxe L (2009) Full vector model for magnetization in sediments. *Earth and Planetary Science Letters* 286: 535–545.

p0510 The work of deMenocal et al. (1990) called for a deep lock-in depth of up to ~16 cm for marine sediments based on a compilation of deep-sea sediment records with oxygen isotopes and the Matuyama–Brunhes boundary (MBB). However, Tauxe et al. (1996) updated the compilation with twice the number of records and, using the same logic, concluded that, on average, the magnetization is recorded within the top few centimeters. This is supported by coincidence of ^{10}Be production peak and relative paleointensity low during the Iceland Basin excursion in two ODP cores from the Atlantic Ocean (Knudsen et al., 2008).

p0515 Several papers have revived the deep lock-in debate (e.g., Bleil and von Dobeneck, 1999; Channell et al., 2004). The former used a complicated lock-in model to explain results not observed anywhere else (substantial reversely magnetized intervals in apparently late Brunhes age equatorial sediments). The latter noted that in North Atlantic drift deposits, the midpoint of the MBB is 'younger' isotopically than records with lower sedimentation rates, implying a deep lock-in. However, drift deposits by nature collect sediments from a large catchment area. A particular bit of plankton from the surface waters of the North Atlantic will be transported along the bottom for some time before it finds a permanent home in the drift. The age offset between the isotopic (acquired at the surface) and magnetic ages (acquired at the final point of deposition) obviates the need for a deep lock-in depth.

p0520 The most quoted examples of significant smoothing in natural sediments are those of Lund and Keigwin (1994) and Kent and Schneider (1995). On close examination, the evidence is weak. Lund and Keigwin (1994) postulated that the PSV record of the Bermuda Rise, western North Atlantic Ocean, was systematically subdued with respect to the PSV recorded in Lake St. Croix stemming from the observed difference in sediment accumulation rate, the Lake St. Croix record having been deposited at a rate several times that of the Bermuda Rise record. They suggested that smoothing the Lake St. Croix data with a 10 or 20 cm moving average window reproduced the Bermuda Rise data with high-frequency features smoothed out and the amplitude of variation significantly reduced. However, they ignored the age constraints available in the original St. Croix record. Tauxe et al. (2006) showed that a substantially better fit of the Bermuda data could be achieved when the available age constraints are used and no smoothing was required by the data.

p0525 The study of Kent and Schneider (1995) showed three records of relative paleointensity across the MBB and interpreted these in terms of sedimentary smoothing. These records came from low and moderate sediment accumulation rates. Hartl and Tauxe (1996) augmented the database of relative paleointensity records spanning the MBB with additional ten records obtained from a wide range of sediment accumulation rates and showed that the single low sedimentation rate core of

Kent and Schneider (V16-58) most probably had a poorly constrained timescale. Once again, little, if any, smoothing of sedimentary paleointensity records is required.

p0530   As sediments lose water and consolidate, compaction can have a strong effect on DRM intensity (e.g., Anson and Kodama, 1987). Consolidation is a continuous process starting from the sediment/water interface when sedimentary particles first gel (see, e.g., Figure 12(b)) and continuing until the sediment is completely compacted, perhaps as deep as hundreds of meters. The effect on magnetic remanence depends on volume loss during compaction, which depends largely on clay content, so clay-rich sediments will have the largest effect.

p0535   Recently, Suganuma et al. (2010, 2011) revived again the issue of lock-in depth and smoothing of remanence in postdepositional processes. They found a lock-in depth of $\sim$15 cm from within-core offsets of paleointensity minima at the Matuyama–Brunhes polarity transition between normalized remanence intensity and paleointensity estimated from cosmogenic nuclide ^{10}Be in three sediment cores from the Pacific Ocean with relatively low sedimentation rates, $\sim$20 m My^{-1} or less. Furthermore, they suggested that a Gaussian lock-in function, in which the rate of remanence lock-in increases in the middle of the lock-in zone, can explain the observation that indicates relatively little smoothing of the geomagnetic signals. When using an exponential lock-in function, which was often used for simulating remanence acquisition with sediment compaction and dewatering, the geomagnetic signals are overly smoothed.

p0540   The inevitable conclusion from this section is that, despite the long history of research in the matter, much remains to be learned for remanent magnetization acquisition processes of sediments. Nonetheless, sedimentary paleointensity remains a useful tool in high-resolution Quaternary geochronology, as summarized in a recent review by Roberts et al. (2013).

s0110   ### 107.4.3   Note on Aeolian Deposits

p0545   The theoretical and experimental foundations of relative paleointensity studies have all been done on waterborne sedimentary deposits. Nonetheless, it is clear that aeolian sediments, in particular, loess, can retain an NRM that appears to record the direction of the geomagnetic field (e.g., Heller and Liu, 1982). Details of how the geomagnetic field is impressed on loess deposits are not well known, but mechanisms must include viscous remanence, pedogenic modification (chemical remanence), and perhaps also a remanence acquired at dry deposition and postdepositional wetting (Spassov et al., 2003; Wang and Lovlie, 2010; Zhao and Roberts, 2010). What controls the intensity of remanence acquired during deposition of windblown dust is unknown, yet there have been several attempts to use the normalized remanence in loess as a proxy for geomagnetic intensity variations (e.g., Liu et al., 2005; Pan et al., 2001; Zhu et al., 1994). These studies rely heavily on the theoretical and experimental work developed for water-lain sediments (see also Spassov et al., 2003); theoretical and experimental efforts must be carried out for the mechanism involved in remanence acquisition in loess.

107.4.4   Normalization   s0115

Until now, we have considered only how magnetic moments   p0550 behave when placed in a magnetic field and are allowed to rotate freely. Paleointensity studies in sediments make the a priori assumption that DRM is quasilinear with the applied field (although as we have seen in the section on DRM theory, that is only true under certain circumstances). However, we have not yet considered the effect of changing the magnetic content of the sediment, which of course will have a profound effect on the intensity of the remanence. Such changes must be compensated for through some sort of normalization process (see, e.g., Kent, 1982). Methods of normalization were reviewed thoroughly by King et al. (1983) and Tauxe (1993), but there have been a few contributions to the subject published since. Here, we briefly summarize the most commonly used methods of normalization.

Most studies use some easily measured bulk magnetic   p0555 parameters such as saturation remanence (Johnson et al., 1948), magnetic susceptibility (χ, Harrison, 1966), and ARM (Johnson et al., 1975), which will compensate for changes in concentration of the magnetic minerals in a relatively crude way. Levi and Banerjee (1976) proposed a more sophisticated approach in which the natural remanence was partially demagnetized as was the anhysteretic remanent normalizer to ensure that the same coercivity fraction was used to normalize the remanence as was carrying the NRM. Following up on this line of reasoning, Tauxe et al. (1995) suggested that the NRM be normalized by ARM in a manner similar to the KTT experiments for thermal remanences using a technique known as 'pseudo-Thellier' normalization. King et al. (1983) reminded us that ARM itself is a strong function of concentration with higher magnetite concentrations being less efficient at ARM acquisition than lower concentrations. As a result, zones with   Au27 varying concentrations will be normalized differently (in effect, different α's in eqn [1]) and violate the fundamental assumptions of the method. More recently, Brachfeld and Banerjee (2000) proposed a secondary correction for normalized intensity that attempted to remove some of the nonlinear effects of the normalization process. Tauxe and Wu (1990) argued that if the power spectrum of the normalizer was coherent with the normalized remanence, the normalization process was insufficient. Constable et al. (1998) expanded on this idea, suggesting that the normalizer most coherent with the remanence should be used.

One of the important implications of the composite   p0560 floc model of DRM of Tauxe et al. (2006) described in Section 107.4.1 is that current methods of normalizing sedimentary records for changes in magnetic grain size and concentration do not account for changes in floc size and hence will be only partially effective in isolating the geomagnetic contribution to changes in DRM. This has practical implications in the role of climate in influencing relative paleointensity records. For example, changes in the clay content could well lead to differences in flocculation, which in turn could influence paleointensity with no observable change in the magnetic mineralogy apart from a change in concentration. Other 'stealth' influences could be miniscule changes in salinity of lakes, which could result in profound changes in the paleointensity recorded, with no means of detecting it. However, in stable environments with   Au28

TGP2: 00107

only small changes in magnetic mineralogy and concentration, we can only hope that the normalization procedures chosen will give records that are reasonably linear with the applied field.

p0565   Recently, it was revealed that magnetic mineral assemblages of pelagic sediments are often dominated by biogenic magnetite (Roberts et al., 2012; Yamazaki and Ikehara, 2012). Variations in the relative proportion of biogenic and terrigenous magnetic mineral components emerge as variations of ARM/ SIRM ratio (Yamazaki, 2012; Yamazaki and Ikehara, 2012), reflecting differences in grain-size distribution. Normalized intensities (with either ARM or IRM) sometimes correlate with ARM/SIRM ratios (Hoffmann and Fabian, 2009; Xuan and Channell, 2008a; Yamazaki et al., 2013), which suggests that neither ARM nor IRM can compensate well for variations in relative proportion of biogenic and terrigenous components and that such sediments are not suitable for relative paleointensity estimation. Using a regional group of sediment cores, Hoffmann and Fabian (2009) tried to correct for the influence of lithologic variations including those appearing as ARM/ SIRM ratio variations.

s0120   **107.5   Remagnetization**

p0570   Theoretical treatment of how rocks get magnetized and how that magnetization might be used for paleointensity studies assume that the remanence was blocked either thermally (Section 107.3) or depositionally (Section 107.4). Yet almost no NRM remains completely unchanged for long. Thermodynamics teaches us that all substances out of equilibrium with their environments will approach equilibrium as the energy available permits. Magnetic particles out of equilibrium with the magnetic field in which they sit are subject to magnetic viscosity. If they are out of chemical equilibrium, they will alter chemically. The former results in the acquisition of a viscous remanence and the latter a chemical one. These are discussed in more detail in Chapter 102. We will briefly describe their importance to paleointensity in the following.

s0125   **107.5.1   Magnetic Viscosity**

p0575   Returning to Figure 2, we see that magnetic moments can respond to external fields even if the magnetic crystal itself is fixed on timescales determined by the magnetic relaxation time τ. When the relaxation time is short relative to the time span of observation, the magnetization is in equilibrium with the external field and the particles are called 'superparamagnetic.' This means that magnetic particles have sufficient thermal energy to overcome intervening energy barriers and flip their magnetic moments from one easy direction to another. The energy barrier is in part controlled by the external field, with a lower threshold into the direction of the applied field than out of it. Therefore, magnetic moments will tend to 'pool' in the direction of the applied field.

p0580   The magnetization that is acquired in this isochemical, isothermal fashion is termed viscous remanent magnetization. With time, more and more grains will have sufficient thermal energy to overcome anisotropy energy barriers and flip their magnetizations to an angle more in alignment with the external field. The lower the value of τ, the quicker the approach to equilibrium.

p0585   According to eqn [2], relaxation time varies with external factors such as temperature (as seen in Figure 2) and applied field B and with factors specific to the magnetic particle such as volume and its intrinsic resistance to changing external fields reflected in its anisotropy constant K. In any natural substance, there will be a range of values for τ that could span from seconds (or less) to billions of years. It is interesting to note that a TRM is in effect the equilibrium magnetization (see, e.g., Yu and Tauxe, 2006) and TRMs will only be subject to magnetic viscosity if the field changes. DRMs, however, are typically one or two orders of magnitude less than the TRM that would be acquired in the same field and hence are almost never in equilibrium and therefore will nearly always be subject to viscous remagnetization, depending on the spectrum of τ values (see Kok and Tauxe, 1996a, for discussion).

s0130   **107.5.2   Chemical Alteration**

p0590   Geologic materials form in one environment (e.g., extruding red hot from the mouth of a volcano!) and wind up in quite different environments. Inevitably, they will break down as part of the rock cycle. Magnetic minerals are no exception and growth, alteration, and dissolution of magnetic minerals change the original remanence. The magnetization that is fixed by growth or alteration of magnetic minerals is termed chemical remanent magnetization, and while this too is controlled in part by the external magnetic field, the theory of how to normalize CRM to retrieve the geomagnetic signal has never been properly developed. In general, paleointensity studies strive to recognize CRMs and exclude such remanences from interpretation.

s0135   **107.6   Evaluating Paleointensity Data**

s0140   **107.6.1   Thermally Blocked Remanences**

p0595   A well-done paleointensity experiment allows us to test (1) whether the NRM was a single component magnetization, (2) whether alteration occurred during laboratory reheating, (3) whether blocking and unblocking were reciprocal, and (4) whether the TRM is a linear function of the applied field. Parameters can be calculated to provide measures of overall quality (scatter about the best-fit line, distribution of temperature steps, fraction of the NRM, etc.) of a given experiment. Some useful parameters are listed for convenience in Table 1. This subject has been debated rather intensely in the recent literature (e.g., Biggin et al., 2003; Kissel et al., 2004; Paterson et al., 2010; Shaar and Tauxe, 2013; Tauxe and Staudigel, 2004), and it appears that as yet there is no consensus on what constitutes a standard method for determining reliability. This is a rapidly developing field, so stay tuned.

s0145   **107.6.2   Depositional Remanences**

p0600   How can sedimentary relative paleointensity data be judged? Here are some thoughts:

TGP2: 00107

t0010   **Table 1**   Parameters

Parameter	Name	Definition/notes	References
$\lvert b \rvert$	Best-fit slope	Slope of pTRM acquired versus NRM remaining	Coe et al. (1978)
B_{anc}	Ancient field estimate	$\lvert b \rvert$ times the laboratory field	Coe et al. (1978)
β	Scatter parameter	Standard error of the slope over $\lvert b \rvert$	Coe et al. (1978)
Q	Quality factor	Combines several parameters	Coe et al. (1978)
VDS	Vector difference sum	Sum of vector differences of sequential demagnetization steps	Tauxe (1998)
F_{vds}	Fraction of the total NRM	Total NRM is VDS	Tauxe and Staudigel (2004)
δ_i	pTRM check	Difference between pTRM at pTRM check step at T_i	Tauxe and Staudigel (2004)
T_{max}	Maximum blocking temperature	Highest step in calculation of $\lvert b \rvert$	Tauxe and Staudigel (2004)
DRATS	Difference ratio sum	$\sum \delta_i$ normalized by pTRM (T_{max})	Tauxe and Staudigel (2004)
N_{pTRM}	Number of pTRM checks	Below T_{max}	Tauxe and Staudigel (2004)
Δ_i	pTRM tail check	Difference between NRMs remaining after the first and second zero-field steps	Tauxe and Staudigel (2004)
$MD\%$	Percent maximum difference	$100 \times$ maximum value of Δ_i/VDS	Tauxe and Staudigel (2004)
T	Orientation matrix	Matrix of sums of squares and products of demagnetization data	Tauxe (1998)
τ_i	Eigenvalues of **T**	$\tau_1 > \tau_2 > \tau_3$	Tauxe (1998)
$\mathbf{V}_i$	Eigenvectors of T	Best-fit direction is $\mathbf{V}_1$	Tauxe (1998)
MAD	Maximum angle of deviation	$\tan^{-1}(\sqrt{(\tau_2^2 + \tau_3^2)}/\tau_1)$	Kirschvink (1980)
DANG	Deviation angle	Angle between origin and $\mathbf{V}_1$	Tauxe and Staudigel (2004)

Source: Tauxe L (2006) Long term trends in paleointensity: The contribution of DSDP/ODP submarine basaltic glass collections. *Physics of the Earth and Planetary Interiors* 244: 515–529.

o0010   1. The NRM must be carried by a detrital phase of high magnetic stability. Furthermore, the portion of the natural remanent vector used for paleointensity should be a single, well-defined component of magnetization. The nature of the NRM can be checked with progressive demagnetization using AF and thermal techniques. Supplementary information from hysteresis and rock magnetic experiments can also be useful.

o0015   2. The detrital remanence must be an excellent recorder of the geomagnetic field and exhibit no inclination error, and if both polarities are present, the two populations should be antipodal. The associated directional data should therefore be plotted on equal area projections (or at least histograms of inclination) whenever possible.

o0020   3. Large changes in concentration (more than about an order of magnitude) and changes in magnetic mineralogy or grain size should be minimized. These changes can be detected with the use of biplots of, for example, IRM versus χ. Such biplots should be linear, with low scatter.

o0025   4. The relative paleointensity estimates that are coherent with bulk rock magnetic and lithologic parameters should be treated with caution. Coherence can be assessed using standard spectral techniques.

o0030   5. Records from a given region should be coherent within the limits of a common timescale. Whenever possible, duplicate records should be obtained and compared.

o0035   6. For a relative paleointensity record to have the maximum utility, it should have an independent timescale. Many deep-sea sediment records are calibrated using oxygen isotopic curves or magnetostratigraphic age constraints (or

both). Lake sediments are more difficult to date and rely for the most part on radiocarbon ages.

107.7   Current State of the Paleointensity Data   s0150

107.7.1   Paleomagnetic Databases   s0155

p0635   There has been an enormous effort in collecting and preserving paleomagnetic data since the early 1960s (e.g., Irving, 1964), but since the 1987 meeting of the IAGA in Vancouver, the effort has been more concerted with seven IAGA-sponsored databases. Absolute paleointensities have been assembled in a series of compilations by Tanaka and Kono (1994), Tanaka et al. (1995a,b), Perrin and Shcherbakov (1997), Perrin et al. (1998), Perrin and Schnepp (2004), Tauxe and Yamazaki (2007), and Biggin (2010). In their assessment of the most recent release of the absolute paleointensity database, Perrin and Schnepp (2004) stated:

> For the future, a harmonization or a combination of all IAGA databases would be desirable. Furthermore, the input of raw data at the specimen level would be useful in order to allow reinterpretation of data with more developed and sophisticated methods based on our increasing understanding of rock magnetism.   dq0010

p0640   In order to address this widely felt sentiment, the MagIC database was created and is accessible at http://earthref.org/MAGIC/. This database has merged several of the existing IAGA databases and allows for data ranging from original magnetometer output (including magnetometer, hysteresis,

thermomagnetic, susceptibility, and other measurements) and their interpretations. Detailed descriptions of the data are possible by using 'method codes.' The database is constantly updated to include data as they are published and existing entries are inspected for errors and corrected. The absolute paleointensity database can be accessed through the MagIC website by searching on the method code 'LP–PI–TRM' (lab protocol–paleointensity–thermal remanence). The search for data for the period from 50 ka to 200 Ma can be retrieved at http://earthref.org/MAGIC/search#1382302391017. We will call this PINT13 in the following.

p0645   The data in the databases include information on geographic location (see map of data locations in **Figure 16(a)**), rock type and age of the sampling sites, type of paleointensity experiment, the remanence vector (including direction if available), and summary statistics such as the standard deviation of replicate specimens from a given cooling unit. In many cases, the database includes even the measurement data. If no measurement data are available, we may know that, for example, pTRM checks were performed (e.g., studies with pTRM listed under alteration check), but we do not know whether they 'passed' any particular criterion. The only reliability criterion

included is the standard deviation of the replicate measurements from a given cooling unit. Because there are many useful reliability criteria for judging paleointensity data (see **Section 107.6**), efforts should be made to update the contributions in the MagIC database to include as many of these as are available.

Perrin and Schnepp (2004) ably summarized the characteristics of the PINT03 database and we will not repeat their analysis here. Nonetheless, it is useful to reiterate that most of the data come from the last million years and are from the northern hemisphere. The temporal bias is particularly egregious when only the most 'reliable' data are used (i.e., that employed TRM normalization with pTRM checks).   p0650

There was no IAGA database for relative paleointensity data (except those included in the TRANS database) prior to the compilation of Tauxe and Yamazaki (2007). As a step toward rectifying this problem, they summarized the published literature with relative paleointensity data in **Table 2**. Locations of records are shown in **Figure 16(b)**. There are data from nearly 100 references and contributed them to the MagIC database (obtainable individually through the original reference or collectively through this reference). We refer to this compilation   p0655
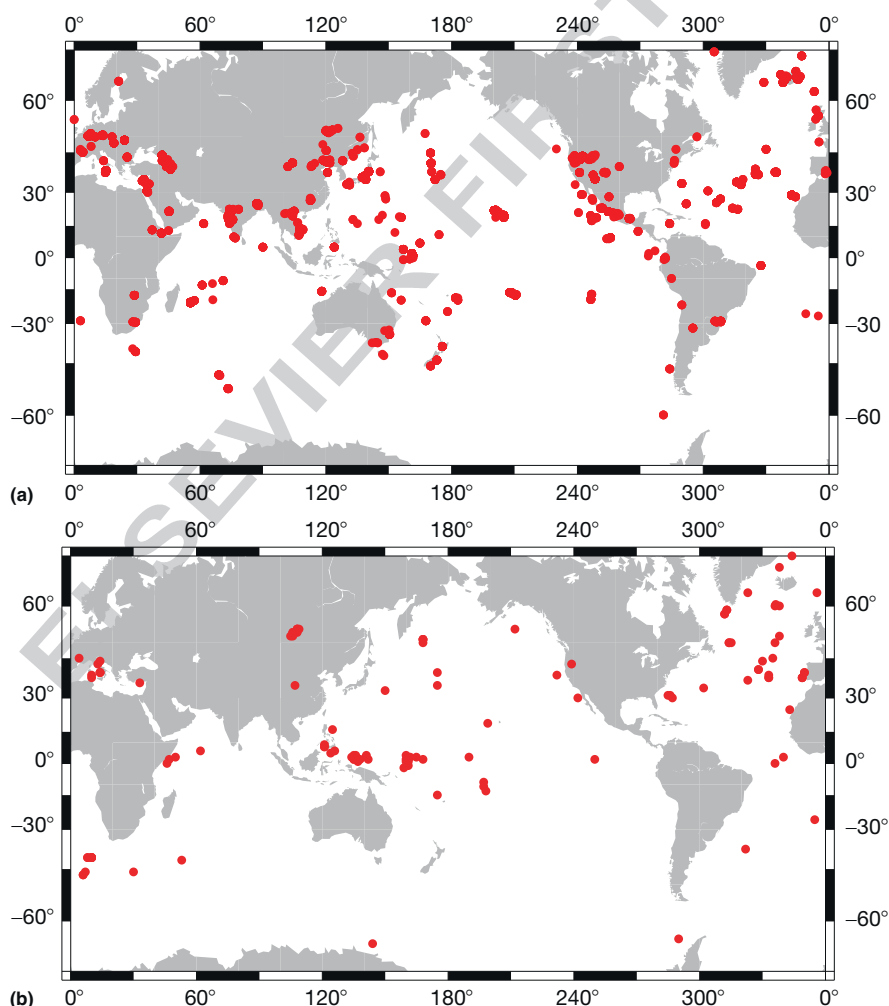
f0085   **Figure 16**   Locations of all paleointensity data in the (a) absolute (PINT13) and (b) relative (SEDPI06) databases compiled for this paper.

TGP2: 00107

t0015   **Table 2**   Summary of relative paleointensity records

Record	Latitude/ longitude	Age range	Dating methods	Comp.	TS	References
10-pc03[a]	−47/6	23–115 ka	RPI	Stoner et al. (2002)	Martinson et al. (1987)	Channell and Kleiven (2000), Stoner et al. (2002)
1010[a]	30/−118	19–2036 ka	POL, MS	Guyodo and Valet (2006)	Bassinot et al. (1994), Cande and Kent (1995)	Hayashida et al. (1999), Leonhardt et al. (1999)
1021[a,b]	39/−128	13–1562 ka	POL	Guyodo and Valet (1999)	Cande and Kent (1995), Bassinot et al. (1994)	Guyodo et al. (1999), Leonhardt et al. (1999)
1089[a]	−41/10	20–578 ka	δ^{18}O	Stoner et al. (2002)	Martinson et al. (1987)	Stoner et al. (2003)
1092	−46/7	5.9–3.5 Ma	POL		Cande and Kent (1995)	Evans and Channell (2003)
1101[a,b]	−64/−70	706–1105 ka	POL, MS, δ^{18}O	Guyodo and Valet (2006)	Cande and Kent (1995), Shackleton et al. (1990)	Guyodo et al. (2001)
21-pc02[a]	−41/8	0–81 ka	δ^{18}O	Stoner et al. (2002)	Martinson et al. (1987)	Channell and Kleiven (2000), Stoner et al. (2002, 2003)
305-a5[a]	53/106	0–11 ka			Martinson et al. (1987)	Peck et al. (1996)
337-t2[a]	53/106	13–84 ka	RPI		Martinson et al. (1987)	Peck et al. (1996)
4-pc03[a]	−41/10	9–44 ka	RPI	Stoner et al. (2002)	Martinson et al. (1987)	Channell and Kleiven (2000), Stoner et al. (2002)
5-pc01[a]	−41/10	8–64 ka	RPI	Stoner et al. (2002)	Martinson et al. (1987)	Channell and Kleiven (2000), Stoner et al. (2002)
522[a]	−26/−5	22.8–34.7 Ma	POL		Cande and Kent (1995)	Tauxe and Hartl (1997)
606a[a]	37/323	773–792 ka	POL	Hartl and Tauxe (1996)	Cande and Kent (1995)	Clement and Kent (1986)
609b[a]	50/336	777–825 ka	POL	Hartl and Tauxe (1996)	Cande and Kent (1995)	Hartl and Tauxe (1996)
664d[a]	0/336	670–807 ka	POL	Hartl and Tauxe (1996)	Cande and Kent (1995)	Valet et al. (1989
665a[a]	3/340	770–817 ka	POL	Hartl and Tauxe (1996)	Cande and Kent (1995)	Valet et al. (1989
767[a,b]	5/124	601–1518 ka	POL	Guyodo and Valet (2006)	Cande and Kent (1995)	Guyodo and Valet (2006), Schneider et al. (1992)
767b[a]	5/124	759–829 ka	POL	Guyodo and Valet (2006)	Cande and Kent (1995)	Guyodo and Valet (2006), Schneider et al. (1992)
768a[a]	8/121	5–94 ka	δ^{18}O, ^{14}C	Guyodo and Valet (1999)	Linsley and Thunnell (1990), Tiedemann et al. (1994)	Schneider and Mello (1996)
768b[a]	8/121	9–130 ka	δ^{18}O, ^{14}C	Guyodo and Valet (1999)	Linsley and Thunnell (1990), Tiedemann et al. (1994)	Schneider and Mello (1996)
769[a]	9/121	5–831 ka	δ^{18}O, ^{14}C	Guyodo and Valet (1999)	Linsley and Thunnell (1990), Shackleton et al. (1990), Tiedemann et al. (1994)	Schneider (1993), Schneider and Mello (1996)
803a[a,b]	2/161	783–2178 ka	POL	Guyodo and Valet (2006)	Cande and Kent (1995)	Kok and Tauxe (1999)
803b[a,b]	2/161	1487–2786 ka	POL	Guyodo and Valet (2006)	Cande and Kent (1995)	Kok and Tauxe (1999)
804c[a]	1/161	1448–1470 ka	POL	Hartl and Tauxe (1996)	Cande and Kent (1995)	Hartl and Tauxe (1996)
805b[a]	1/160	770–821 ka	POL	Hartl and Tauxe (1996)	Cande and Kent (1995)	Hartl and Tauxe (1996)
848–851[a]	2/−110	34–4035 ka	POL	Guyodo and Valet (1999)	Cande and Kent (1995)	Valet and Meynadier (1993)
877[a]	54/−148	9.4–11.3 Ma	POL		Cande and Kent (1995)	Bowles et al. (2003)
882b	50/168	0–200 ka	∼		Shackleton et al. (1990)	Okada (1995)

TGP2: 00107

Table 2 (Continued)

Record	Latitude/ longitude	Age range	Dating methods	Comp.	TS	References
883	51/168	15–200 ka	δ^{18}O		Shackleton et al. (1990)	Roberts et al. (1997)
884	51/168	15–200 ka	MS		Shackleton et al. (1990)	Roberts et al. (1997)
884[a,b]	51/168	9.9–10.3 Ma	POL		Cande and Kent (1995)	Roberts and Lewin-Harris (2000)
983[a,b]	60/−24.1	0–1889 ka	POL, δ^{18}O	Guyodo and Valet (2006), Laj et al. (2000)	Cande and Kent (1995), Shackleton et al. (1990)	Channell (1999), Channell et al. (1997, 1998, 2000, 2002, 2004)
984[a,b]	60.4/−23.6	0–2151 ka	POL, δ^{18}O		Cande and Kent (1995), Shackleton et al. (1990)	Channell et al. (1998, 2002, 2004)
Chewaucan	43/−121	65–102 ka	^{14}C, ThL			Roberts et al. (1994)
Sed-17aK[a]	25/−17	9–224 ka	δ^{18}O		1984	Haag (2000)
ch88-10p[a]	30/−73	10–70 ka			Martinson et al. (1987)	Schwartz et al. (1996)
ch88-11p	31/−74	10–70 ka	∼		Martinson et al. (1987)	Schwartz et al. (1996)
ch89-1p	31/−75	12–71 ka	∼		Martinson et al. (1987)	Schwartz et al. (1998)
con-01-603-2	54/109	10–200 ka	POL, ^{14}C, ∼			Demory et al. (2005)
con-01-604-2	52/106	0–60 ka	ARM			Demory et al. (2005)
con-01-605-3	52/105	0–40 ka	ARM			Demory et al. (2005)
ded8707[a]	40/14	10–60 ka	ash	Guyodo and Valet (1999)	1984	Tric et al. (1992)
ded8708	40/14	40–80 ka	ash		1984	Tric et al. (1992)
e113p[a,b]	−2/159	4–380 ka	δ^{18}O	Guyodo and Valet (2006)	Bassinot et al. (1994)	Tauxe and Wu (1990)
hu90-013-012	59/−47	10–110 ka	RPI, δ^{18}O, ^{14}C			Stoner et al. (1995)
hu90-013-013	58/−48	10–110 ka	RPI, ^{14}C			Stoner et al. (1995)
hu91-045-094	50/−45	10–110 ka	RPI, δ^{18}O, ^{14}C			Stoner et al. (1995)
ket8251[a]	40/14	8–95 ka	ash	Guyodo and Valet (1999)	1984	Tric et al. (1992)
kh73-4-7	3/165	0–2000 ka	POL			Sato and Kobayashi (1989)
kh73-4-8	2/168	0–2000 ka	POL			Sato and Kobayashi (1989)
kh90-3-5	4/160	32–1159 ka	POL		Cande and Kent (1995)	Sato et al. (1998)
kk78-030[a]	19/−161	601–1785 ka	POL	Guyodo and Valet (2006)	Cande and Kent (1995)	Laj et al. (1996a,b)
kr9912-pc2[a]	−11/−163	1003–3000 ka	POL, ARM		Cande and Kent (1995), Lisiecki and Raymo (2005)	Yamazaki and Oda (2005)
kr9912-pc4[a]	−13/−162	2002–2845 ka	POL		Cande and Kent (1995), Lisiecki and Raymo (2005)	Yamazaki and Oda (2005)
kr9912-pc5[a]	−9/−163	1295–2118 ka	POL		Cande and Kent (1995), Lisiecki and Raymo (2005)	Yamazaki and Oda (2005)
ks87-752[a,b]	−38/−38	311–1023 ka	POL, MS	Guyodo and Valet (1999)	Cande and Kent (1995)	Valet et al. (1994)
lc07[a]	38/10	754–1033 ka	POL, ∼	Guyodo and Valet (2006)	Shackleton et al. (1990)	Dinares-Turell et al. (2002)
ldb[a]	45/4	20–308 ka	MS, ^{14}C		Dansgaard et al. (1993)	Thouveny et al. (1994), Williams et al. (1998)
Massicore	44/14	32–35 Ma	POL		Cande and Kent (1995)	Lanci and Lowrie (1997)
md01-2440	38/−11	2–400 ka	RPI, MS		Martinson et al. (1987)	Thouveny et al. (2004)
md01-2441	38/−11	30–54 ka	RPI, MS		Martinson et al. (1987)	Thouveny et al. (2004)

Au8

(*Continued*)

TGP2: 00107

Table 2   (Continued)

Record	Latitude/ longitude	Age range	Dating methods	Comp.	TS	References
md84-528	−42/53	15–80 ka	δ^{18}O		1984	Tric et al. (1992)
md84-629	36/33	15–62 ka	δ^{18}O		1984	Tric et al. (1992)
md85-668[a]	0/46	21–187 ka	δ^{18}O	Guyodo and Valet (1999)	Martinson et al. (1987)	Meynadier et al. (1992)
md85-669[a]	2/47	20–138 ka	RPI	Guyodo and Valet (1999)	Martinson et al. (1987)	Meynadier et al. (1992)
md85-674[a]	3/50	18–138 ka	RPI	Guyodo and Valet (1999)	Martinson et al. (1987)	Meynadier et al. (1992)
md90-0940[a]	6/62	108–1954 ka	POL, MS, fossils	Guyodo and Valet (1999)	Cande and Kent (1995)	Meynadier et al. (1994)
md95-2009[a]	63/−4	10–76 ka	ARM	Laj et al. (2000)	Grootes and Stuiver (1997)	Kissel et al. (1999), Laj et al. (2000)
md95-2024[a]	50/−46	1–117 ka	MS, δ^{18}O	Stoner et al. (2000)	Bender et al. (1994)	Stoner et al. (2000)
md95-2034[a]	34/−58	12–76 ka	ARM	Laj et al. (2000)	Grootes and Stuiver (1997)	Kissel et al. (1999), Laj et al. (2000)
md95-2039	40/−10	0–320 ka	δ^{18}O, ^{14}C		Martinson et al. (1987)	Thouveny et al. (2004)
md95-2042	40/−10	32–160 ka	δ^{18}O, ^{14}C		Martinson et al. (1987)	Thouveny et al. (2004)
md97-2140[a,b]	2/142	568–1465 ka	POL		Cande and Kent (1995)	Carcaillet et al. (2003)
md97-2143[a,b]	16/125	601–2226 ka	POL, δ^{18}O	Guyodo and Valet (2006)	Cande and Kent (1995), Laskar et al. (1993)	Horng et al. (2003)
md98-2181[a]	6/126	12–660 ka	δ^{18}O, ^{14}C		Sowers et al. (1993)	Stott et al. (2002)
md98-2183[a,b]	2/135	20–1193 ka	POL, MS, ARM	Yamazaki and Oda (2005)	Cande and Kent (1995), Lisiecki and Raymo (2005)	Yamazaki and Oda (2005)
md98-2185[a,b]	3/134	9–2256 ka	POL, MS, ARM	Guyodo and Valet (2006)	Cande and Kent (1995), Lisiecki and Raymo (2005)	Yamazaki and Oda (2005)
md98-2187[a,b]	4/135	51–3053 ka	POL, MS, ARM		Cande and Kent (1995), Lisiecki and Raymo (2005)	Yamazaki and Oda (2005)
md99-2334	38/−11	0–38 ka	RPI		Martinson et al. (1987)	Thouveny et al. (2004)
ngc16[a]	2/135	2–191 ka	MS	Guyodo and Valet (1999)	Martinson et al. (1987)	Yamazaki and Ioka (1994)
ngc26[a]	3/135	1–120 ka	MS	Guyodo and Valet (1999)	Martinson et al. (1987)	Yamazaki and Ioka (1994)
ngc29[a]	4/136	2–192 ka	MS	Guyodo and Valet (1999)	Martinson et al. (1987)	Yamazaki and Ioka (1994)
ngc36[a]	−1/161	1–546 ka	δ^{18}O	Guyodo and Valet (1999)	1984, Bassinot et al. (1994)	Yamazaki et al. (1995)
ngc38[a]	−15/175	9–406 ka	δ^{18}O	Guyodo and Valet (1999)	1984, Bassinot et al. (1994)	Yamazaki et al. (1995)
ngc65[a]	35/175	6–635 ka	S		Bassinot et al. (1994)	Yamazaki (1999)
ngc69[a,b]	40/175	7–881 ka	S		Bassinot et al. (1994)	Yamazaki (1999)
np35[a]	4/141	127–798 ka	δ^{18}O	Guyodo and Valet (1999)	1984, Bassinot et al. (1994)	Yamazaki et al. (1995)
np5[a]	1/137	8–196 ka	δ^{18}O	Guyodo and Valet (1999)	Martinson et al. (1987)	Yamazaki and Ioka (1994)
np7[a]	2/138	6–199 ka	MS	Guyodo and Valet (1999)	Martinson et al. (1987)	Yamazaki and Ioka (1994)
p012[a]	59/−47	14–177 ka	RPI	Guyodo and Valet (1999)	Guyodo and Valet (1999)	Stoner et al. (1998)
p013[a]	58/−48	14–277 ka	RPI	Guyodo and Valet (1999)	Guyodo and Valet (1999)	Stoner et al. (1998)
p094[a]	50/−46	2–111 ka	RPI	Guyodo and Valet (1999)	Guyodo and Valet (1999)	Stoner et al. (1998)

(*Continued*)

TGP2: 00107

Table 2 (Continued)

Record	Latitude/ longitude	Age range	Dating methods	Comp.	TS	References
p226[a]	3/−170	41−780 ka	POL	Guyodo and Valet (1999)	Cande and Kent (1995)	Yamazaki et al. (1995)
ps1535-10	79/2	0−100 ka	^{14}C			Nowaczyk et al. (2003)
ps1535-6	79/2	0−100 ka	^{14}C			Nowaczyk et al. (2003)
ps1535-8	79/2	0−100 ka	^{14}C			Nowaczyk et al. (2003)
ps1707-2	73/−14	0−80 ka	MS		Martinson et al. (1987)	Nowaczyk and Antonow (1997)
ps1852-2[a]	70/−16	4−283 ka	MS		1984,Martinson et al. (1987)	Nowaczyk and Frederichs (1999)
ps1878-3	73/−9	0−100 ka	^{14}C			Nowaczyk et al. (2003)
ps1878-3	73/−10	0−45 ka	δ^{18}O, ^{14}C		Martinson et al. (1987)	Nowaczyk and Antonow (1997)
ps2138-1	82/31	10−75 ka	δ^{18}O, ^{14}C			Nowaczyk and Knies (2000)
ps2644-5[a]	68/−22	12−76 ka	ARM	Laj et al. (2000)	Grootes and Stuiver (1997)	Kissel et al. (1999), Laj et al. (2000)
rc10-167[a]	33/150	11−781 ka	POL	Guyodo and Valet (1999), Hartl and Tauxe (1996)	Cande and Kent (1995)	Kent and Opdyke (1977)
rndb75p[a]	2/160	124−668 ka	δ^{18}O	Guyodo and Valet (1999)	1984,Shackleton et al. (1990)	Tauxe and Shackleton (1994)
su90-24[a]	63/−37	11−76 ka	ARM	Laj et al. (2000)	Grootes and Stuiver (1997)	Kissel et al. (1999), Laj et al. (2000)
su90-33[a]	60/−22	12−76 ka	ARM	Laj et al. (2000)	Grootes and Stuiver (1997)	Kissel et al. (1999), Laj et al. (2000)
su9003	41/−32	10−240 ka	Color		Pisias et al. (1984)	Weeks et al. (1995)
su9004	41/−32	0−240 ka	Color		Pisias et al. (1984)	Weeks et al. (1995)
su9008	44/−30	10−180 ka	δ^{18}O		Pisias et al. (1984)	Weeks et al. (1995)
su9039	52/−22	0−240 ka	δ^{18}O		Pisias et al. (1984)	Weeks et al. (1995)
su92-17[a]	39/−27	4−280 ka	Color		Martinson et al. (1987)	Lehman et al. (1996)
su92-18[a]	38/−27	4−280 ka	δ^{18}O	Guyodo and Valet (1999)	Martinson et al. (1987)	Lehman et al. (1996)
su92-19[a]	38/−27	4−279 ka	Color	Guyodo and Valet (1999)	Martinson et al. (1987)	Lehman et al. (1996)
v16-58[a]	−46/30	767−770 ka	POL	Hartl and Tauxe (1996)	Cande and Kent (1995)	Kent and Schneider (1995)
ver98-1-1	53/108	20−60 ka	ARM			Demory et al. (2005)
ver98-1-14	54/108	0−350 ka	ARM			Demory et al. (2005)
ver98-1-3	54/108	50−250 ka	ARM			Demory et al. (2005)
ver98-1-6[a]	54/108	65−235 ka	Silica		Martinson et al. (1987)	Oda et al. (2002)
Kotsiana	36/24	−				Laj et al. (1996b)
Lingtai[a]	35/107	10−73 ka	MS, ^{14}C, ThL			Pan et al. (2001)
Potamida	36/24	−				Laj et al. (1996b)
lr[a,b]	43/13	90−94.9 Ma	POL, fossils		Stratigraphy (2004)	Cronin et al. (2001)
WEGAstack	−65/144	0−800 ka	RPI, ^{14}C, fossils			Macri et al. (2005)
MBstack[a]	3/162	32−1159 ka	POL	Guyodo and Valet (2006)	Cande and Kent (1995)	Sato et al. (1998)
PMstack[a]	39/10	0−402 ka	RPI, δ^{18}O, ^{14}C		Martinson et al. (1987)	Thouveny et al. (2004)
NAstack[a]	45/−25	10−250 ka	δ^{18}O		Pisias et al. (1984)	Weeks et al. (1995)

[a]Submitted to the MagIC database.

[b]Ages recalculated.

Dating methods: RPI: relative paleointensity; POL: polarity stratigraphy; MS: correlation of magnetic susceptibility; ARM: correlation of ARM; carb.: correlation of calcium carbonate; ash: tephrostratigraphy; color: correlation of color; δ^{18}O: oxygen isotopes; ^{14}C: radiocarbon; $\sim$: correlation of some unspecified wiggle; ThL: thermoluminescence; S: correlation of high to low coercivity IRM; silica: correlation of silica variations; fossil: correlation based on fossils.

of relative paleointensity data as SEDPI06 in the following. Authors are encouraged to contribute or augment their own data in the database. In **Section 107.8**, we will discuss the highlights of the available paleointensity data from both the PINT13 (absolute) and SEDPI06 (relative) compilations. Before we discuss the global data set, we will first describe methods of converting to virtual dipole moment (VDM).

s0160   107.7.2   Conversion to VDM

s0165   107.7.2.1   Absolute paleointensity data

p0660   The intensity of the magnetic field varies by a factor of two from equator to pole simply as a result of a dipole source, so data from different latitudes must be normalized to take this inherent dipole variation into account. In the following, we discuss methods for converting intensities to 'virtual dipole moments' in both absolute and relative paleointensity data sets.

p0665   There are several ways to calculate equivalent dipole moments for paleointensity data. Early studies tended to present a given intensity result as a ratio with some expected field. For example, Thellier and Thellier (1959) normalized intensity data to a reference inclination of 65°, using the paleomagnetically determined inclination and the relationship between inclination and field strength expected from a magnetic dipole. Most studies published over the last few decades, however, express paleointensity in terms of the equivalent geocentric dipole moment, which would have produced the observed intensity at that (paleo)latitude. There are two ways in which this is done, the VDM (**Figure 17(a)**) and the virtual axial dipole moment (VADM; **Figure 17(b)**). The VDM (Smith, 1967) is the moment of a geocentric dipole that would give rise to the observed magnetic field vector at location P. (The piercing point on the surface of the globe of this moment is the virtual geomagnetic pole or VGP.) To get the VDM, we first calculate the magnetic (paleo)colatitude θ_m from the observed inclination I and the so-called dipole formula ($\tan I = 2 \cot \theta_m$). Then, assuming a centered (but not axial) magnetic dipole with moment VDM, we have

$$VDM = \frac{4\pi r^3}{\mu_o} B_{anc} \left(1 + 3\cos^2 \theta_m\right)^{-1/2} \qquad [11]$$

p0670   The VDM calculation requires a good estimate for the inclination, which is not always available, especially when unoriented specimens are used. In such cases, it may be possible to use either the site (co)latitude or a paleo(co)latitude estimated by a plate reconstruction in the place of magnetic colatitude in eqn [11]. This moment is known as the virtual axial dipole moment (Barbetti, 1977). [Au32]

p0675   In order to compare the two forms of normalization, we selected data from the PINT13 database for the last 200 My that (1) were obtained with thermal normalization and used pTRM checks and (2) had multiple specimens that had standard deviations < 15% of the mean or were less than 5 μT. We estimated paleolatitudes for the sampling sites using the global apparent polar wander paths of Besse and Courtillot (2002) and used these to calculate VADMs for many sites. We show the two estimates of dipole moment in **Figure 17(c)**; the two are essentially equivalent representations.

p0680   It is important to note here that neither VDMs nor VADMs actually represent the true dipole moment (see Korte and Constable, 2005). They do not take into account the rather substantial effect of the nondipole field contributions and in fact overestimate the true dipole moment based on an evaluation of data for the last 7000 years.

107.7.2.2   Relative paleointensity data   s0170

p0685   Sedimentary paleointensity data are at best 'relative' paleointensity. Nonetheless, several studies have attempted to calibrate relative paleointensity data into a quasiabsolute form and cast them as 'VADMs' in order to compare them with the igneous data sets. There are different strategies for accomplishing this conversion (see **Figure 18**): setting the 'floor' to some minimum value expected for the field (Constable and Tauxe, 1996), setting parts of the sedimentary record to be equal to coeval igneous records (e.g., Guyodo and Valet, 1999; Valet et al., 2005), and setting the mean value to be some assumed value.

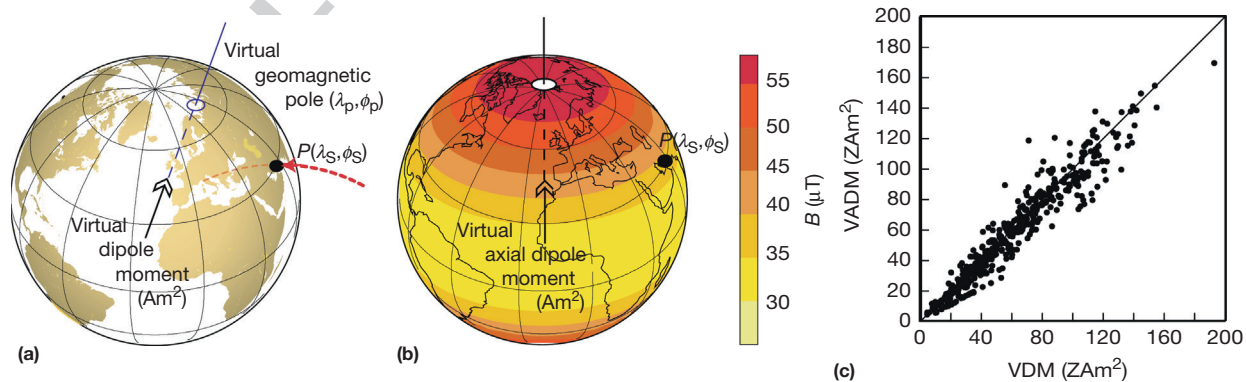f0090   **Figure 17**   (a) The virtual dipole moment (VDM) is the geocentric dipole that would give rise to the observed geomagnetic field vector at the location P. λ_s, ϕ_s are the site latitude and longitude, respectively. (b) The virtual axial dipole moment is the geocentric axial dipole that would give rise to the observed intensity at P. (c) Comparison of VDM and VADM for paleointensity data (see text).
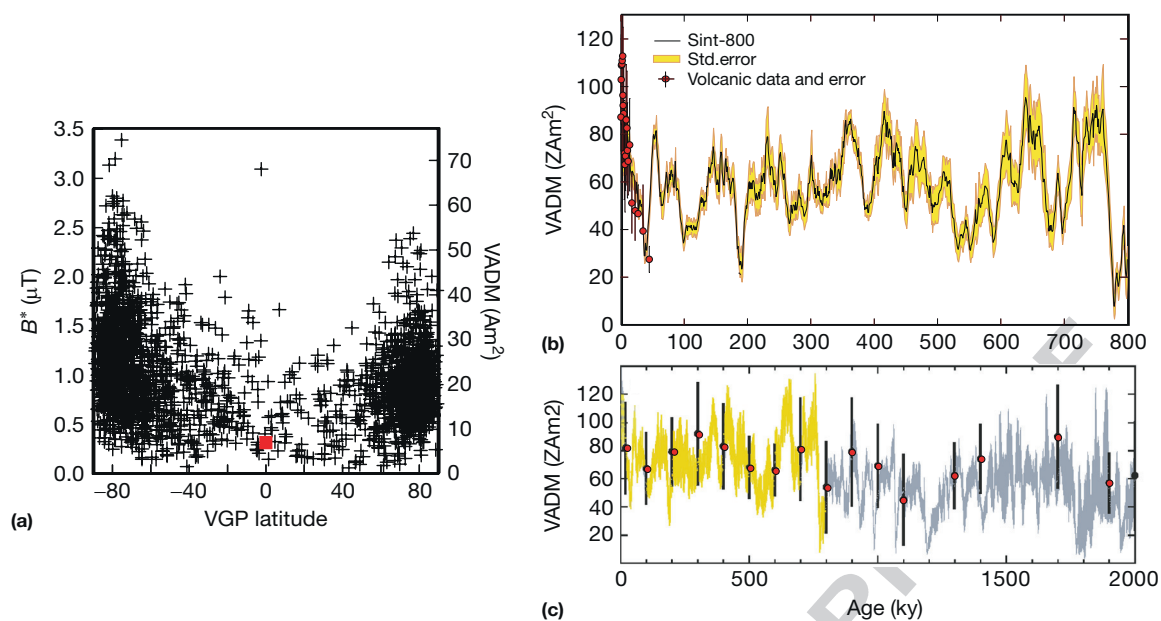
TGP2: 00107

f0095   **Figure 18**   Calibration of sedimentary relative paleointensity data to quasiabsolute values. (a) Approach of Constable and Tauxe (1996) on relative paleointensity data from the Oligocene record at DSDP Site 522. Data associated with transitional fields (low virtual geomagnetic pole (VGP) latitudes) are assumed to be on average 7.5 μT, the value of the present average non-GAD field. This inverts the relative intensity data to μT. Taking a paleolatitude of 32°, Tauxe and Staudigel (2004) converted these data to VADM using eqn [12]. (b) Stacked record of relative paleointensity data spanning the last 800 ky (SINT-800) of Guyodo and Valet (1999). They used the VADM data from contemporaneous lava flows to calibrate the record to VADM. (c) Similar to (b) but data span the last 2 My (SINT-2000) from Valet et al. (2005). They used averages of the PINT03 database (red dots) to calibrate the SINT record to VADM.

p0690   In the Constable and Tauxe (1996) method, the nonaxial dipole field is assumed to be on average 7.5 μT as it is for the present field. Reasoning that because the axial dipole must go through zero in a polarity transition, the average transitional field should be about 7.5 μT. **Figure 18(a)** illustrates an application of this method to calibrate the Oligocene relative paleointensity data from DSDP Site 522 of Tauxe and Hartl (1997; see **Table 2**) into VADM values. Setting the average value of the intensity in transitional records (red square in **Figure 18(a)**) to a value of 7.5 μT calibrates the entire record to B^* in μT. Assuming a paleolatitude of 32° S allows these B^* values to be converted to VADM values using eqn [11]. The problem with this method is that it is extremely sensitive to the choice of the nonaxial dipole field 'floor' value, which is not known for ancient times. Small changes in the choice of floor result in large changes for the calibrated record. Channell et al. (2009) followed Constable and Tauxe (1996) for calibrating their PISO-1500 stack, which covers for the last 1.5 My with sediment cores of relatively high sedimentation rates mainly from the North Atlantic Ocean.

p0695   A different approach was taken by Guyodo and Valet (1999) who collected together many relative paleointensity records spanning the last 800 ky (Guyodo and Valet, 1999). The 'SINT-800' stack (see **Figure 18(b)**) overlapped a sequence of absolute paleointensity data whose ages were well known (red dots). These absolute data were used to calibrate the SINT-800 stack into VADM. Valet et al. (2005) extended the relative paleointensity stack to span the last 2 My (see **Figure 18(c)**). In this latest version, known as the SINT-2000 stack (a subset of the records compiled in Guyodo and Valet (2006)), they took the global paleointensity data in the PINT03 database (with no selection

criteria) and averaged them in 100 000-year bins (red dots). These were used to convert the SINT-2000 stack to VADM values. The two calibrations are somewhat different, with the latter version being higher on average. Ziegler et al. (2011) also combined relative and absolute paleointensity data but in a different way; they constructed the PADM2M time-varying axial dipole intensity model over the last 2 My based on a penalized maximum likelihood inversion procedure using a joint set of absolute paleointensity data and relative paleointensity time series.

p0700   Because amplitudes of relative paleointensity records must be related to latitude, it is preferable to convert individual records to VADM prior to stacking, instead of stacking first and then converting to VADM. However, the 'floor setting' method of Constable and Tauxe (1996) required transitional data, which are not always available, and has severe drawbacks of its own as mentioned before.

107.8   Discussion   s0175

p0705   In the following, we will discuss some of the 'hot topics' in paleointensity. The issues for many of these are still under debate and conclusions are still tentative. Nonetheless, the spirit of this volume is to present the 'state of the field' and we will endeavor to do so.

107.8.1   Selection Criteria from the PINT13 Database   s0180

p0710   For the purpose of this discussion, we plot all the available data from the PINT13 database as white triangles and those that had standard deviations either ≤5 μT or 15% of the mean as green
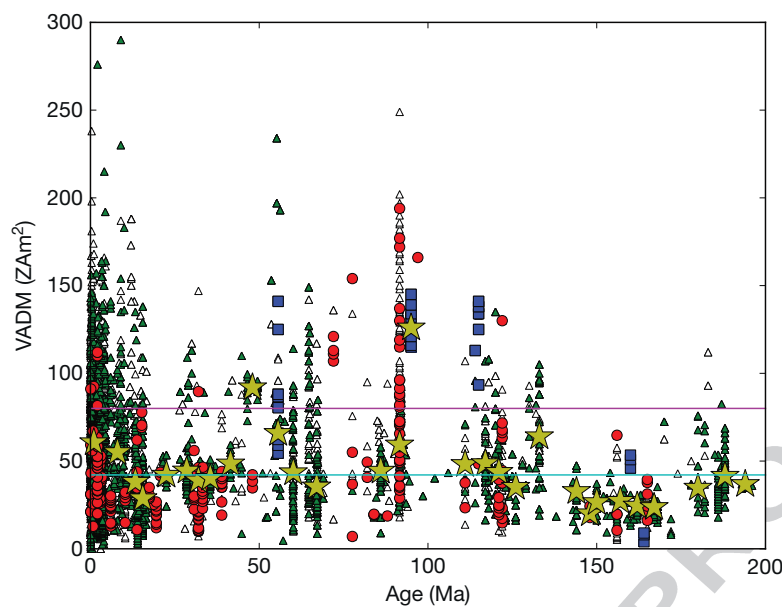
f0100   **Figure 19**   Summary of published data downloaded from the MagIC database for the last 200 Ma. Red dots are submarine basaltic glass data. Blue squares are single crystal results. Triangles are all other data and the light green triangles meet the consistency criteria ($<$15% of mean or $<$5 μT); VADMs calculated using the paleolatitudes indicated in the database (model_lat) for data points older than 5 Ma. Magenta dashed line is present field and solid cyan line is long-term stable value for the last 140 Ma. Modified from Tauxe L, Gee JS, Steiner M, and Staudigel H (2013) Paleointensity results from the Jurassic: New constraints from submarine basaltic glasses of ODP Site 801C. *Geochemistry, Geophysics, Geosystems*. http://dx.doi.org/10.1002/ggge.20282.

triangles in **Figure 19**. Data that came from submarine basaltic glass are marked as red circles, while those from single crystals are blue squares. Following the treatment of Tauxe et al. (2013), we calculate median values for 5 My bins for bins with at least ten reliable data points (green triangles); these are shown as stars. The median value of all the median values is 42 ZAm^2 (shown as the solid cyan line) and the present field value is shown as the dashed magenta line.

p0715   There are a total of 4475 cooling unit averages with an estimate for either VADM or VDM, of which 2887 meet the cooling unit consistency test applied here. The median value of all results from the last 140 Ma is 42 ZAm^2 ('Z' stands for Zetta (1021)). We have deliberately chosen a very loose standard for acceptance as there is no agreement in the community as to what constitutes a 'reliable' result and it is not clear that, without the original measurement data, an intelligent selection can be made.

p0720   As an example of the problem of data selection, there are a total of 3328 cooling unit averages with checks of alteration during the experiment (method code of 'LP–PI–ALT') and the rest have no such test. The two data sets are plotted as cumulative distributions in **Figure 20**. One might expect a significant difference between the two distributions, but, in fact, there is no statistical difference between the two. This does not mean that experimental design makes no difference; the discussion of theory makes it quite clear that many things can give an erroneous result and these things should be tested for. The problem is that there is insufficient information in the database to make a meaningful selection.

p0725   The difficulty with the published data as a whole becomes apparent when we plot the intensity data from the last 5 My against latitude (**Figure 21**). Stars are median values in 10°
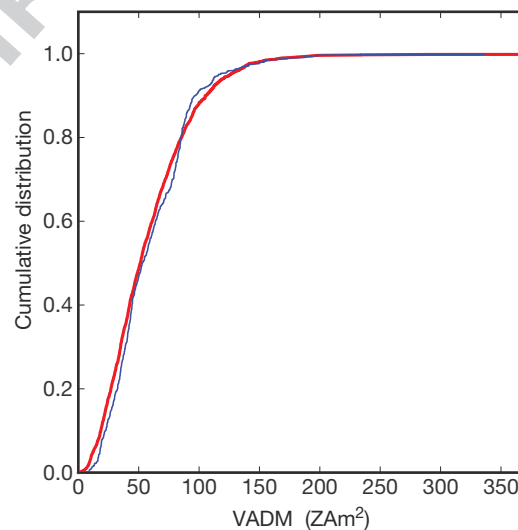
Figure 20   Cumulative distributions of data that come from experiments   f0105 with a check for alteration (heavy red line) versus those that did not (light blue line). The two data sets cannot be distinguished from one another at the 95% level of confidence, based on a two-tailed Kolmogorov–Smirnov test.

latitudinal bins, and the intensity at each latitude expected from the median dipole moment of 61 ZAm^2 for the same interval is shown as the cyan line. The overall fit of the paleointensity data shown in **Figure 21** to a dipole field is poor as pointed out by Lawrence et al. (2009). Reasons for the failure of the dipole hypothesis in the PINT13 data compilation include the following: (1) the data may be 'no good,' (2)

TGP2: 00107

f0110   **Figure 21**   Paleointensity versus latitude for data from the last 5 My. Stars are median values for 10° bins.

there may be long-term nonaxial dipole field contributions to the geomagnetic field, (3) the average may be nonstationary and the data in different bins in **Figure 21** are from different ages and average fields, and (4) there may be long-term hemispheric asymmetry (Cromwell et al., 2013).
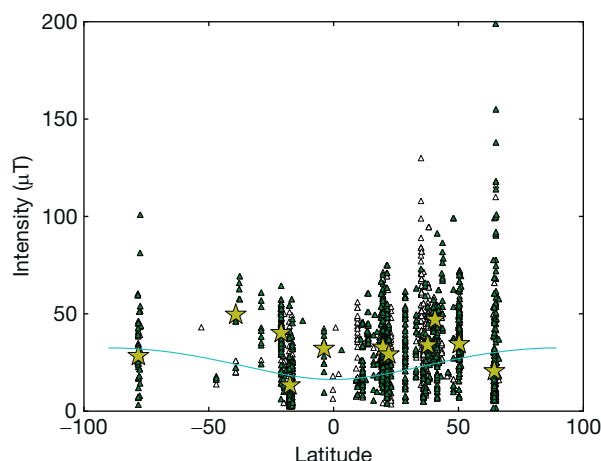
p0730   Although the PINT13 data set is by now quite large, the age distribution of paleointensity data for the last 200 Ma is still patchy with 24% of the data being younger than 1 Ma. By far, most data come from the northern hemisphere (see **Figure 16(a)**). So one point of agreement among all papers on the subject is that more and better data would be helpful for defining the average paleofield intensity and its variation.

s0185   **107.8.2   What Is Long-Term Strength of the Geomagnetic Field?**

p0735   The present Earth's magnetic field is well approximated by a geocentric magnetic dipole with a moment of about 80 ZAm^2. But what is the average value of the dipole moment? A great deal of effort has been put into assembling paleointensity databases over more than three decades, yet there remains little consensus on the answer to this most basic question.

p0740   Early studies suggested that the average field strength has been either quite a bit lower than the present (e.g., Coe, 1967; Smith, 1967) or approximately equivalent to today's field (Bol'shakov and Solodonikov, 1980; Kono, 1971; McFadden and McElhinny, 1982). Some studies found no trend with age in VDMs (e.g., Bol'shakov and Solodonikov, 1980) over the last few hundred million years, while others found a significant increase in dipole moment from the Mesozoic to the present (e.g., Smith, 1967). Tanaka et al. (1995a,b) estimated the average dipole moment for the last 20 My to be approximately 84 ZAm^2 with significantly lower values in the Mesozoic (the so-called Mesozoic dipole low of Prévot et al., 1990), a view also held by Perrin and Shcherbakov (1997) and reiterated by Biggin et al. (2003). But a series of more recent papers have

Au33   argued for a lower average (Juarez and Tauxe, 2000; Juarez et al., 1998; Selkin and Tauxe, 2000; Tauxe, 2006; Tauxe et al., 2013; Yamamoto and Tsunakawa, 2005).

p0745   The lack of consensus on the 'stable' value of the field stems in part from differing views on which data to include as well as the explosive growth of paleointensity data available (compare, e.g., Biggin et al., 2003; Goguitchaichvili et al., 2004; Heller et al., 2002; Selkin and Tauxe, 2000; Tauxe et al., 2013). While Biggin et al. (2003) argued that because such procedures as the so-called pTRM check designed to identify alteration during the paleointensity experiment cannot guarantee the quality of a particular result, there is no need to reject data that do not have pTRM checks; others (e.g., Riisager and Riisager, 2001; Tauxe and Staudigel, 2004) have tried to develop more rigorous experimental protocols to detect and reject 'bad' data. Here, we take the broad view advocated by Biggin et al. (2003), relying strongly on strict consistency tests at the cooling unit level.   Au17

p0750   Tauxe et al. (2013) considered the subject anew and calculated the median value of the field, as opposed to the arithmetic average. The arithmetic average is heavily influenced by outliers, of which there are many in the database. In their treatment, the median value of the field (shown as the cyan line in **Figure 19**) is 42 ZAm^2 and is quite stable through time, with the only long-term departure from this value occurring in the Jurassic and early Cretaceous (the Mesozoic dipole low).

p0755   One clear result from the data in **Figure 19** is that the geomagnetic field is highly variable on both short and long timescales. Therefore, it is likely that unless the same time period is considered in all latitudinal bins in figures like **Figure 21**, there will be scatter introduced from comparing times with different average field strength. Some effort should be put in obtaining data for certain time slices as a function of paleolatitude.

s0190   **107.8.3   Are There Any Trends?**

s0195   *107.8.3.1   Intensity versus polarity interval length*

p0760   Although there are no clear long-term trends in the paleointensity data shown in **Figure 19**, there are times when the field is stronger than others as noted previously. Cox (1968) suggested that strong geomagnetic fields could inhibit reversals of the geomagnetic field and this makes sense with the observation that geomagnetic fields are low when the field is reversing.

p0765   Tauxe and Hartl (1997) and Constable et al. (1998) demonstrated a weak correlation between the length of a given polarity interval and the average paleointensity in the relative paleointensity data from DSDP Site 522 (but Yamazaki et al. (2013) suggested that this data set may be influenced by sediment property changes). So one of the primary motivations for initiating the study of the DSDP/ODP submarine basaltic glasses for paleointensity was to test the hypothesis that long intervals of stable polarity (like the Cretaceous Normal Superchron or CNS in **Figure 19**) were associated with unusually strong fields (see, e.g., Pick and Tauxe, 1993). It was therefore puzzling and a bit disappointing when Selkin and Tauxe (2000) compared paleofield strength with reversal rate and found no clear relationship. There were just too few data from the CNS to make a definitive statement.

p0770   Now, there are many more data from the last 175 Ma with several data sets available from intervals whose polarity chrons are known and the data can be associated with known polarity

interval length. In **Figure 22**, we also show the data from **Figure 19** associated with known polarity intervals. These data are from SBG obtained from holes drilled on clearly identifiable magnetic anomalies compiled by Tauxe (2006) and data from lava flows in magnetostratigraphic sections correlated to the timescale (Herrero-Bervera and Valet, 2005; Riisager et al., 2003). It appears that the correlation suggested by Tauxe and Hartl (1997) and Constable et al. (1998) based on relative paleointensity in sediments is supported by the absolute paleointensity data set, although not strongly.
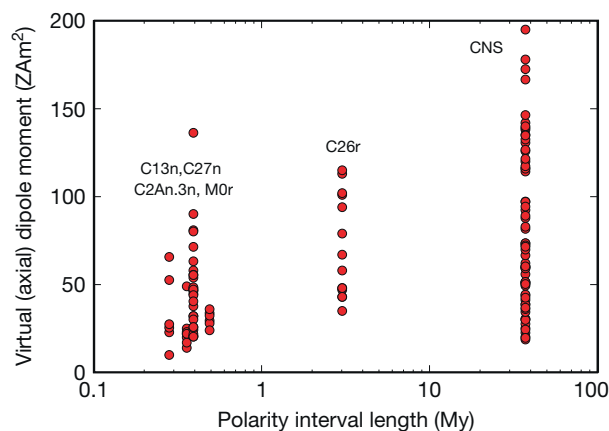

f0115 **Figure 22** VADM data from the PINT13 database from polarity intervals of known duration. Data from the CNS are from Cottrell and Tarduno (2000), Riisager et al. (2003), Sherwood et al. (1993), Tarduno et al. (2001, 2002), Tauxe (2006), Tauxe and Staudigel (2004), Tanaka and Kono (2002), Zhu et al. (2004), and Zhu et al. (2004); C26r and C27n from Riisager and Abrahmsen (2000); C12n, C13n, C32n are from Tauxe (2006); M0r are from Riisager et al. (2003), Tauxe (2006), and Zhu et al. (2001); and C2An.3n are from Herrero-Bervera and Valet (2005).

107.8.3.2   Source of scatter in the CNS   s0200

Another prediction made from the relative paleointensity data   p0775
from Site 522 was that the scatter in the data is proportional to the average value and strongly linked to polarity interval length (Constable et al., 1998). This observation also appears to be weakly supported by the absolute paleointensity data set. One question that springs to mind, however, is whether the scatter is geomagnetic in origin. To address this issue, Granot et al. (2007) assembled a data set from the Troodos Ophiolite, which formed during the CNS. Their data set includes new data from gabbros as well as the submarine basaltic glass data of Tauxe and Staudigel (2004). Many of the gabbro data came from a sequence of small plutons with a clear relationship to the ancient spreading axis and their relative age relationships were therefore known. Tauxe and Staudigel (2004) had sampled two transects through the entire oceanic extrusive layer, separated by some 10 km. Data from these two transects are in stratigraphic order, so their age relationships are also known. In **Figure 23**, we show their plot of the three time sequences. The data exhibit remarkable serial correlation, which Granot et al. (2007) used to argue that the scatter in the CNS data is largely geomagnetic in origin. Magnetic anomaly data of Granot et al. (2012) seem to support the geomagnetic origin of the scatter; the amplitude envelope of magnetic contrasts from inversion of a deep-tow magnetic anomaly profile from the Central Atlantic Ocean spanning the entire CNS shows some similarity with time variations of the paleointensity data scatter.

107.8.3.3   The oldest paleointensity records   s0205

Under the topic of 'trends in paleointensity,' one of the most   p0780
interesting questions concerns the earliest records of paleointensity. In **Figure 24**, we show published results satisfying minimum consistency constraints obtained from Archean-aged rocks. Until the 1990s, there were very few studies that
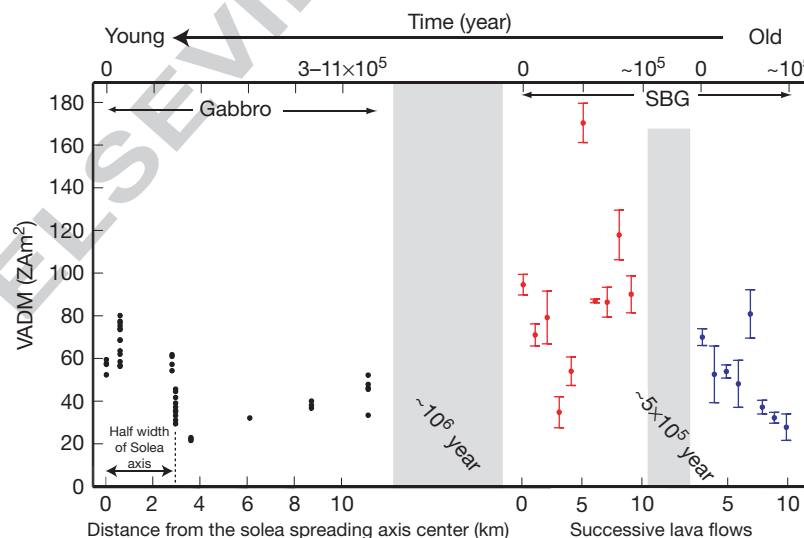
f0120 **Figure 23** Three time series of paleointensity data during the late CNS from the gabbros and glasses. Gray areas represent gaps in time estimated from moderate spreading rate (full spreading rate of 20–75 mm year^{-1}). Results for the gabbro specimens are shown as individual points and are corrected for cooling rate and anisotropy. Results for the SBG sites correspond to the average results from successive cooling units. Data are from Granot et al. (2007) and Tauxe and Staudigel (2004). Modified from Granot R, Tauxe L, Gee JS, and Ron H (2007) A view into the Cretaceous geomagnetic field from analysis of gabbros and submarine glasses. *Earth and Planetary Science Letters* 256: 1–11.

TGP2: 00107

f0125   **Figure 24**   Archean data from the database that have standard deviations of <20% of the mean or are <5 µT. Age uncertainties are indicated by the horizontal bars. Triangles are data from KTT-type experiments with pTRM checks and squares are from other types of experiments. The diamonds are from single crystal experiments. Data ar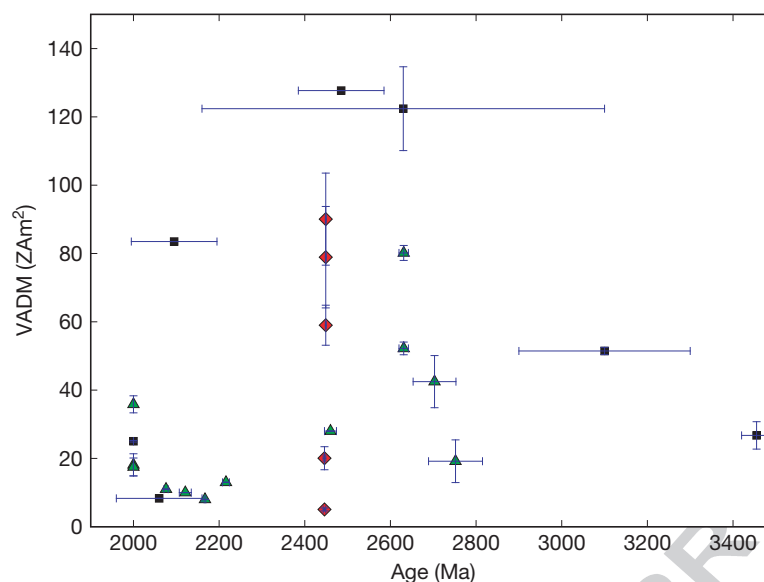e from Morimoto et al. (1997), Yoshihara and Hamano (2000), Sumita et al. (2001), Macouin et al. (2003), Bergh (1970), Hale (1987), McElhinny and Evans (1968), Schwartz and Simons (1969), Smirnov and Tarduno (2003), Smirnov et al. (2003, 2005), and Selkin et al. (2000).

were based on experiments that used pTRM checks (triangles and diamonds in **Figure 24**). Recent data meet the highest experimental standards and show that the field had a large range in intensity, similar to more recent times, although the highest values come from experiments not done with pTRM checks (squares in **Figure 24**). The inescapable conclusion from these data is that the geomagnetic field was 'alive and well' by ~3 Ga.

s0210   ***107.8.3.4   The paleointensity 'sawtooth'***

Au34 p0785   Valet and Meynadier (1993) (detailed data set in Meynadier et al., 1995) presented a relative paleointensity record for the last 4 My using sediment cores of ODP Leg 138 taken from the eastern equatorial Pacific (see **Figure 25**). They postulated an 'asymmetrical sawtooth pattern' of paleointensity variations, that is, a rapid intensity growth just after a polarity transition and a gradual decrease since then toward the next reversal (see **Figure 25**). They also suggested that the length of a polarity zone is proportional to the magnitude of the intensity jump. The latter observation is consistent with the data shown in **Figure 22** whereby long polarity intervals appear to have higher average fields. Nonetheless, the 'sawtooth' idea became the subject of heated arguments.

p0790   The sawtooth was originally epitomized by the long-term decreasing trends observed in the Matuyama, one toward the Brunhes and one toward the Olduvai, and in the Gauss, one toward the Kaena and one toward the Matuyama boundaries. The sawtooth envisioned by Valet et al. (2005) (see SINT-2000 in **Figure 25**), however, is a shorter trend immediately preceding the reversal boundary. We will refer to this more restricted view as the 'short sawtooth' hypothesis in the following. First, we review the debate about the sawtooth in the literature.

p0795   While all transitional records with paleointensity data have low field intensities associated with transitional directions, not all records display a long-term decreasing trend toward a reversal. Arguments supporting the existence of the sawtooth pattern were presented in rapid succession. Valet et al. (1994) examined paleointensity records near the Matuyama–Brunhes transition from the Atlantic, Indian, and Pacific Oceans and found the rapid intensity growth after the transition. Meynadier et al. (1994) recognized the 'sawtooth pattern' in a relative paleointensity record spanning the last 4 My obtained from a core in the Indian Ocean. Verosub et al. (1996) presented a record focused near the MBB and the Jaramillo subchron of a sediment core from the central north Pacific, which supported the 'sawtooth pattern.'

p0800   Counterarguments to the sawtooth also began to appear. For example, Laj et al. (1996a, 1997 (for correction)) failed to see the 'sawtooth pattern' utilizing the same core as that of Verosub et al. (1996) when examining a longer period of time up to the Olduvai subchron. Laj et al. (1996b) reported that no rapid intensity increase after polarity transitions was observed in relative paleointensity records from two Late Miocene sections in Crete (Kotsiana and Potamida in **Table 2**).

p0805   Arguments against the 'sawtooth pattern' were presented also from paleointensity estimations based on recording mechanisms different from sediments. Records of $^{10}Be/^9Be$ reflect geomagnetic paleointensity through a control on the production rate of the cosmogenic nuclide (^{10}Be). Raisbeck et al. (1994) argued that a $^{10}Be/^9Be$ record at Site 851 of ODP Leg 138, which is the same site as of Valet and Meynadier (1993), is inconsistent with the 'sawtooth pattern.' Westphal and Munschy (1994) showed that the 'sawtooth pattern' cannot [Au35] explain the shape of stacked magnetic anomaly profiles over the Southeast Indian Ridge, Juan de Fuca Ridge, and East [Au36]

TGP2: 00107
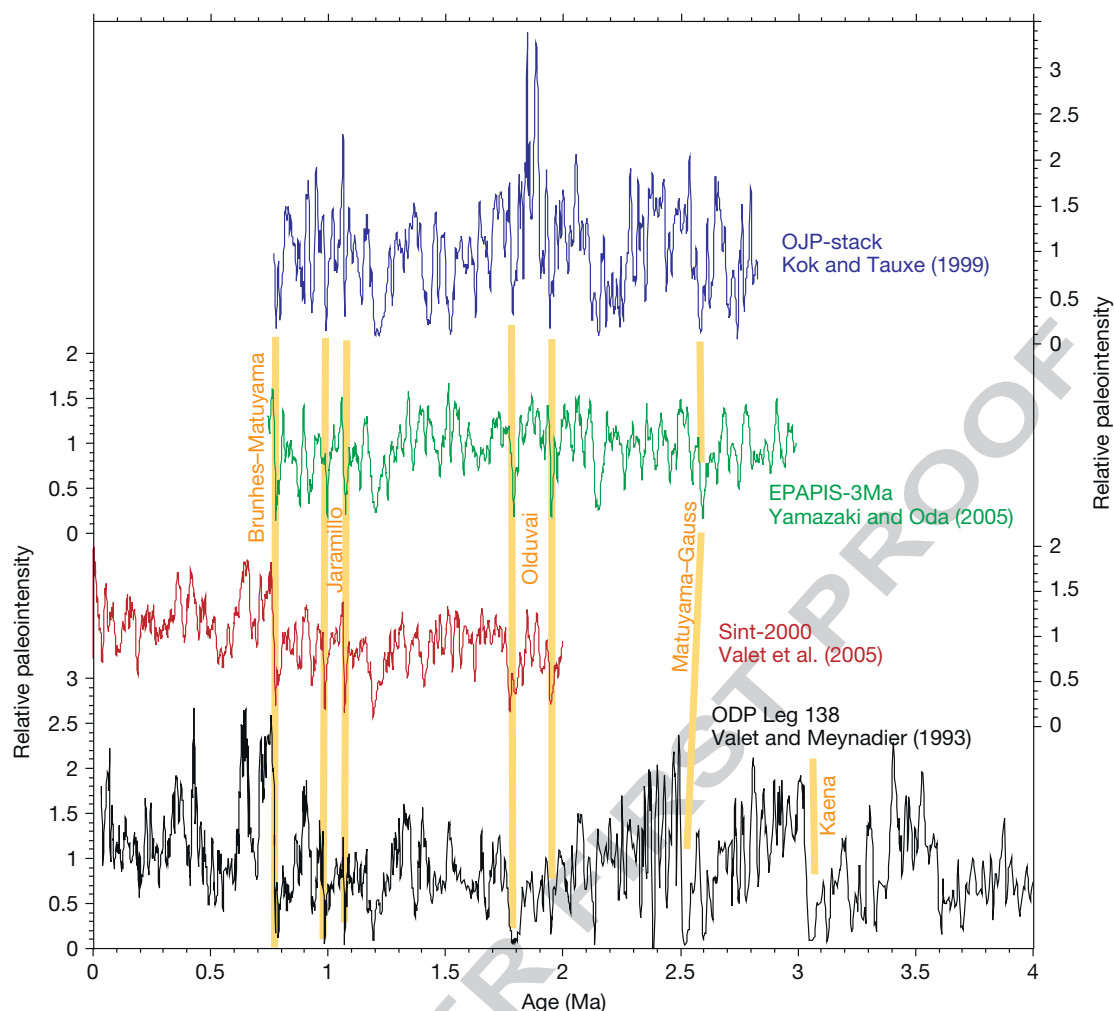
f0130   **Figure 25**   The paleointensity record from ODP Leg 138 cores (Valet and Meynadier, 1993) showed the 'asymmetrical sawtooth pattern,' whereas other records, which reached the Gauss–Matuyama boundary, do not show such pattern: Ontong Java Plateau stack of Kok and Tauxe (1999) and equatorial Pacific paleointensity stack of Yamazaki and Oda (2005).

Pacific Rise. McFadden and Merrill (1997) presented an analysis of the Cenozoic polarity reversal chronology that effective inhibition of a future reversal can only last for about 50 ky at most, which contradicts the 'sawtooth pattern' requiring much longer inhibition.

p0810   The 'sawtooth pattern' was also questioned from remanent magnetization acquisition processes. Kok and Tauxe (1996a) proposed a cumulative viscous remanence model for remanence acquisition of sediments that can yield intensity variations like the 'sawtooth' pattern. Then, Kok and Tauxe (1996b) reproduced the 'sawtooth pattern' of the ODP Leg 138 sediments by the cumulative viscous remanence model using the values of the equilibrium magnetization constrained by results of a Thellier-type paleointensity experiments applied to the ODP Leg 138 sediments. Furthermore, they resampled the Site 851 sediments near the Gauss–Gilbert boundary and showed that the 'sawtooth pattern' disappeared by thermal demagnetization to 400 °C.

p0815   Meynadier et al. (1998) made a counterargument to the cumulative viscous remanence model of Kok and Tauxe (1996a,b). They suggested that to produce the sawtooth pattern and to preserve the magnetostratigraphy with the

cumulative viscous remanence model, a very narrow distribution of the relaxation times is required. They also showed that the sawtooth pattern of the Site 851 sediments did not change by thermal demagnetization and AF demagnetization of stronger fields, which is inconsistent with the result of Kok and Tauxe (1996b) despite using the sediments from the same site. Kok and Tauxe (2000) on the comments to Meynadier et al. (1998) stressed the nonuniqueness of relaxation time distribution explaining the 'sawtooth pattern' and pointed out that the τ distribution of Kok and Tauxe (1996b) is not all relaxation times present in the sediments, but merely a part of them that behave viscously. In the reply, Meynadier and Au37 Valet (2000) mentioned that the remanent magnetization with blocking temperatures between 150 and 300 °C, which may carry cumulative viscous remanence, is only a minor part of NRM of the sediments. The two groups also argued about the validity of thermal demagnetization on relative paleointensity estimation from sediments (Kok and Tauxe, 1999; Kok and Ynsen, 2002; Valet and Meynadier, 2001).

Mazaud (1996) proposed another model of magnetization p0820 acquisition, which produces the 'sawtooth pattern': a large

TGP2: 00107

fraction (say, two-thirds) of magnetic grains acquire NRM at deposition time, while the remaining grains reorientate or acquire magnetization after deposition. Although Meynadier and Valet (1996) considered this model unlikely from the knowledge of pDRM acquisition processes that prevailed at that time, recent studies suggest that this model may have difficulties. As discussed in **Section 107.4**, pDRM acquisition with compaction that can be expressed by an exponential function is unlikely to occur, although there are still different opinions for the amount of depth-lag. An experiment of Katari et al. (2000) using natural undisturbed sediments suggests that pDRM (reorientation of magnetic particles) is a rare phenomenon, probably because of the effects of flocculation: magnetic minerals would be aggregated with clay.

p0825   In the 851 record of Valet and Meynadier (1993), the 'sawtooth pattern' is most apparent in the early Matuyama chron after the Gauss–Matuyama transition and during the Gauss chron. The number of paleointensity records reported so far that reached the Gauss–Matuyama transition is still small. However, available records from different groups do not support the 'sawtooth pattern': neither a stacked record since 2.8 Ma from the Ontong Java Plateau (Kok and Tauxe, 1999; OJP-stack in **Figure 25**) nor a stacked record since 3.0 Ma from the equatorial Pacific (Yamazaki and Oda, 2005; EPAPIS stack in **Figure 25**) shows variations like the 'sawtooth pattern' after the Gauss–Matuyama transition. More recently, a record from between 2.1 and 2.75 Ma at IODP Site U1314 in the North Atlantic (Ohno et al., 2012) also fails to reproduce the sawtooth.

p0830   We do not yet understand well the rock magnetic processes, which produce the 'sawtooth pattern' only for some sediments. If the DRM acquisition model of Mazaud (1996) works in general, all sedimentary paleointensity records should display 'sawtooth'-like changes. From the cumulative viscous remanence model of Kok and Tauxe (1996a), the sediments producing the 'sawtooth pattern' are expected to have a particular magnetic grain-size distribution favorable for the long-term viscous remanence acquisition, but this has not yet been fully tested.

p0835   Valet et al. (2005) used 10 of the 15 records of relative paleointensity data compiled by Guyodo and Valet (2006) to create the so-called SINT-2000 stack (see **Table 2** and Au38 **Figure 25**). Based on this subset of the data, Valet et al. (2000) argued for the 'short sawtooth' pattern in the 80 ky interval immediately prior to the four reversals included in the stack. Of the four reversals in the SINT-2000 stack (Figure 4 of Valet et al., 2000), only the upper Jaramillo and the lower Olduvai show convincing short sawtooth patterns.

p0840   Relative paleointensity records spanning the last 2 My have steadily been produced (see, e.g., **Table 2**). Because the SINT-2000 is a stack that did not include many of the records in **Table 2**, we have plotted those records that span at least the period from 800 to 900 ky in **Figure 26** for the interval including the Brunhes and Jaramillo. Considering all the records, it appears that even the short sawtooth is only observed in a small subset of the records, although an intensity peak just Au39 after the B/M boundary (Guyodo and Valet, 1999; Valet et al., 2005) does appear in all records. In general, the long-term sawtooth pattern originally observed by Valet and Meynadier (1993) has not been universally observed, as would be

expected from the behavior of a dipole source. Recently, however, Ziegler and Constable (2011) showed asymmetry in Au40 growth and decay of the geomagnetic dipole that is not restricted near polarity boundaries. They found that on the 25–150 ky timescale, growth rates are larger than decay rates in their PADM2M model of paleointensity variations (Ziegler et al., 2011), in which the data sets of relative paleointensity mentioned earlier are incorporated.

107.8.4   High-Resolution Temporal Correlation   s0215

107.8.4.1   Sediments   s0220
Oxygen isotope stratigraphy revolutionized paleoceanography   p0845 by providing a global signal with a resolution on the order of 10 s of thousands of years (e.g., Hays et al., 1976). Yet oxygen isotope stratigraphy has its drawbacks. It cannot be applied in sediments deeper than the carbonate compensation depth or lakes. Oxygen isotopic data are often difficult to interpret in marginal seas, where records may not reflect global ice-volume changes. Finally, temporal resolution better than 10^4 years is critical for assessing the global nature of climatic events and their durations. The prospect of using relative paleointensity from sediments as a high-resolution correlation and dating tool has therefore been met with great enthusiasm (e.g., Stott et al., 2002) and was reviewed recently by Roberts et al. (2013). Here, we examine the prospects and problems with the so-called paleointensity-assisted chronology or PAC.

The importance of PAC is not simply as a substitution for   p0850 δ^{18}O. It can also be used to examine consistency of other chronologies such as δ^{18}O and ^{14}C, because it is quasi-independent of them. Regional and global intercore correlations tied by paleointensity variations revealed discrepancies of up to several thousand years between those based on ^{14}C and δ^{18}O (Stoner et al., 1995) and between GISP2 and the δ^{18}O chronologies (Stoner et al., 1995, 2000) during the last c.100 ky. Moreover, paleointensity stratigraphy can have higher resolution than δ^{18}O stratigraphy because the variations contain shorter wavelength components than those of δ^{18}O. Truly dipolar features of geomagnetic field variations have a potential for providing a time reference for an interhemispheric paleoclimatic relationship with unprecedented resolution.

On a more limited scale, there is a possibility that intercore   p0855 correlation and age estimation can be performed using paleointensity by correlating patterns among cores with a standard curve such as SINT-800 (Guyodo et al., 2001) and NAPIS-75 (Laj et al., 2000), which is exemplified by Stoner et al. (1995) in the Labrador Sea, Demory et al. (2005) in Lake Baikal, and Macri (2005).

We feel that while regional correlations can be achieved,   p0860 much is lost by using PAC as a primary dating tool. These records can no longer be used to constrain paleointensity models or global stacks, because the age information is not independent and features correlate by assumption. Such records have been clearly labeled in **Table 2** (RPI) and in the MagIC database.

If we desire a global correlation tool, we require a dipolar   p0865 signal. However, it is as yet unclear at which wavelength the dipole terms give way to nondipole terms. Korte and Constable (2005) cautioned us that variations in VADMs may not be global and their variations need not be synchronous because they can
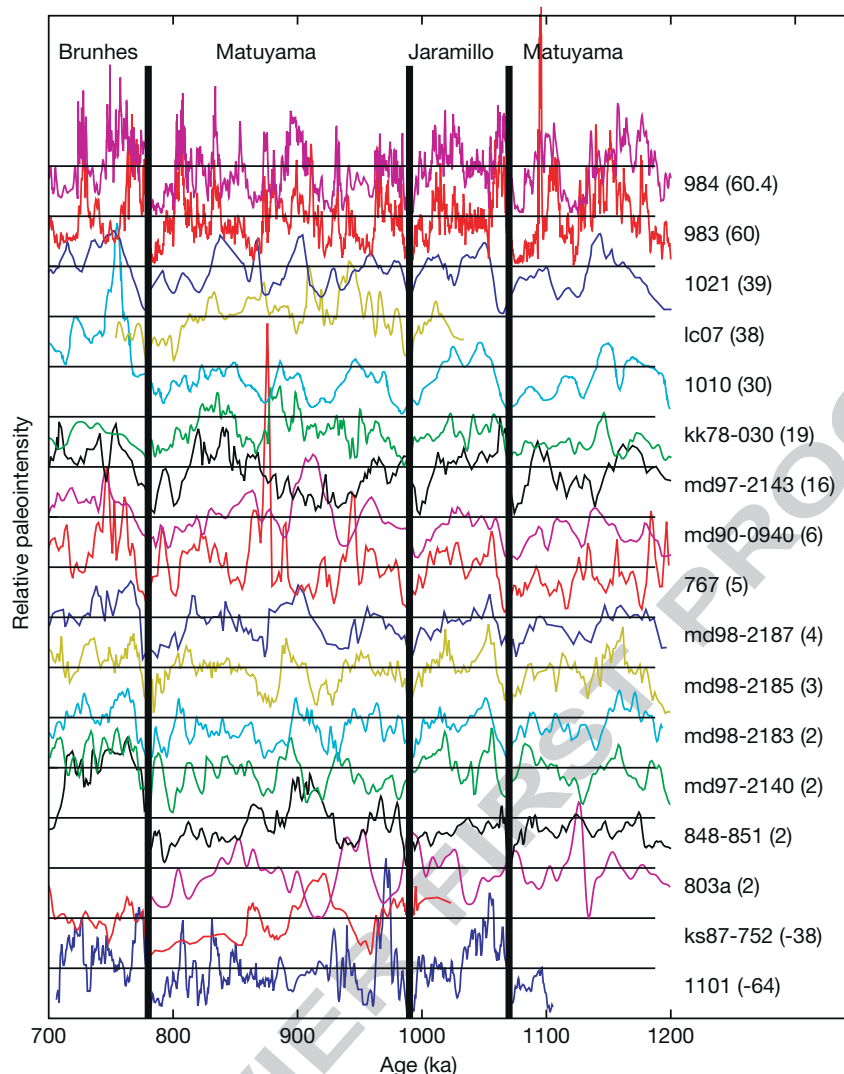
TGP2: 00107

Figure 26   Plot of all records spanning at least the period from 800 to 900 ka in the MagIC database (see **Table 2**) for the range 700–1200 ka. Records are plotted in order of latitude (in parentheses to right of record name). The positions of the Matuyama–Brunhes and the upper and lower Jaramillo transitions are indicated by heavy black lines.

be strongly influenced by nondipole field effects. Moreover, the duration of a polarity reversal is known to be dependent on latitudes, ranging from about 2 ky near the equator to 10 ky at $\pm 60°$ (Clement, 2004). Furthermore, the contribution of non-dipole effects may be higher when paleointensity is low, and both the duration and shape of a particular paleointensity low will be site-dependent. Nonetheless, there is an astonishing correlation between the 'paleointensity dipole stack' of Ziegler et al. (2011) and the magnetic anomaly inversion of Gee et al. (2000) as illustrated in Figure fig:padmVanom.

Au41

p0870   Doubts about the global nature of paleointensity features notwithstanding, global intercore correlations on a millennial scale have been attempted. A series of papers by Channell et al. (2000), Stoner et al. (2000), and Mazaud et al. (2002) correlated records between the high latitudes of the North Atlantic and the South Atlantic and Indian Ocean sectors. As an example of the method, we show the records of Stott et al.

(2002), who tied cores together between the North Atlantic and the western equatorial Pacific (see **Figure 27**). The large-scale features (labeled H1–H10 and L1–L8) correlate reasonably well and are consistent with the oxygen isotopic records from the two cores. These allow correlation with a resolution of 2–3 ky. The difficulty of identifying global features on a submillennial scale is made apparent by the rather unconvincing correlation of features marked by the stars. Although these features may well be synchronous, they do not resemble each other very much in the two hemispheres, and without the excellent and very detailed chronological control of the independent oxygen isotopic records, their identification would not have been possible. How much should these 'millennial' features look like each other and how synchronous they are expected to be require much more detailed knowledge of the process of secular variation, a topic of active research (see **Chapter 103**).
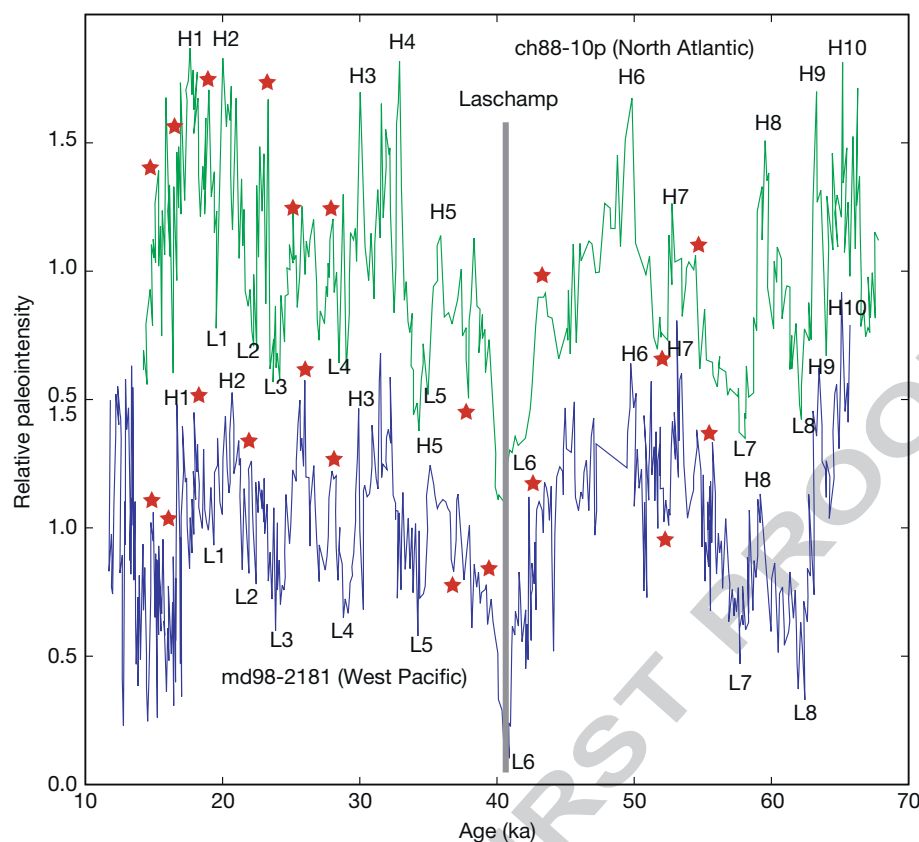
TGP2: 00107

f0140   **Figure 27**   Comparison of deep-sea sediment relative paleointensity records from MD98-2181 and the North Atlantic Ocean site CH88-10P. The two records were dated by correlation of their individual oxygen isotopic stratigraphies to the GISP2 record. Distinctive paleointensity highs (H1–H10) and lows (L1–L8) are identified in the two records. Less convincing features (stars) are marked as well. The ages of the named features are synchronous to within an uncertainty of less than ±500 years. The 'Laschamp excursion' correlates with a distinctive 36Cl excursion in the GISP2 record and provides an independent tie point to ice cores. Redrawn from supplement to Stott L, Poulsen C, Lund S, and Thunell R (2002) Super ENSO and global climate oscillations at millennial time scales. *Science* 297: 222–226.

s0225   ### 107.8.4.2   Ridge crest processes

p0875   The potential of paleointensity for high-resolution dating is not restricted to sediments. Thellier-type paleointensity data can be used to estimate ages of basalts near mid-ocean ridges, and it is expected that paleointensity will be useful for studying crustal accretion processes at ridges (Bowles et al., 2006; Gee et al., 2000; Ravilly et al., 2001). This work is discussed in more detail in Chapter 106 (Figure 28).

s0230   ### 107.8.4.3   Archaeomagnetic dating

p0880   A thorough review of the possibilities of using paleointensity estimates to provide age constraints for archaeological materials is beyond the scope of this chapter (but see Chapter 5.9 of this volume). Nonetheless, it is worth mentioning that the so-called archaeointensity results are increasingly used for this purpose (e.g., Ben-Yosef et al., 2008a,b; Pavón-Carrasco et al., 2011).

[Au42]

s0235   ### 107.8.5   Atmospheric Interaction

p0885   Radioactive forms of carbon, beryllium, and chlorine are produced in the atmosphere by cosmic ray bombardment. The
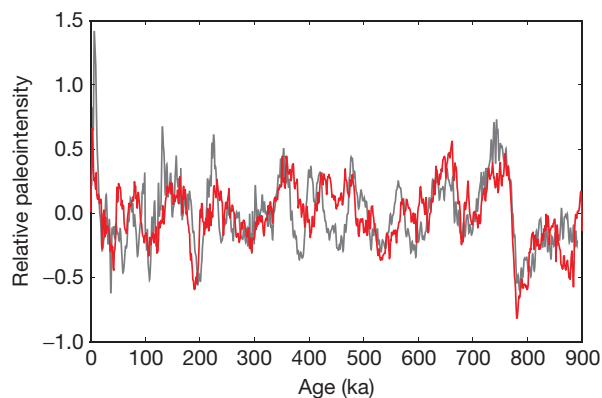
Figure 28   Comparison of predicted relative paleointensity from the   f0145 magnetization inverted from a high-resolution marine magnetic anomaly stack (gray; data from Gee et al., 2000) and dipole moments from the PADM2M paleointensity stack (red; Ziegler et al., 2011). Ages for the magnetic anomaly record were rescaled to a common age for the Matuyama–Brunhes boundary. Redrawn from Roberts AP, Tauxe L, and Heslop D (2013) Magnetic paleointensity stratigraphy and high resolution Quaternary geochronology: Successes and future challenges. *Quaternary Science Reviews* 61: 1–16.

decay of these isotopes is used for dating purposes in a wide variety of disciplines. There are large variations in ages predicted from tree ring, varve, ice layer counting, or U/Th dating and those estimated by radiocarbon dating. An example of such a comparison is shown in **Figure 29(a)**, which shows the age based on ^{14}C dating from a core in the Cariaco Basin versus layer counting in the Greenland Ice Sheet Project 2 ice core from a core in the Cariaco Basin (Hughen et al., 2004). The correlation of the marine sediment core to the ice core was based on tying dark sedimentary layers to interstadials in the GISP2 core.

p0890   The difference between radiocarbon and other age estimates in **Figure 29(a)** is used to calculate variations in initial radiocarbon in the atmosphere relative to the concentration in the modern atmosphere (see atmospheric Δ^{14}C plotted as dots in **Figure 29(b)**). An excess of radiocarbon (positive Δ^{14}C) results in an underestimate of the age because there is 'too much' radiocarbon in the sample for its age. Changes in Δ^{14}C have been attributed to differences in the production of radiocarbon in the atmosphere by cosmic ray bombardment and changes in the carbon balance between the atmosphere and the deep ocean, which is a reservoir of old carbon (see, e.g., Bard et al., 1990). If, for example, the transfer of atmospheric carbon into the ocean was less efficient in the past or the release of old carbon from the deep ocean was less efficient ('ventilation' was slower), then there would be an excess of radiocarbon in the atmosphere relative to the modern atmosphere, resulting in 'too young' ^{14}C ages.

p0895   Radiocarbon production is thought to be strongly controlled by changes in magnetic field strength because the magnetic field shields the atmosphere from cosmic rays (see **Chapter 103**). Changes in the intensity of the magnetic field should therefore result in changes in radiocarbon production (among other things); hence, the variation in intensity is a key parameter in deriving accurate age information. Hughen et al. (2004) used a paleointensity stack from the North Atlantic (the NAPIS stack of Laj et al., 2000) as a proxy for changes in the dipole moment of the Earth's magnetic field over the last 70 ky. Au43 By using the Monte Carlo simulations of the relationship between geomagnetic field strength and radiocarbon production of Masarik and Beer (1999), Hughen et al. (2004) predicted radiocarbon production for the past 50 ky (**Figure 29 (c)**). The different curves in **Figure 29(a)–29(d)** use the predicted radiocarbon production values as input into box models using different ocean/atmosphere boundary conditions relating to different models of deep-sea ventilation, resulting in different estimates for atmospheric Δ_{14}C.

p0900   None of the curves in **Figure 29(b)** based on the model predictions using the NAPIS stack provide a satisfactory fit to Au44 the observed variations. Hughen et al. (2002) suggested that either the model of Masarik and Beer (1999) for translating geomagnetic field intensity to radiocarbon production is incorrect at low field strengths or our understanding of the global carbon cycle is insufficient. It is of course also possible that the NAPIS model of North Atlantic relative paleointensity is a poor proxy for the global paleomagnetic field intensity variations.

p0905   Roberts et al. (2013) considered the problem but used the PADM2M model of Ziegler et al. (2011) with the variations predicted from the ^{10}Be stack of Frank et al. (1997) (**Figure 30**). The agreement is remarkably good. Overall,
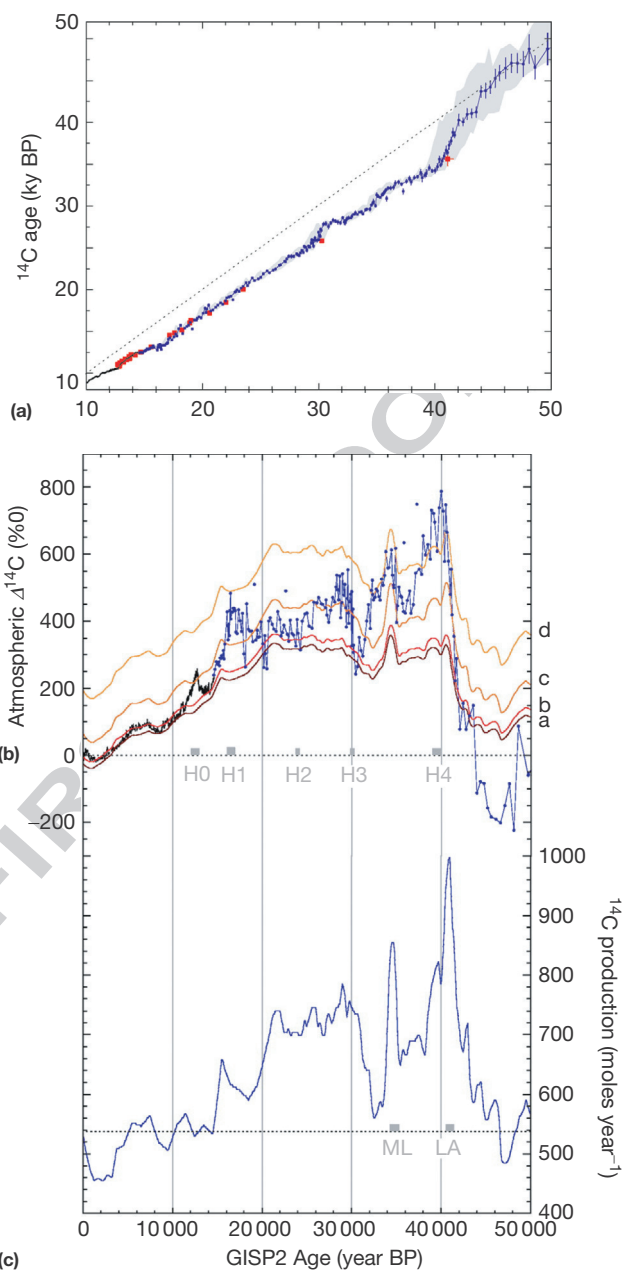
Figure 29   (a) Radiocarbon calibration data from Cariaco ODP Leg 165, f0150 Holes 1002D and 1002E (blue circles), plotted versus calendar age assigned by correlation of detailed paleoclimate records to the Greenland Ice Core GISP2. The thin black line is high-resolution radiocarbon calibration data from tree rings joined at 12 cal. ka BP to the varve counting chronology. Red squares are paired 14C-U/Th dates from corals. Light gray shading represents the uncertainties in the Cariaco calibration. The radiocarbon dates are 'too young,' falling well below the dashed line of 1:1 correlation. (b) Compilation of data interpreted as production rate changes in radiocarbon (Δ^{14}C) versus calendar age (symbols same as in (a)). (c) Predicted variation of Δ^{14}C from the geomagnetic field intensity variations from sediments of the North Atlantic (Laj et al., 2000) using the model of Masarik and Beer (1999). Modified from Hughen K, Lehman S, Southon J, et al. (2004) C-14 activity and global carbon cycle changes over the past 50,000 years. *Science* 303(5655): 202–207.

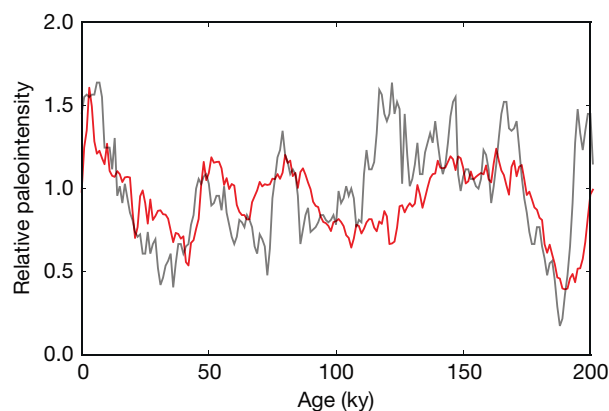# TGP2: 00107

f0155   **Figure 30**   Comparison of relative paleointensity and the relative paleointensity (gray) predicted from normalized ^{10}Be stacks (reproduced from Frank M, Schwarz B, Baumann S, Kubik P, Suter M, and Mangini A (1997) A 200 kyr record of cosmogenic radionuclide production rate and geomagnetic field intensity from ^{10}Be in globally stacked deep-sea sediments. *Earth and Planetary Science Letters* 149: 121–129) and relative paleointensity (red) from the PADM2M model (Ziegler et al., 2011) for the last 200 ka. Redrawn from Roberts AP, Tauxe L, and Heslop D (2013) Magnetic paleointensity stratigraphy and high resolution Quaternary geochronology: Successes and future challenges. *Quaternary Science Reviews* 61: 1–16.

variations in dipole intensity are not as well constrained as we would like. As these variations are key to refining the radiocarbon calibration, more records with independent and accurate age constraints are needed.

s0240   **107.8.6   Frequency of Intensity Fluctuations and the Climatic Connection**

p0910   Arguments regarding the possible relationship between the intensity of the geomagnetic field and climate have a long history of more than 30 years (e.g., Wollin et al., 1971). Discussions in the 1970s were based on the remanent intensity variations, which were not corrected for differences in magnetizability of sediments. The relationship was convincingly rejected by Kent (1982), who showed that the remanent intensity variations of the relevant sediment cores were controlled by climatically induced variations in carbonate contents. Kent and Opdyke (1977) were the first to suggest the presence of the obliquity frequency, ~43 ky in a normalized intensity record, but this idea was not seriously discussed at that time.

p0915   Rapid progress in relative paleointensity studies revived the orbital modulation issue in the late 1990s, and it has been
Au45   heatedly argued since then. Tauxe and Shackleton (1994) found significant power in the power spectrum of a record from the Ontong Java Plateau in the 30–50 ky band but showed that the intensity fluctuations came in and out of phase of the associated oxygen isotopic record, arguing against a strong relationship between climate and paleointensity. In contrast, Channell et al. (1998) and Channell (1999) proposed a ~40 ky obliquity frequency from a power spectrum analysis of their relative paleointensity records during the Brunhes chron obtained from ODP Sites 983 and 984 in the North Atlantic. They interpreted it as geomagnetic field behavior from the observations that no power exists at ~40 ky in

bulk magnetic properties and there is no coherence between the relative intensity and the normalizer (IRM), percent carbonate, and a magnetic grain-size proxy at ~40 ky. Their paleointensity records showed significant power also at the ~100 ky eccentricity frequency, but they rejected this because this frequency was observed also in bulk magnetic properties. Yamazaki (1999) instead proposed the possible presence of the ~100 ky frequency in his relative paleointensity records from the North Pacific based on the same logic as that of Channell et al. (1998): occurrence of ~100 ky power in relative paleointensity but not in the normalizer on the power spectra. Possible occurrence of ~100 ky period in paleointensity records would not be limited to the Brunhes chron: Yamazaki and Oda (2005) (see **Figure 31**) found significant power at ~100 ky period in paleointensity records from 0.8 to 3.0 Ma. Kok and Tauxe (1999) found a peak at ~150 ky in paleointensity records during the Matuyama chron from the Ontong Java Plateau.

p0920   Yokoyama and Yamazaki (2000) applied a wavelet analysis to five paleointensity records from the Pacific Ocean reported in Yamazaki et al. (1995) and Yamazaki (1999) and found a quasiperiod of ~100 ky. They considered the ~100 ky period inherent to the geomagnetic field, because of the good coincidence of the relative intensity records in this scale despite significant phase differences in magnetic properties. Thouveny et al. (2004) reported a ~100 ky period in a paleointensity record during the last 400 ky from Portuguese Margin sediments, North Atlantic. Yokoyama et al. (2007) reached the same conclusion using a similar approach with the data set of Yamazaki and Oda (2002, 2005) and Yamazaki and Kanamatsu (2007). Yokoyama et al. (2010) showed that variations in the geomagnetic vertical component were synchronous with the first derivative of the eccentricity and suggested that changes in the eccentricity may excite the geomagnetic variations. Saracco et al. (2009), using complex wavelet transform, found orbital frequencies in paleointensity proxy records based on production of cosmogenic nuclide (^{10}Be/^{9}Be) and magnetic anomalies of oceanic crust as well as in sedimentary relative paleointensity records. Heslop (2007) and Xuan and Channell (2008a), on the other hand, showed in their cross wavelet analyses that common power exists at orbital periods in relative paleointensity records and orbital parameters, but they did not have a constant phase relationship, from which they concluded that there is no direct causal relationship. However, this does not exclude a possibility for a nonlinear interaction or a linear interaction in a different physical dimension (Yokoyama et al., 2010).

p0925   Whether the orbital frequencies found in sedimentary paleointensity records reflect geomagnetic field behavior or not has been discussed mainly on the following three points: significance and stability of the orbital periodicities, error in age control, and lithologic contamination to paleointensity records. Guyodo and Valet (1999) argued that there is no stable periodicity during the Brunhes chron by a spectrum analysis on the SINT-800 stack using sliding windows. However, the orbital modulation may be a nonstationary process. Sato et al. (1998) suggested that there is no constant period but continuous shifts between 50 and 140 ky based on a stacked paleointensity record from three cores in the western equatorial Pacific during the last 1.1 My. Horng et al. (2003) argued
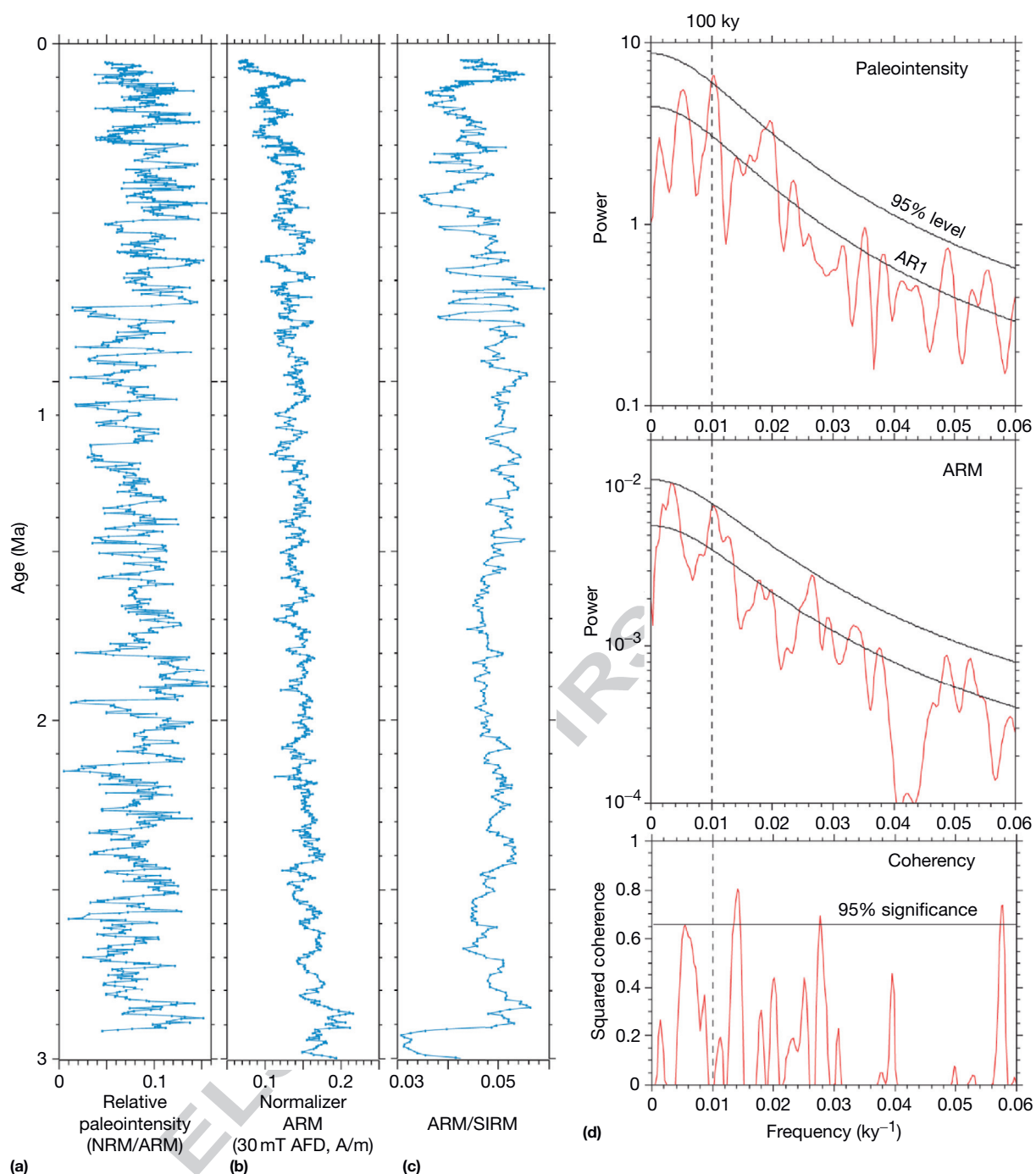
f0160 **Figure 31**   (a) Relative paleointensity, (b) normalizer ARM, and (c) ARM/SIRM ratio of Core MD982187 in the western equatorial Pacific (Yamazaki and Oda, 2005). This core is one of six cores that were used to construct the EPAPIS-3 Ma curve shown in **Figure 26** and covers the longest period of time among them. (d) Power spectra of relative paleointensity and the normalizer (ARM), and cross correlation between them (Yamazaki and Oda, 2005). The relative paleointensity variations contain quasiperiod of ~100 ky but no significant correlation between relative paleointensity and the normalizer. The statistical significance of the spectral peaks was tested against the red-noise background from a first-order autoregressive (AR1) process, and the 95% confidence level is indicated.

that the orbital frequencies in paleointensity variations are not statistically significant by applying a wavelet analysis on their relative paleointensity record during the last 2.14 My from the Western Philippine Sea. On the other hand, Teanby and Gubbins (2000) proposed that the periodicities of several

tens of thousand years observed from sedimentary paleointensity records could be due to aliasing, an artifact of coarse sampling, and simulated using archaeointensity data with a 2 ky period how false longer periods appear by aliasing. However, orbital periodicities have been reported even from

TGP2: 00107

sediment cores with significant variations in sedimentation rates, which is difficult to be explained by aliasing. Guyodo and Channell (2002) performed numerical simulation of paleointensity records with various sedimentation rates and variable quality of age control and showed how spectral information is lost with decreasing sedimentation rates: the power spectra are reliable for periods as short as 4 ky in records with a sedimentation rate of 15 cm ky^{-1} with good age control, whereas periods of only c.50 ky or longer are reliable in records with a sedimentation rate of 1 cm ky^{-1}. McMillan et al. (2002, 2004) evaluated effects of various sources of errors such as dating errors, misidentified tie points, changes in sedimentation rate, and the effect of nondipole components. They simulated coherence of records among various sites and evaluated the accuracy of a stacked record suggesting that dipole variations with periods of longer than 20 ky can be recovered (but shorter ones would be problematic).

p0930 Strong arguments against orbital modulation of the geomagnetic field come from possible lithologic contamination to sedimentary paleointensity records. Because paleointensity records during the last 200 ky look coherent with the oxygen isotope curve, Kok (1999) suspected that sedimentary paleointensity records including those derived from ^{10}Be are controlled by paleoclimate due to inadequate normalization. Guyodo et al. (2000) and Xuan and Channell (2008a) found correlation between paleointensity and magnetic grain-size proxy (ARM/k or ARM/IRM) in orbital frequencies and concluded that orbital frequencies in relative paleointensity records are caused by lithologic contamination. As mentioned before in Chapter 13.4.4, changes in relative abundance of biogenic and terrigenous magnetic mineral components appear as variations in ARM/SIRM ratio (Yamazaki and Ikehara, 2012), and such changes may not be compensated well by the normalization with either ARM or SIRM, resulting in contamination to relative paleointensity.

p0935 The possibility of orbital modulation of paleointensity cannot be excluded only from the existence of correlation between records of relative paleointensity and magnetic properties because the two can also have coherency if the orbital parameters affect both the geomagnetic field and depositional environment. To solve the problem, it is necessary to understand quantitative relation between the magnitude of magnetic property (e.g., magnetic grain-size and mineralogy) changes and the magnitude of induced changes in normalized intensity. At present, we cannot even predict whether normalized intensity increases or decreases when magnetic grain size increases in a certain grain-size range. It is also important to examine phase relationships in coherency analyses. Patterns of lithologic and magnetic property variations induced by paleoclimatic changes may vary place to place; for example, magnetic grain size would increase in a certain period of time in some areas, but in other areas, it would decrease in the same period of time. Paleointensity, on the other hand, should be globally synchronous. Thus, even when paleointensity and magnetic property variations have coherency, lithologic contamination is suggested to be minor if the phase angles between the two from various places differ significantly. The conclusion of lithologic contamination by Guyodo et al. (2000) and Xuan and Channell (2008a) mentioned earlier was based on analyses of a record from a single

site or a set of records from nearby sites that belong to a similar sedimentary environment, and thus, further studies are still required. For isolating true geomagnetic signals and climatic contamination components from normalized intensity records, principal component analysis will be useful as demonstrated by Valet et al. (2011).

p0940 On the possibility of orbital modulation of the geomagnetic field, a relationship of excursions (see Chapter 5.10 in the volume) and reversals with paleoclimate has also been discussed since the 1970s. Rampino (1979, 1981) suggested that excursions may have occurred at about 100 ky intervals and the ages of the excursions seem to coincide with times of peak eccentricity of the Earth's orbit (but see Rampino and Kent, 1983). Worm (1997) revisited the problem and suggested that excursions and reversals tend to have occurred during periods of global cooling or during cold stages. On the contrary, Kent and Carlut (2001) rejected the relationship. They concluded that six excursions in the Brunhes chron and 21 reversals since 5.3 Ma have no tendency to occur at a consistent amplitude or phase of obliquity and eccentricity. The number of possible excursions during the Brunhes chron has increased significantly (up to ca. 20) (Lund et al., 2001). Hence, the problem of the possible connection between excursions and paleoclimate is not independent of the arguments on the orbital frequencies in relative paleointensity. Fuller (2006) revived the problem by suggesting relationships between the obliquity signal and intensity, excursions, and reversals. His arguments include that reversals tend to occur when average amplitude of the obliquity is low with a particular phase within the obliquity signal. This was supported by Thouveny et al. (2008). However, a statistical test by Xuan and Channell (2008b) with a longer reversal sequence did not support the conclusion. Besides paleointensity and excursions, a discussion of orbital frequencies in paleomagnetic directions has been revitalized. Yamazaki and Oda (2002) reported a ∼100 ky periodicity in an inclination record during the last 2.2 My from the western equatorial Pacific, whereas Roberts et al. (2003) concluded that it is not statistically significant.

p0945 As a possible mechanism for relation between the geomagnetic field and climate, orbital forcing on the geodynamo through changes in the moment of inertia by ice-volume changes has often been invoked (e.g., Rampino, 1979; Worm, 1997), but the opposite way of the geomagnetic–climate connection, that is, possibility of a geomagnetic control on climate, has become a matter of debate (Courtillot et al., 2007); changes on galactic cosmic ray flux, which is controlled by the strength and morphology of the geomagnetic field, may affect cloud cover and then global temperature (Svensmark and Friis-Christensen, 1997). Kitaba et al. (2013) reported climate cooling at paleointensity minima during the Matuyama–Brunhes and lower Jaramillo polarity reversals.

p0950 As noted in Section 107.4, there can be a 'stealth' link between lithologic factors, like clay content, which are controlled by climate and the relative paleointensity records, which would be difficult to detect using the standard methods of normalization. To date, the significance and implications of possible climatic controls on paleointensity have not yet been adequately addressed.

TGP2: 00107

s0245   107.9   Conclusions

p0955   Scientists have dreamed of analyzing the ancient magnetic field intensity for over four centuries. Since the first serious attempts to acquire paleointensity data in the 1930s, experimental design has improved dramatically. The theoretical foundations for interpreting paleointensity data from both thermal and depositional remanences are steadily improving, and there has been explosive growth in publications with paleointensity data. The data are slowly being contributed to the communal database whose scope has increased dramatically recently.

p0960   We have highlighted some of the major topics involving paleointensity data in this treatise. While these topics are still fresh and arguments abound, we can make the following statements regarding paleointensity:

o0040   1. Everyone agrees that more and better data could resolve many of the current debates. Experiments with built-in assessments of the fundamental assumptions of the method and the ability to estimate reliability indices are essential. Data sets are being contributed to the MagIC database, including measurements and full documentation of methods and data processing. This new generation of a database has the potential to go a long way toward settling some of the major issues discussed in this chapter.

o0045   2. In general, the ancient magnetic field has been highly variable on both short and long timescales. There have been extended periods of time with intensities lower than the present field, but there have also been intervals with field strengths greater than the present field in the past. These periods of increased field strength may be related to the length of the polarity interval in which they are found.

o0050   3. The geomagnetic field in the Archean appears to have been 'alive and well.'

o0055   4. Arguments against the 'asymmetrical sawtooth' in paleointensity data associated with polarity reversals appear to be winning, while arguments about the coherence of paleointensity with orbital frequencies and the ability to correlate globally paleointensity features on a millennial scale remain unresolved.

Acknowledgments

References   Au47

Aitken MJ, Allsop AL, Bussell GD, and Winter MB (1988) Determination of the intensity of the Earth's magnetic field during archeological times: Reliability of the Thellier technique. *Reviews of Geophysics* 26: 3–12.

Anson GL and Kodama KP (1987) Compaction-induced inclination shallowing of the post-depositional remanent magnetization in a synthetic sediment. *Geophysical Journal of the Royal Astronomical Society* 88: 673–692.

Barbetti M (1977) Measurements of recent geomagnetic secular variation in southeastern Australia and the question of dipole wobble. *Earth and Planetary Science Letters* 36: 207–218.

Bard E, Hamelin B, Fairbanks RG, and Zindler A (1990) Calibration of the 14C timescale over the past 30,000 years using mass spectrometric U-Th ages from Barbados corals. *Nature* 345: 405–410.

Bassinot FC, Labeyrie LD, Vincent E, Quidelleur X, Shackleton NJ, and Lancelot Y (1994) The astronomical theory of climate and the age of the Brunhes–Matuyama magnetic reversal. *Earth and Planetary Science Letters* 126: 91–108.

Ben Yosef E, Tauxe L, Levy T, Shaar R, Ron H, and Najjar M (2009) Archaeomagnetic intensity spike recorded in high resolution slag deposit from historical biblical archaeology site in southern Jordan. *Earth and Planetary Science Letters* 287: 529–539.

Bender M, Sowers T, Dickson ML, et al. (1994) Climate correlations between Greenland and Antarctica during the past 100,000 years. *Nature* 372(6507): 663–666.

Ben-Yosef E, Ron H, Tauxe L, et al. (2008) Application of copper slag in geomagnetic archaeointensity research. *Journal of Geophysical Research* 113. http://dx.doi.org/10.1029/2007JB005235.

Ben-Yosef E, Tauxe L, Ron H, et al. (2008) A new approach for geomagnetic archeointensity research: Insights on ancient metallurgy in the Southern Levant. *Journal of Archaeological Science* 35: 2863–2879.

Besse J and Courtillot V (2002) Apparent and true polar wander and the geometry of the geomagnetic field over the last 200 Myr. *Journal of Geophysical Research* 107. http://dx.doi.org/10.1029/2000JB000050.

Biggin A (2010) Paleointensity database updated and upgraded. *EOS, Transactions AGU* 91: 15.

Biggin AJ, Bohnel HN, and Zuniga FR (2003) How many paleointensity determinations are required from a single lava flow to constitute a reliable average? *Geophysical Research Letters* 30(11).

Biggin A, Perrin M, and Shaw J (2007) A comparison of a quasi-perpendicular method of absolute paleointensity determination with other thermal and microwave techniques. *Earth and Planetary Science Letters* 257: 564–581.

Bleil U and von Dobeneck T (1999) *Geomagnetic Events and Relative Paleointensity Records: Clues to High-Resolution Paleomagnetic Chronostratigraphies of Late Quaternary Marine Sediments*. Berlin: Springer-Verlag, pp. 635–654.

Bohnel H, Biggin AJ, Walton D, Shaw J, and Share JA (2003) Microwave palaeointensities from a recent Mexican lava flow, baked sediments and reheated pottery. *Earth and Planetary Science Letters* 214(1–2): 221–236.

Bol'shakov A and Shcherbakova V (1979) A thermomagnetic criterion for determining the domain structure of ferrimagnetics. *Izvestiya, Physics of the Solid Earth* 15: 111–117.

Bol'shakov A and Solodonikov GM (1980) Paleomagnetic data on the intensity of the magnetic field of the Earth. *Izvestiya, Physics of the Solid Earth* 16: 602–614.

Bowles J, Gee JS, Burgess K, and Cooper R (2011) Timing of magnetite formation in basaltic glass: Insights from synthetic analogs and relevance for geomagnetic paleointensity analysis. *Geochemistry, Geophysics, Geosystems* 12.

Bowles J, Gee JS, Kent D, Bergmanis E, and Sinton J (2005) Cooling rate effects on paleointensity estimates in submarine basaltic glass and implications for dating young flows. *Geochemistry, Geophysics, Geosystems* 6: Q07002. http://dx.doi.org/10.1029/2004GC000900.

Bowles J, Gee J, Kent DV, Perfit M, Soule A, and Fornari D (2006) Paleointensity applications to timing and extent of eruptive activity, 9°–10° N East Pacific rise. *Geochemistry, Geophysics, Geosystems* 7, Q06006.

Bowles J, Tauxe L, Gee J, McMillan D, and Cande SC (2003) Source of tiny wiggles in Chron C5: A comparison of sedimentary relative intensity and marine magnetic anomalies. *Geochemistry, Geophysics, Geosystems* 4(6): 1049. http://dx.doi.org/10.1029/2002GC000489.

Boyd M (1986) A new method for measuring paleomagnetic intensities. *Nature* 3196: 208–209.

Brachfeld SA and Banerjee SK (2000) A new high-resolution geomagnetic relative paleointensity record for the North American Holocene: A comparison of sedimentary and absolute intensity data. *Journal of Geophysical Research* 105(B1): 821–834.

TGP2: 00107

Cande SC and Kent DV (1995) Revised calibration of the geomagnetic polarity timescale for the late Cretaceous and Cenozoic. *Journal of Geophysical Research* 100: 6093–6095.

Carcaillet JT, Thouveny N, and Bourles DL (2003) Geomagnetic moment instability between 0.6 and 1.3 Ma from cosmonuclide evidence. *Geophysical Research Letters* 30(15): 1792.

Carter-Stiglitz B, Jackson M, and Moskowitz B (2002) Low-temperature remanence in stable single domain magnetite. *Geophysical Research Letters* 29.

Carter-Stiglitz B, Moskowitz B, and Jackson M (2003) Correction to "Low-temperature remanence in stable single domain magnetite" *Geophysical Research Letters* 30(21): 2113.

Channell JET (1999) Geomagnetic paleointensity and directional secular variation at Ocean Drilling Program (ODP) Site 984 (Bjorn Drift) since 500 ka: Comparisons with ODP Site 983 (Gardar Drift). *Journal of Geophysical Research: Solid Earth* 104(B10): 22937–22951.

Channell JET, Curtis JH, and Flower BP (2004) The Matuyama–Brunhes boundary interval (500–900 ka) in North Atlantic drift sediments. *Geophysical Journal International* 158(2): 489–505.

Channell JET, Hodell DA, and Lehman B (1997) Relative geomagnetic paleointensity and 18O at ODP Site 983 (Gardar Drift, North Atlantic) since 350 ka. *Earth and Planetary Science Letters* 153: 103–118.

Channell JET, Hodell DA, McManus J, and Lehman B (1998) Orbital modulation of the Earth's magnetic field intensity. *Nature* 394(6692): 464–468.

Channell JET and Kleiven HF (2000) Geomagnetic palaeointensities and astrochronological ages for the Matuyama-Brunhes boundary and the boundaries of the Jaramillo Subchron: Palaeomagnetic and oxygen isotope records from ODP Site 983. *Philosophical Transactions of the Royal Society of London Series A: Mathematical Physical and Engineering Sciences* 358(1768): 1027–1047.

Channell JET, Mazaud A, Sullivan P, Turner S, and Raymo ME (2002) Geomagnetic excursions and paleointensities in the Matuyama Chron at Ocean Drilling Program Sites 983 and 984 (Iceland Basin). *Journal of Geophysical Research: Solid Earth* 107(B6).

Channell J, Stoner J, Hodell D, and Charles C (2000) Geomagnetic paleointensity for the last 100 kyr from the sub-antarctic South Atlantic: A tool for inter-hemispheric correlation. *Earth and Planetary Science Letters* 175: 145–160.

Channell JET, Xuan C, and Hodell D (2009) Stacking paleointensity and oxygen isotope data for the last 1.5 Myr (PISO-1500). *Earth and Planetary Science Letters* 283: 14–23.

Chauvin A, Roperch P, and Levi S (2005) Reliability of geomagnetic paleointensity data: The effects of the NRM fraction and concave-up behavior on paleointensity determinations by the Thellier method. *Physics of the Earth and Planetary Interiors* 150(4): 265–286.

Cisowski S and Fuller M (1986) *Lunar Paleointensities via the IRM(s) Normalization Method and the Early Magnetic History of the Moon*. Houston, TX: Lunar and Planetary Science Institute, pp. 411–424.

Clement BM (2004) Dependence of the duration of geomagnetic polarity reversals on site latitude. *Nature* 428(6983): 637–640.

Clement BM and Kent DV (1986) Short polarity intervals within the Matuyama: Transitional field records from hydraulic piston cored sediments from the North Atlantic. *Earth and Planetary Science Letters* 81: 253–264.

Coe RS (1967) The determination of paleo-intensities of the Earth's magnetic field with emphasis on mechanisms which could cause non-ideal behavior in Thellier's method. *Journal of Geomagnetism and Geoelectricity* 19: 157–178.

Coe RS, Grommé S, and Mankinen EA (1978) Geomagnetic paleointensities from radiocarbon-dated lava flows on Hawaii and the question of the Pacific nondipole low. *Journal of Geophysical Research* 83: 1740–1756.

Coffey W, Kalmykov Y, and Waldron J (1996) *The Langevin Equation with Applications in Physics, Chemistry and Electrical Engineering*. Vol. 11 of World Scientific Series in Contemporary Chemical Physics. Singapore: World Scientific.

Collinson DW (1965) DRM in sediments. *Journal of Geophysical Research* 70: 4663–4668.

Constable C and Tauxe L (1996) Towards absolute calibration of sedimentary paleointensity records. *Earth and Planetary Science Letters* 143: 269–274.

Constable CG, Tauxe L, and Parker RL (1998) Analysis of 11 Myr of geomagnetic intensity variation. *Journal of Geophysical Research: Solid Earth* 103(B8): 17735–17748.

Cottrell R and Tarduno J (2000) Late Cretaceous true polar wander: Not so fast. *Science* 288: 2283.

Courtillot V, Gallet Y, Le Mouël J-L, Fluteau F, and Genevey A (2007) Are there connections between the Earth's magnetic field and climate? *Earth and Planetary Science Letters* 253: 328–339.

Cox AV (1968) Lengths of geomagnetic polarity intervals. *Journal of Geophysical Research* 73: 3247–3260.

Cromwell G, Tauxe L, Staudigel H, Constable C, Koppers A, and Pedersen R-B (2013) Evidence for long-term hemispheric asymmetry in the geomagnetic field: Results from high northern latitudes. *Geochemistry, Geophysics, Geosystems* 14. http://dx.doi.org/10.1002/ggge.20174.

Cronin M, Tauxe L, Constable C, Selkin P, and Pick T (2001) Noise in the quiet zone. *Earth and Planetary Science Letters* 190: 13–30.

Dansgaard W, Johnsen S, Clausen H, et al. (1993) Evidence for general instability of past climate from a 250-kyr ice core record. *Nature* 364: 218–220.

de Groot L, Dekkers M, and Mullender T (2012) Exploring the potential of acquisition curves of the anhysteretic remanent magnetization as a tool to detect subtle magnetic alteration induced by heating. *Physics of the Earth and Planetary Interiors* 194–195: 71–84.

Deamer GA and Kodama KP (1990) Compaction-induced inclination shallowing in synthetic and natural clay-rich sediments. *Journal of Geophysical Research* 95: 4511–4529.

Dekkers M and Böhnel H (2006) Reliable absolute paleointensities independent of magnetic domain state. *Earth and Planetary Science Letters* 248: 508–517.

deMenocal PB, Ruddiman WF, and Kent DV (1990) Depth of p-DRM acquisition in deep-sea sediments – A case study of the B/M reversal and oxygen isotopic stage 19.1. *Earth and Planetary Science Letters* 99: 1–13.

Demory F, Nowaczyk NR, Witt A, and Oberhansli H (2005) High-resolution magnetostratigraphy of late Quaternary sediments from Lake Baikal, Siberia: Timing of intracontinental paleoclimatic responses. *Global and Planetary Change* 46(1–4): 167–186.

Denham CR and Chave AD (1982) Detrital remanent magnetization: Viscosity theory of the lock-in zone. *Journal of Geophysical Research* 87: 7126–7130.

Dinares-Turell J, Sagnotti L, and Roberts AP (2002) Relative geomagnetic paleointensity from the Jaramillo Subchron to the Matuyama/Brunhes boundary as recorded in a Mediterranean piston core. *Earth and Planetary Science Letters* 194(3–4): 327–341.

Dunlop D and Argyle K (1997) Thermoremanence, anhysteretic remanence and susceptibility of submicron magnetites: Nonlinear field dependence and variation with grain size. *Journal of Geophysical Research* 102: 20199–20210.

Dunlop D and Ozdemir O (1997) *Rock Magnetism: Fundamentals and Frontiers*, Cambridge Studies in Magnetism. Cambridge: Cambridge University Press.

Dunlop DJ and Xu S (1994) Theory of partial thermoremanent magnetization in multidomain grains: 1. Repeated identical barriers to wall motion (single microcoercivity). *Journal of Geophysical Research* 99: 9005–9023.

Evans HF and Channell JET (2003) Upper Miocene magnetic stratigraphy at ODP site 1092 (sub-Antarctic South Atlantic): Recognition of 'cryptochrons' in C5n.2n. *Geophysical Journal International* 153(2): 483–496.

Fabian K (2003) Some additional parameters to estimate domain state from isothermal magnetization measurements. *Earth and Planetary Science Letters* 213(3–4): 337–345.

Fabian K and Leonhardt R (2010) Multiple-specimen absolute paleointensity determination: An optimal protocol including pTRM normalization, domain-state correction, and alteration test. *Earth and Planetary Science Letters* 297: 84–94.

Folgheraiter M (1899) Sur les variations séculaires de l'inclinaison magnétique dans l'antiquité. *Journal de Physique* 5: 660–667.

Fox JMW and Aitken MJ (1980) Cooling-rate dependence of thermoremanent magnetization. *Nature* 283: 462–463.

Frank M, Schwarz B, Baumann S, Kubik P, Suter M, and Mangini A (1997) A 200 kyr record of cosmogenic radionuclide production rate and geomagnetic field intensity from [10]Be in globally stacked deep-sea sediments. *Earth and Planetary Science Letters* 149: 121–129.

Fuller M (2006) Geomagnetic field intensity, excursions, reversals and the 41,000-yr obliquity signal. *Earth and Planetary Science Letters* 245: 605–615.

Gallet Y and Le Goff M (2006) High-temperature archeointensity measurements from Mesopotamia. *Earth and Planetary Science Letters* 241: 159–173.

Gattacceca J and Rochette P (2004) Toward a robust normalized magnetic paleointensity method applied to meteorites. *Earth and Planetary Science Letters* 227: 377–393.

Gee JS and Bowles J (2010) Paleointensity estimates from ignimbrites: An evaluation of the Bishop Tuff'. *Geochemistry, Geophysics, Geosystems* 11: Q03010. http://dx.doi.org/10.1029/2009GC002834.

Gee J, Cande S, Hildebrand J, Donnelly K, and Parker R (2000) Geomagnetic intensity variations over the past 780 kyr obtained from near-seafloor magnetic anomalies. *Nature* 408: 827–832.

Genevey A and Gallet Y (2003) Eight thousand years of geomagnetic field intensity variations in the eastern Mediterranean. *Journal of Geophysical Research* 108. http://dx.doi.org/10.1029/2001JB001612.

Gibbs R (1985) Estuarine flocs: Their size, settling velocity and density. *Journal of Geophysical Research* 90: 3249–3251.

TGP2: 00107

Goguitchaichvili A, Alva-Valdivia LM, Luis M, Rosas-Elguera J, Urrutia-Fucugauchi J, and Sole J (2004) Absolute geomagnetic paleointensity after the Cretaceous Normal Superchron and just prior to the Cretaceous-Tertiary transition. *Journal of Geophysical Research* 109: B01105. http://dx.doi.org/10.1029/2003JB002477.

Granot R, Dymont J, and Gallet Y (2012) Geomagnetic field variability during the Cretaceous Normal Superchron. *Nature Geoscience* 5: 220–223.

Granot R, Tauxe L, Gee JS, and Ron H (2007) A view into the Cretaceous geomagnetic field from analysis of gabbros and submarine glasses. *Earth and Planetary Science Letters* 256: 1–11.

Grootes P and Stuiver M (1997) Oxygen 18/16 variability in Greenland snow and ice with 10^{-3} to 10^5 year time resolution. *Journal of Geophysical Research* 102: 26455–26470.

Guyodo Y, Acton GD, Brachfeld S, and Channell JET (2001) A sedimentary paleomagnetic record of the Matuyama chron from the Western Antarctic margin (ODP Site 1101). *Earth and Planetary Science Letters* 191(1–2): 61–74.

Guyodo Y and Channell JET (2002) Effects of variable sedimentation rates and age errors on the resolution of sedimentary paleointensity records. *Geochemistry, Geophysics, Geosystems* 3: 1–18, art. no. –1048.

Guyodo Y, Gaillot P, and Channell JET (2000) Wavelet analysis of relative geomagnetic paleointensity at ODP Site 983. *Earth and Planetary Science Letters* 184(1): 109–123.

Guyodo Y, Richter C, and Valet JP (1999) Paleointensity record from Pleistocene sediments off the California Margin. *Journal of Geophysics* 104: 22953–22965.

Guyodo Y and Valet JP (1999) Global changes in intensity of the Earth's magnetic field during the past 800 kyr. *Nature* 399(6733): 249–252.

Guyodo Y and Valet JP (2006) A comparison of relative paleointensity records of the Matuyama Chron for the period 0.75–1.25 Ma. *Physics of the Earth and Planetary Interiors* 156: 205–212.

Haag M (2000) Reliability of relative palaeointensities of a sediment core with climatically-triggered strong magnetisation changes. *Earth and Planetary Science Letters* 180(1–2): 49–59.

Halgedahl S, Day R, and Fuller M (1980) The effect of cooling rate on the intensity of weak-field TRM in single-domain magnetite. *Journal of Geophysical Research* 95: 3690–3698.

Harrison CGA (1966) The paleomagnetism of deep sea sediments. *Journal of Geophysical Research* 71: 3033–3043.

Hartl P and Tauxe L (1996) A precursor to the Matuyama/Brunhes transition-field instability as recorded in pelagic sediments. *Earth and Planetary Science Letters* 138: 121–135.

Hayashida A, Verosub KL, Heider F, and Leonhardt R (1999) Magnetostratigraphy and relative palaeointensity of late Neogene sediments at ODP Leg 167 Site 1010 off Baja California. *Geophysical Journal International* 139(3): 829–840.

Hays JD, Imbrie J, and Shackleton NJ (1976) Variations in the Earth's orbit: Pacemaker of the ice ages. *Science* 194: 1121–1132.

Heller F and Liu T (1982) Magnetostratigraphical dating of loess deposits in China. *Nature* 300: 431–433.

Heller F and Peterson N (1982) The Laschamp excursion. *Philosophical Transactions of the Royal Society London, Series A* 306: 169–177.

Herrero-Bervera E and Valet JP (2005) Absolute paleointensity and reversal records from the Waianae sequence (Oahu, Hawaii, USA). *Earth and Planetary Science Letters* 234: 279–296.

Heslop D (2007) Are hydrodynamic shape effects important when modelling the formation of depositional remanent magnetization? *Geophysical Journal International* 171: 1029–1035.

Hill MJ, Gratton M, and Shaw J (2002) A comparison of thermal and microwave paleomagnetic techniques using lava containing laboratory induced remanence. *Geophysical Journal International* 151: 157–163.

Hoffman KA and Biggin AJ (2005) A rapid multi-sample approach to the determination of absolute paleointensity. *Journal of Geophysical Research* 110: B12108. http://dx.doi.org/10.1029/2005JB003646.

Hoffman KA, Constantine VL, and Morse DL (1989) Determination of absolute palaeointensity using a multi-specimen procedure. *Nature* 339: 295–297.

Hoffmann D and Fabian K (2009) Correcting relative paleointensity records for variations in sediment composition: Results from a South Atlantic stratigraphic network. *Earth and Planetary Science Letters* 284: 34–43.

Horng CS, Roberts AP, and Liang WT (2003) A 2.14-Myr astronomically tuned record of relative geomagnetic paleointensity from the western Philippine Sea. *Journal of Geophysical Research: Solid Earth* 108(B1).

Hughen K, Lehman S, Southon J, et al. (2004) C-14 activity and global carbon cycle changes over the past 50,000 years. *Science* 303(5655): 202–207.

Imbrie J, Hays JD, Martinson DG, et al. (1984) The orbital theory of Pleistocene climate: Support from a revised chronology of the marine δ18 O record. In: *Part 1, Milankovitch and Climate*. Hingham, MA: Reidel.

International Commission on Stratigraphy (2004) *Geologic Time Scale 2004*. Cambridge: Cambridge University Press.

Irving E (1964) *Paleomagnetism and Its Application to Geological and Geophysical Problems*. New York: Wiley.

Johnson HP, Lowrie W, and Kent DV (1975) Stability of anhysteretic remanent magnetization in fine and coarse magnetite and maghemite particles. *Geophysical Journal of the Royal Astronomical Society* 41: 1–10.

Johnson EA, Murphy T, and Torreson OW (1948) Pre-history of the Earth's magnetic field. *Terrestrial Magnetism and Atmospheric Electricity* 53: 349–372.

Juarez M and Tauxe L (2000) The intensity of the time averaged geomagnetic field: The last 5 m.y. *Earth and Planetary Science Letters* 175: 169–180.

Juarez T, Tauxe L, Gee JS, and Pick T (1998) The intensity of the Earth's magnetic field over the past 160 million years. *Nature* 394: 878–881.

Katari K and Bloxham J (2001) Effects of sediment aggregate size on DRM intensity: A new theory. *Earth and Planetary Science Letters* 186(1): 113–122.

Katari K, Tauxe L, and King J (2000) A reassessment of post depositional remanent magnetism: Preliminary experiments with natural sediments. *Earth and Planetary Science Letters* 183: 147–160.

Kent DV (1973) Post-depositional remanent magnetization in deep-sea sediment. *Nature* 246: 32–34.

Kent DV (1982) Apparent correlation of paleomagnetic intensity and climatic records in deep-sea sediments. *Nature* 299: 538–539.

Kent DV and Carlut J (2001) A negative test of orbital control of geomagnetic reversals and excursions. *Geophysical Research Letters* 28(18): 3561–3564.

Kent DV and Opdyke ND (1977) Paleomagnetic field intensity variation recorded in a Brunhes epoch deep-sea sediment core. *Nature* 266: 156–159.

Kent DV and Schneider DA (1995) Correlation of paleointensity variation records in the Brunhes/Matuyama polarity transition interval. *Earth and Planetary Science Letters* 129: 135–144.

King RF (1955) The remanent magnetism of artificially deposited sediments. *Monthly Notices of the Royal Astronomical Society, Geophysical Supplement* 7: 115–134.

King JW, Banerjee SK, and Marvin J (1983) A new rock magnetic approach to selecting sediments for geomagnetic paleointensity studies: Application to paleointensity for the last 4000 years. *Journal of Geophysical Research* 88: 5911–5921.

King RF and Rees AI (1966) Detrital magnetism in sediments: An examination of some theoretical models. *Journal of Geophysical Research* 71: 561–571.

Kirschvink JL (1980) The least-squares line and plane and the analysis of paleomagnetic data. *Geophysical Journal of the Royal Astronomical Society* 62: 699–718.

Kissel C and Laj C (2004) Improvements in procedure and paleointensity selection criteria (PICRIT 03) for Thellier and Thellier determinations: Application to Hawaiian basaltic long cores. *Physics of the Earth and Planetary Interiors* 147(2–3): 155–169.

Kissel C, Laj C, Labeyrie L, Dokken T, Voelker A, and Blamart D (1999) Rapid climatic variations during marine isotopic stage 3: Magnetic analysis of sediments from Nordic Seas and North Atlantic. *Earth and Planetary Science Letters* 171(3): 489–502.

Kitaba I, Hyodo M, Katoh S, Dettman D, and Sato H (2013) Midlatitude cooling caused by geomagnetic field minimum during polarity reversal. *Proceedings of the National Academy of Sciences of the United States of America* 110: 1215–1220.

Kletetschka G, Acuna MH, Kohout T, Wasilewski PJ, and Connerney JEP (2004) An empirical scaling law for acquisition of thermoremanent magnetization. *Earth and Planetary Science Letters* 226(3–4): 521–528.

Kletetschka G, Fuller M, Kohout T, et al. (2006) TRM in low magnetic fields: A minimum field that can be recorded by large multidomain grains. *Physics of the Earth and Planetary Interiors* 154: 290–298.

Knudsen M, Henderson G, Frank M, Niocaill C, and Kubik P (2008) In-phase anomalies in Beryllium-10 production and palaeomagnetic field behaviour during the Iceland Basin geomagnetic excursion. *Earth and Planetary Science Letters* 265: 588–599.

Koenigsberger J (1936) Die abhaengigkeit der natuerlichen remanenten magnetisierung bei eruptivgesteinen von deren alter und zusammensetzung. *Beitrage Angewandte Geophysik* 5: 193–246.

Koenigsberger J (1938a) Natural residual magnetism of eruptive rocks, Pt I. *Terrestrial Magnetism and Atmospheric Electricity* 43: 119–127.

Koenigsberger J (1938b) Natural residual magnetism of eruptive rocks, Pt II. *Terrestrial Magnetism and Atmospheric Electricity* 43: 299–320.

Kok YS and Tauxe L (1996a) Saw-toothed pattern of relative paleointensity records and cumulative viscous remanence. *Nature* 137: 95–99.

Kok YS and Tauxe L (1996b) Saw-toothed pattern of sedimentary paleointensity records explained by cumulative viscous remanence. *Earth and Planetary Science Letters* 144: E9–E14.

Kok YS and Tauxe L (1999) A relative geomagnetic paleointensity stack from Ontong-Java Plateau sediments for the Matuyama. *Journal of Geophysical Research: Solid Earth* 104(B11): 25401–25413.

TGP2: 00107

Kok Y and Tauxe L (2000) Comment on "Saw-toothed variations of relative paleointensity and cumulative viscous remanence: Testing the records and the model", by L. Meynadier, J.-P. Valet, Y. Guyodo, and C. Richter. *Journal of Geophysical Research* 105: 16609–16612.

Kok YS and Ynsen I (2002) Reply to comment by J.-P. Valet and L. Meynadier on "A relative geomagnetic paleointensity stack from Ontong-Java Plateau sediments for the Matuyama" *Journal of Geophysical Research* 107(B3), EPM 3-1–EPM 3-2.

Kono M (1971) Intensity of the earth's magnetic field during the Pliocene and Pleistocene in relation to the amplitude of mid-ocean ridge magnetic anomalies. *Earth and Planetary Science Letters* 11: 10–17.

Kono M (1974) Intensities of the Earth's magnetic field about 60 m.y. ago determined from the Deccan Trap basalts, India. *Journal of Geophysical Research* 79: 1135–1141.

Kono M and Ueno N (1977) Paleointensity determination by a modified Thellier method. *Physics of the Earth and Planetary Interiors* 13: 305–314.

Korte M and Constable C (2005) The geomagnetic dipole moment over the last 7000 years – New results from a global model. *Earth and Planetary Science Letters* 236: 348–358.

Laj C, Kissel C, and Garnier F (1996) Relative geomagnetic field intensity and reversals for the last 1.8 My from a central equatorial Pacific core. *Geophysical Research Letters* 23: 3393–3396.

Laj C, Kissel C, and Lefevre I (1996) Relative geomagnetic field intensity and reversals from Upper Miocene sections in Crete. *Earth and Planetary Science Letters* 141(1–4): 67–78.

Laj C, Kissel C, Mazaud A, Channell JET, and Beer J (2000) North Atlantic palaeointensity stack since 75 ka (NAPIS-75) and the duration of the Laschamp event. *Philosophical Transactions of the Royal Society* 358(1768): 1009–1025.

Laj C, Rais A, Surmont J, et al. (1997) Changes of the geomagnetic field vector obtained from lava sequences on the island of Vulcano (Aeolian Islands, Sicily). *Physics of the Earth and Planetary Interiors* 99: 161–177.

Lanci L and Lowrie W (1997) Magnetostratigraphic evidence that "tiny wiggles" in the oceanic magnetic anomaly record represent geomagnetic paleointensity variations. *Earth and Planetary Science Letters* 148(3–4): 581–592.

Laskar J, Joutel F, and Boudin F (1993) Orbital, precessional, and insolation quantities for the Earth from −20 Myr to +10 Myr. *Astronomy and Astrophysics* 270(1–2): 522–533.

Lawrence KP, Tauxe L, Staudigel H, et al. (2009) Paleomagnetic field properties near the southern hemisphere tangent cylinder. *Geochemistry, Geophysics, Geosystems* 10: Q01005. http://dx.doi.org/10.1029/2008GC00207.

Le Goff M and Gallet Y (2004) A new three-axis vibrating sample magnetometer for continuous high-temperature magnetization measurements: Applications to paleo- and archeo-intensity determinations. *Earth and Planetary Science Letters* 229(1–2): 31–43.

Lehman B, Laj C, Kissel C, Mazaud A, Paterne M, and Labeyrie L (1996) Relative changes of the geomagnetic field intensity during the last 280 kyr from piston cores in the Acores area. *Physics of the Earth and Planetary Interiors* 93: 269–284.

Leonhardt R, Heider F, and Hayashida A (1999) Relative geomagnetic field intensity across the Jaramillo subchron in sediments from the California margin: ODP Leg 167. *Journal of Geophysical Research* 104: 29133–29146.

Levi S and Banerjee SK (1976) On the possibility of obtaining relative paleointensities from lake sediments. *Earth and Planetary Science Letters* 29: 219–226.

Linsley B and Thunnell R (1990) The record of deglaciation in the Sulu Sea: Evidence for the Younger Dryas event in the western tropical Pacific. *Paleoceanography* 5: 1025–1039.

Lisiecki L and Raymo ME (2005) A Pliocene-Pleistocene stack of 57 globally distributed benthic δ18O records. *Paleoceanography* 20: PA1003. http://dx.doi.org/10.1029/2004PA001071.

Liu Q, Banerjee SK, Jackson MJ, Deng C, Pan Y, and Zhu R (2005) Inter-profile correlation of the Chinese loess/paleosol sequences during Marine Oxygen Isotope Stage 5 and indications of pedogenesis. *Quaternary Science Reviews* 24(1–2): 195–210.

Lovlie R (1974) Post-depositional remanent magnetization in a re-deposited deep-sea sediment. *Earth and Planetary Science Letters* 21: 315–320.

Lu R, Banerjee SK, and Marvin J (1990) Effects of clay mineralogy and the electrical conductivity of water on the acquisition of depositional remanent magnetization in sediments. *Journal of Geophysical Research* 95: 4531–4538.

Lund SP and Keigwin L (1994) Measurement of the degree of smoothing in sediment paleomagnetic secular variation records: An example from late Quaternary deep-sea sediments of the Bermuda Rise, western North Atlantic Ocean. *Earth and Planetary Science Letters* 122: 317–330.

Lund S, Williams T, Acton GD, Clement BM, and Okada M (2001) Brunhes Chron magnetic field excursions recovered from Leg 172 sediments. *Proceedings of the ODP Science Results*, vol. 172. College Station, TX: Ocean Drilling Program.

Macri P, Sagnotti L, Dinares-Turell J, and Caburlotto A (2005) A composite record of Late Pleistocene relative geomagnetic paleointensity from the Wilkes Land Basin (Antarctica). *Physics of the Earth and Planetary Interiors* 151(3–4): 223–242.

Martinson DG, Pisias NG, Hays JD, Imbrie J Jr., Moore TC, and Shackleton NJ (1987) Age dating and the orbital theory of the Ice ages: Development of a high-resolution 0–300,000 year chronostratigraphy. *Quaternary Research* 27: 1–29.

Masarik J and Beer J (1999) Simulation of particle fluxes and cosmogenic nuclide production in the Earth's atmosphere. *Journal of Geophysical Research* 104(D10): 12099–12111.

Mazaud A (1996) 'Sawtooth' variation in magnetic intensity profiles and delayed acquisition of magnetization in deep sea cores. *Earth and Planetary Science Letters* 139: 379–386.

Mazaud A, Sicre MA, Ezat U, et al. (2002) Geomagnetic-assisted stratigraphy and sea surface temperature changes in core MD94–103 (Southern Indian Ocean): Possible implications for North–South climatic relationships around H4. *Earth and Planetary Science Letters* 201(1): 159–170.

McClelland E and Briden J (1996) An improved methodology for Thellier-type paleointensity determination in igneous rocks and its usefulness for verifying primary thermoremanence. *Journal of Geophysical Research* 101: 21995–22013.

McElhinny MW (1973) *Paleomagnetism and Plate Tectonics*. Cambridge: Cambridge University Press.

McFadden PL and McElhinny MW (1982) Variations in the geomagnetic dipole 2: Statistical analysis of VDM's for the past 5 million years. *Journal of Geomagnetism and Geoelectricity* 34: 163.

McFadden P and Merrill R (1997) Sawtooth paleointensity and reversals of the geomagnetic field. *Physics of the Earth and Planetary Interiors* 103: 247–252.

McMillan DG, Constable CG, and Parker RL (2002) Limitations on stratigraphic analyses due to incomplete age control and their relevance to sedimentary paleomagnetism. *Earth and Planetary Science Letters* 201(3–4): 509–523.

McMillan DG, Constable C, and Parker RL (2004) Assessing the dipolar signal in stacked paleointensity records using a statistical error model and geodynamo simulations. *Physics of the Earth and Planetary Interiors* 145: 37–54.

Meynadier L and Valet JP (1995) Relative geomagnetic intensity during the last 4 m.y. from the equatorial Pacific'. *Proceedings of the Ocean Drilling Program, Scientific Results*, vol. 138, pp. 779–795. College Station, TX: Ocean Drilling Program.

Meynadier L and Valet JP (1996) Post-depositional realignment of magnetic grains and asymmetrical saw-tooth patterns o magnetization intensity. *Earth and Planetary Science Letters* 126: 109–127.

Meynadier L, Valet JP, Bassinot F, Shackleton NJ, and Guyodo Y (1994) Asymmetrical saw-tooth pattern of the geomagnetic field intensity from equatorial sediments in the Pacific and Indian Oceans. *Earth and Planetary Science Letters* 126: 109–127.

Meynadier L, Valet JP, Guyodo Y, and Richter C (1998) Saw-toothed variations of relative paleointensity and cumulative viscous remanence: Testing the records and the model. *Journal of Geophysical Research* 103: 7095–7105.

Meynadier L, Valet JP, Weeks R, Shackleton NJ, and Hagee VL (1992) Relative geomagnetic intensity of the field during the last 140 ka. *Earth and Planetary Science Letters* 114: 39–57.

Mitra R and Tauxe L (2009) Full vector model for magnetization in sediments. *Earth and Planetary Science Letters* 286: 535–545.

Mochizuki N, Tsunakawa H, Oishi Y, Wakai S, Wakabayashi K, and Yamamoto Y (2004) Paleointensity study of the Oshima 1986 lava in Japan: Implications for the reliability of the Thellier and LTD-DHT Shaw methods. *Physics of the Earth and Planetary Interiors* 146: 395–416.

Muxworthy A (2010) Revisiting a domain-state independent method of paleointensity determination. *Physics of the Earth and Planetary Interiors* 179: 21–31.

Nagata T (1961) *Rock Magnetism*. Tokyo: Maruzen.

Nagata T, Arai Y, and Momose K (1963) Secular variation of the geomagnetic total force during the last 5000 years. *Journal of Geophysical Research* 68: 5277–5282.

Néel L (1949) Théorie du trainage magnétique des ferromagneétiques en grains fines avec applications aux terres cuites. *Annales de Geophysique* 5: 99–136.

Néel L (1955) Some theoretical aspects of rock-magnetism. *Advances in Physics* 4: 191–243.

Nowaczyk NR and Antonow M (1997) High-resolution magnetostratigraphy of four sediment cores from the Greenland Sea.1. Identification of the Mono Lake excursion, Laschamp and Biwa I Jamaica geomagnetic polarity events. *Geophysical Journal International* 131(2): 310–324.

Nowaczyk NR, Antonow M, Knies J, and Spielhagen RF (2003) Further rock magnetic and chronostratigraphic results on reversal excursions during the last 50 ka as derived from northern high latitudes and discrepancies in precise AMS C-14 dating. *Geophysical Journal International* 155(3): 1065–1080.

Nowaczyk NR and Frederichs TW (1999) Geomagnetic events and relative palaeointensity variations during the past 300 ka as recorded in Kolbeinsey Ridge

TGP2: 00107

sediments, Iceland Sea: Indication for a strongly variable geomagnetic field. *International Journal of Earth Sciences* 88(1): 116–131.

Nowaczyk NR and Knies J (2000) Magnetostratigraphic results from the eastern Arctic Ocean: AMS 14C ages and relative palaeointensity data of the Mono Lake and Laschamp geomagnetic reversal excursions. *Geophysical Journal International* 140(1): 185–197.

Oda H, Nakamura K, Ikehara K, Nakano T, Nishimura M, and Khlystov O (2002) Paleomagnetic record from Academician Ridge, Lake Baikal: A reversal excursion at the base of marine oxygen isotope stage 6. *Earth and Planetary Science Letters* 202(1): 117–132.

Ohno M, Hayashi T, Komatsu F, et al. (2012) A detailed paleomagnetic record between 2.1 and 2.75 Ma at IODP Site U1314 in the North Atlantic: Geomagnetic excursions and the Gauss-Matuyama transition. *Geochemistry, Geophysics, Geosystems* 13: Q12Z39. http://dx.doi.org/10.1029/2012GC004080.

Okada M (1995) Detailed variation of geomagnetic field intensity during the late Pleistocene at Site 882. *Proceedings of the Ocean Drilling Program, Scientific Results*, vol. 145, pp. 469–474. College Station, TX: Ocean Drilling Program.

Ozima M, Ozima M, and Akimoto S (1964) Low temperature characteristics of remanent magnetization of magnetite. *Journal of Geomagnetism and Geoelectricity* 16: 165–177.

Pan Y, Zhu R, Shaw J, Liu Q, and Guo B (2001) Can relative paleointensities be determined from the normalized magnetization of the wind-blown loess of China? *Journal of Geophysical Research* 106: 19221–19232.

Paterson G, Biggin A, Yamamoto Y, and Pan YX (2012) Towards the robust selection of Thellier-type paleointensity data: The influence of experimental noise. *Geochemistry, Geophysics, Geosystems* 13: Q05Z43. http://dx.doi.org/10.1029/2012GC004046.

Paterson G, Heslop D, and Muxworthy A (2010) Deriving confidence in paleointensity estimates. *Geochemistry, Geophysics, Geosystems* 11: Q07Z18. http://dx.doi.org/10.1029/2010GC003071.

Pavón-Carrasco J, Rodríguez-González J, Osete M, and Torta J (2011) A Matlab tool for archaeomagnetic dating. *Journal of Archaeological Science* 38: 408–419.

Peck J, King J, Colman S, and Kravchinsky V (1996) An 84-kyr paleomagnetic record from the sediments of Lake Baikal, Siberia. *Journal of Geophysical Research* 101: 1365–1385.

Perrin M and Schnepp E (2004) IAGA paleointensity database: Distribution and quality of the data set. *Physics of the Earth and Planetary Interiors* 147(2–3): 255–267.

Perrin M, Schnepp E, and Shcherbakov V (1998) Paleointensity database updated. *EOS, Transactions AGU* 79: 198.

Perrin M and Shcherbakov V (1997) Paleointensity of the Earth's magnetic field for the past 400 Ma: Evidence for a dipole structure during the Mesozoic low. *Journal of Geomagnetism and Geoelectricity* 49: 601–614.

Pick T and Tauxe L (1993) Geomagnetic paleointensities during the Cretaceous normal superchron measured using submarine basaltic glass. *Nature* 366: 238–242.

Pick T and Tauxe L (1994) Characteristics of magnetite in submarine basaltic glass. *Geophysical Journal International* 119: 116–128.

Pisias NG, Martinson DG, Moore TC, et al. (1984) High-resolution stratigraphic correlation of benthic oxygen isotopic records spanning the last 300,000 years. *Marine Geology* 56(1–4): 119–136.

Prévot M, Derder MEM, McWilliams M, and Thompson J (1990) Intensity of the Earth's magnetic field: Evidence for a Mesozoic dipole low. *Earth and Planetary Science Letters* 97: 129–139.

Raisbeck G, Yiou F, and Zhou S (1994) Paleointensity puzzle. *Nature* 371: 207–208.

Rampino M (1979) Possible relations between changes in global ice volume, geomagnetic excursions, and the eccentricity of the Earth's orbit. *Geology* 7: 584–587.

Rampino MR (1981) Revised age estimates of Brunhes paleomagnetic events: Support for a link between geomagnetism and eccentricity. *Journal of Geophysical Research Letters* 8: 1047–1050.

Rampino MR and Kent DV (1983) Geomagnetic excursions and climate change. *Nature* 302: 455.

Ravilly M, Horen H, Perrin M, Dyment J, Gente P, and Guillou H (2001) NRM intensity of altered oceanic basalts across the MAR (21 degrees N, 0–1.5 Ma): A record of geomagnetic palaeointensity variations? *Geophysical Journal International* 145(2): 401–422.

Riisager P and Abrahamsen N (2000) Palaeointensity of West Greenland Palaeocene basalts: Asymmetric intensity around the C27n-C26r transition. *Physics of the Earth and Planetary Interiors* 118(1–2): 53–64.

Riisager P and Riisager J (2001) Detecting multidomain magnetic grains in Thellier palaeointensity experiments. *Physics of the Earth and Planetary Interiors* 125(1–4): 111–117.

Riisager J, Riisager P, and Pedersen A (2003) The C27n-C26r geomagnetic polarity reversal recorded in the west Greenland flood basalt province: How complex is the

transitional field? *Journal of Geophysical Research* 108. http://dx.doi.org/10.1029/2002JB002124.

Roberts AP (1995) Magnetic properties of sedimentary greigite (Fe₃S₄). *Earth and Planetary Science Letters* 134: 227–236.

Roberts AP, Chang L, Heslop D, Florindo F, and Larrasoaña J (2012) Searching for single domain magnetite in the "pseudo-single-domain" sedimentary haystack: Implications of biogenic magnetite preservation for sediment magnetism and relative paleointensity determinations. *Journal of Geophysical Research* 117, B08104.

Roberts A, Lehman B, Weeks R, Verosub K, and Laj C (1997) Relative paleointensity of the geomagnetic field over the last 200,000 years from ODP Sites 883 and 884, North Pacific Ocean. *Earth and Planetary Science Letters* 152: 11–23.

Roberts AP and Lewin-Harris JC (2000) Marine magnetic anomalies: Evidence that 'tiny wiggles' represent short-period geomagnetic polarity intervals. *Earth and Planetary Science Letters* 183(3–4): 375–388.

Roberts AP, Tauxe L, and Heslop D (2013) Magnetic paleointensity stratigraphy and high resolution Quaternary geochronology: Successes and future challenges. *Quaternary Science Reviews* 61: 1–16.

Roberts AP, Verosub KL, and Negrini RM (1994) Middle Late Pleistocene relative paleointensity of the geomagnetic-field from lacustrine sediments, Lake Chewaucan, Western United States. *Geophysical Journal International* 118(1): 101–110.

Roberts AP, Winklhofer M, Liang WT, and Horng CS (2003) Testing the hypothesis of orbital (eccentricity) influence on Earth's magnetic field. *Earth and Planetary Science Letters* 216(1–2): 187–192.

Rolph TC and Shaw J (1985) A new method of palaeofield magnitude correction for thermally altered samples and its application to Lower Carboniferous lavas. *Geophysical Journal of the Royal Astronomical Society* 80: 773–781.

Saracco G, Thouveny N, Bourlès D, and Carcaillet JT (2009) Extraction of non-continuous orbital frequencies from noisy insolation data and from palaeoproxy records of geomagnetic intensity using the phase of continuous wavelet transform. *Geophysical Journal International* 176: 767–781.

Sato T, Kikuchi H, Nakashizuka M, and Okada M (1998) Quaternary geomagnetic field intensity: Constant periodicity or variable period? *Geophysical Research Letters* 25: 2221–2224.

Sato T and Kobayashi K (1989) Long-period secular variations of the Earth's magnetic field revealed by Pacific deep-sea sediment cores. *Journal of Geomagnetism and Geoelectricity* 41: 147–159.

Sbarbori E, Tauxe L, Gogichaishvili A, Urrutia-Fucugauchi J, and Bohrson W (2009) Paleomagnetic behavior of volcanic rocks from Isla Socorro, Mexico. *Earth, Planets and Space* 61: 191–204.

Schneider DA (1993) An estimate of Late Pleistocene geomagnetic intensity variation From Sulu Sea sediments. *Earth and Planetary Science Letters* 120(3–4): 301–310.

Schneider DA, Kent DV, and Mello GA (1992) A detailed chronology of the Australasian impact event, the Brunhes-Matuyama geomagnetic polarity reversal and global climate change. *Earth and Planetary Science Letters* 111: 395–405.

Schneider D and Mello G (1996) A high-resolution marine sedimentary record of geomagnetic intensity during the Brunhes Chron. *Earth and Planetary Science Letters* 144: 297–314.

Schwartz M, Lund SP, and Johnson TC (1996) Environmental factors as complicating influences in the recovery of quantitative geomagnetic-field paleointensity estimates from sediments. *Geophysical Research Letters* 23: 2693–2696.

Schwartz M, Lund SP, and Johnson TC (1998) Geomagnetic field intensity from 71 to 12 ka as recorded in deep-sea sediments of the Blake Outer Ridge, North Atlantic Ocean. *Journal of Geophysical Research: Solid Earth* 103(B12): 30407–30416.

Selkin P, Gee JS, and Tauxe L (2007) Nonlinear thermoremanence acquisition and implications for paleointensity data. *Earth and Planetary Science Letters* 256: 81–89.

Selkin P, Gee J, Tauxe L, Meurer W, and Newell A (2000) The effect of remanence anisotropy on paleointensity estimates: A case study from the Archean Stillwater complex. *Earth and Planetary Science Letters* 182: 403–416.

Selkin P and Tauxe L (2000) Long-term variations in paleointensity. *Philosophical Transactions of the Royal Society London* 358: 1065–1088.

Shaar R, Ben Yosef E, Ron H, Tauxe L, Agnon A, and Kessel R (2011) Geomagnetic field intensity: How high can it get? How fast can it change? Constraints from Iron-Age copper-slag. *Earth and Planetary Science Letters* 301: 297–306. http://dx.doi.org/10.1016/j.epsl.2010.11.013.

Shaar R, Ron H, Tauxe L, Kessel R, and Agnon A (2011) Paleomagnetic field intensity derived from non-SD: Testing the Thellier IZZI technique on MD slag and a new bootstrap procedure. *Earth and Planetary Science Letters* 310: 213–224.

Shaar R, Ron H, Tauxe L, et al. (2010) Testing the accuracy of absolute intensity estimates of the ancient geomagnetic field using copper slag material. *Earth and Planetary Science Letters* 290: 201–213.

TGP2: 00107

Shaar R and Tauxe L (2013) Thellier_GUI: An integrated tool for analyzing paleointensity data from Thellier-type experiments. *Geochemistry, Geophysics, Geosystems* 14: 677–692.

Shackleton NJ, Berger A, and Peltier WR (1990) An alternative astronomical calibration of the lower Pleistocene timescale based on ODP Site 677. *Transactions of the Royal Society of Edinburgh: Earth Sciences* 81: 251–261.

Shaw J (1974) A new method of determining the magnitude of the paleomagnetic field application to 5 historic lavas and five archeological samples. *Geophysical Journal of the Royal Astronomical Society* 39: 133–141.

Shcherbakov V and Shcherbakova V (1983) On the theory of depositional remanent magnetization in sedimentary rocks. *Geophysical Surveys* 5: 369–380.

Shcherbakova V, Shcherbakov V, and Heider F (2000) Properties of partial thermoremanent magnetization in PSD and MD magnetite grains. *Journal of Geophysical Research* 105: 767–782.

Sherwood G, Shaw J, Baer G, and Mallik S (1993) The strength of the geomagnetic field during the Cretaceous Quiet Zone: Paleointensity results from Israeli and Indian Lavas. *Journal of Geomagnetism and Geoelectricity* 45: 339–360.

Smith PJ (1967) The intensity of the ancient geomagnetic field: A review and analysis. *Geophysical Journal of the Royal Astronomical Society* 12: 321–362.

Sowers T, Bender M, Labeyrie L, et al. (1993) A 135,000 year Vostok-Specmap common temporal framework. *Paleoceanography* 8: 737–766.

Spassov S, Heller F, Evans ME, Yue LP, and von Dobeneck T (2003) A lock-in model for the complex Matuyama-Brunhes boundary record of the loess/palaeosol sequence at Lingtai (Central Chinese Loess Plateau). *Geophysical Journal International* 155(2): 350–366.

Stacey FD (1972) On the role of Brownian motion in the control of detrital remanent magnetization of sediments. *Pure and Applied Geophysics* 98: 139–145.

Stern DP (2003) A millennium of geomagnetism. *Reviews of Geophysics* 41(2): 1007.

Stoner JS, Channell JET, and Hillaire-Marcel C (1995) Late Pleistocene relative geomagnetic paleointensity from the deep Labrador Sea: Regional and global correlations. *Earth and Planetary Science Letters* 134: 237–252.

Stoner JS, Channell JET, and Hillaire-Marcel C (1998) A 200 ka geomagnetic chronostratigraphy for the Labrador Sea: Indirect correlation of the sediment record to SPECMAP. *Earth and Planetary Science Letters* 159(3–4): 165–181.

Stoner J, Channell J, Hillaire-Marcel C, and Kissel C (2000) Geomagnetic paleointensity and environmental record from Labrador Sea core MD95–2024: Global marine sediment and ice core chronostratigraphy for the last 110 kyr. *Earth and Planetary Science Letters* 5626: 1–17.

Stoner JS, Channell JET, Hodell DA, and Charles CD (2003) A ~580 kyr paleomagnetic record from the sub-Antarctic South Atlantic (Ocean Drilling Program Site 1089). *Journal of Geophysical Research* 108(B5).

Stoner JS, Laj C, Channell JET, and Kissel C (2002) South Atlantic and North Atlantic geomagnetic paleointensity stacks (0–80 ka): Implications for inter-hemispheric correlation. *Quaternary Science Reviews* 21(10): 1141–1151.

Stott L, Poulsen C, Lund S, and Thunell R (2002) Super ENSO and global climate oscillations at millennial time scales. *Science* 297: 222–226.

Suganuma Y, Okuno J, Heslop D, Roberts AP, Yamazaki T, and Yokoyama Y (2011) Post-depositional remanent magnetization lock-in for marine sediments deduced from 10Be and paleomagnetic records through the Matuyama-Brunhes boundary. *Earth and Planetary Science Letters* 311: 39–52.

Suganuma Y, Yokoyama Y, Yamazaki T, Kawamura K, Horng C-S, and Matsuzaki H (2010) 10Be evidence for delayed acquisition of remanent magnetization in marine sediments: Implication for a new age for the Matuyama-Brunhes boundary. *Earth and Planetary Science Letters* 296: 443–450.

Sugiura N, Strangway D, Pearce G, Wu Y, and Taylor L (1979) A new magnetic paleointensity value for a 'young lunar glass'. In: *Proceedings of Lunar and Planetary Science Conference X*, pp. 2189–2197.

Svensmark H and Friis-Christensen E (1997) Variation of cosmic ray flux and global cloud coverage – A missing link in solar-climate relationship. *Journal of Atmospheric and Solar – Terrestrial Physics* 59: 1225–1232.

Tanaka H, Athanassopoulos J, Dunn J, and Fuller M (1995) Paleointensity determinations with measurements at high temperature. *Journal of Geomagnetism and Geoelectricity* 47: 103–113.

Tanaka H and Kono M (1991) Preliminary results and reliability of palaeointensity studies on historical and C14 dated Hawaiian lavas. *Journal of Geomagnetism and Geoelectricity* 43: 375–388.

Tanaka H and Kono M (1994) Paleointensity database provides new research. *EOS, Transactions AGU* 75: 498.

Tanaka HF and Kono M (2002) Paleointensities from a Cretaceous basalt platform in Inner Mongolia, Northeastern China. *Physics of the Earth and Planetary Interiors* 133(1–4): 147–157.

Tanaka H, Kono M, and Uchimura H (1995) Some global features of paleointensity in geological time. *Geophysical Journal International* 120: 97–102.

Tarduno JA, Cottrell RD, and Smirnov AV (2001) High geomagnetic intensity during the mid-Cretaceous from Thellier analyses of single plagioclase crystals. *Science* 291(5509): 1779–1783.

Tarduno JA, Cottrell RD, and Smirnov AV (2002) The Cretaceous superchron geodynamo: Observations near the tangent cylinder. *Proceedings of National Academy of Sciences of the United States of America* 99: 14020–14025.

Tarduno J, Cottrell R, and Smirnov A (2006) The paleomagnetism of single silicate crystals: Recording geomagnetic field strength during mixed polarity intervals, superchrons, and inner core growth. *Reviews of Geophysics* 44. http://dx.doi.org/10.1029/2005RG000189.

Tarduno JA, Cottrell RD, Watkeys M, and Bauch D (2007) Geomagnetic field strength 3.2 billion years ago recorded by single silicate crystals. *Nature* 446: 657–660.

Tarduno JA, Cottrell RD, Watkeys M, et al. (2010) Geodynamo, solar wind, and magnetopause 3.4 to 3.45 billion years ago. *Science* 327: 1238–1240.

Tauxe L (1993) Sedimentary records of relative paleointensity of the geomagnetic field: Theory and practice. *Reviews of Geophysics* 31: 319–354.

Tauxe L (1998) *Paleomagnetic Principles and Practice*. Dordrecht: Kluwer Academic Publishers.

Tauxe L (2006) Long term trends in paleointensity: The contribution of DSDP/ODP submarine basaltic glass collections. *Physics of the Earth and Planetary Interiors* 244: 515–529.

Tauxe L, Banerjee SK, Butler R, and van der Voo R (2010) *Essentials of Paleomagnetism*. Berkeley, CA: University of California Press.

Tauxe L, Bertram H, and Seberino C (2002) Physical interpretation of hysteresis loops: Micro-magnetic modelling of fine particle magnetite. *Geochemistry, Geophysics, Geosystems* 3: 1–22. http://dx.doi.org/10.1029/2001GC000280.

Tauxe L, Gee JS, Steiner M, and Staudigel H (2013) Paleointensity results from the Jurassic: New constraints from submarine basaltic glasses of ODP Site 801C. *Geochemistry, Geophysics, Geosystems*. http://dx.doi.org/10.1002/ggge.20282.

Tauxe L and Hartl P (1997) 11 million years of Oligocene geomagnetic field behaviour. *Geophysical Journal International* 128: 217–229.

Tauxe L, Herbert T, Shackleton NJ, and Kok YS (1996) Astronomical calibration of the Matuyama Brunhes Boundary: Consequences for magnetic remanence acquisition in marine carbonates and the Asian loess sequences. *Earth and Planetary Science Letters* 140: 133–146.

Tauxe L and Love J (2003) Paleointensity in Hawaiian Scientific Drilling project Hole (HSDP2): Results from submarine basaltic glass. *Geochemistry, Geophysics, Geosystems* 4: GC000276. http://dx.doi.org/10.1029/2001.

Tauxe L, Pick T, and Kok YS (1995) Relative paleointensity in sediments: A pseudo-Thellier approach. *Geophysical Research Letters* 22: 2885–2888.

Tauxe L and Shackleton NJ (1994) Relative paleointensity records from the Ontong-Java Plateau. *Geophysical Journal International* 117: 769–782.

Tauxe L and Staudigel H (2004) Strength of the geomagnetic field in the Cretaceous Normal Superchron: New data from submarine basaltic glass of the Troodos Ophiolite. *Geochemistry, Geophysics, Geosystems* 5(2): Q02H06. http://dx.doi.org/10.1029/2003GC000635.

Tauxe L, Steindorf J, and Harris A (2006) Depositional remanent magnetization: Toward an improved theoretical and experimental foundation. *Earth and Planetary Science Letters* 244: 515–529.

Tauxe L and Wu G (1990) Normalized remanence in sediments of the Western Equatorial Pacific: Relative paleointensity of the geomagnetic field? *Journal of Geophysical Research* 95(B8): 12337–12350.

Tauxe L and Yamazaki T (2007) Paleointensities. *Treatise on Geophysics*, vol. 5, pp. 509–563. New York: Elsevier. http://dx.doi.org/10.1016/B978-044452748-6/00098-5.

Taylor L (1979) An effective sample preparation technique for paleointensity determinations at elevated temperatures. In: *Proceedings of Lunar and Planetary Science Conference X*, pp. 1209–1211.

Teanby N and Gubbins D (2000) The effects of aliasing and lock-in processes on palaeosecular variation records from sediments. *Geophysical Journal International* 142(2): 563–570.

Thellier E (1938) Sur l'aimantation des terres cuites et ses applications géophysique. *Annales de l'Institut de Physique du Globe de Paris* 16: 157–302.

Thellier E and Thellier O (1959) Sur l'intensité du champ magnétique terrestre dans le passé historique et géologique. *Annales de Geophysique* 15: 285–378.

Thouveny N, Bourlès D, Saracco G, Carcaillet JT, and Basssinot F (2008) Paleoclimatic context of geomagnetic dipole lows and excursions in the Brunhes, clue for an orbital influence on the geodynamo? *Earth and Planetary Science Letters* 275: 269–284.

Thouveny N, Carcaillet J, Moreno E, Leduc G, and Nerini D (2004) Geomagnetic moment variation and paleomagnetic excursions since 400 kyr BP: A stacked record from sedimentary sequences of the Portuguese margin, Pt 1. *Earth and Planetary Science Letters* 219(3–4): 377–396.

TGP2: 00107

Thouveny N, Debeaulieu JL, Bonifay E, et al. (1994) Climate variations in Europe over the past 140-kyr deduced from rock magnetism. *Nature* 371(6497): 503–506.

Tiedemann R, Sarnthein M, and Shackleton NJ (1994) Astronomical timescale for the Pliocene Atlantic delta^{18}O and dust flux records of Ocean Drilling Program site 659. *Paleoceanography* 9: 619–638.

Tric E, Valet JP, Tucholka P, et al. (1992) Paleointensity of the geomagnetic field during the last 80,000 years. *Journal of Geophysical Research* 97: 9337–9351.

Tsunakawa H and Shaw J (1994) The Shaw method of paleointensity determinations and its application to recent volcanic rocks. *Geophysical Journal International* 118: 781–787.

Valet J-P (2003) Time variations in geomagnetic intensity. *Reviews of Geophysics* 41. http://dx.doi.org/10.1029/2001RG000104.

Valet JP, Brassart J, Lemeur I, et al. (1996) Absolute paleointensity and magnetomineralogical changes. *Journal of Geophysical Research* 101(B11): 25029–25044.

Valet J-P and Herrero-Bervera E (2000) Paleointensity experiments using alternating field demagnetization. *Earth and Planetary Science Letters* 177: 43–58.

Valet JP and Meynadier L (1993) Geomagnetic field intensity and reversals during the past four million years. *Nature* 366: 234–238.

Valet JP and Meynadier L (2001) Comment on "A relative geomagnetic paleointensity stack from Ontong-Java plateau sediments for the Matuyama" by Yvo S. Kok and Lisa Tauxe. *Journal of Geophysical Research* 106: 11013–11015.

Valet JP, Meynadier L, Bassinot FC, and Garnier F (1994) Relative paleointensity across the last geomagnetic reversal from sediments of the Atlantic, Indian and Pacific Oceans. *Geophysical Research Letters* 21: 485–488.

Valet JP, Meynadier L, and Guyodo Y (2005) Geomagnetic dipole strength and reversal rate over the past two million years. *Nature* 435: 802–805.

Valet JP, Moreno E, Basssinot F, et al. (2011) Isolating climatic and paleomagnetic imbricated signals in two marine cores using principal component analysis. *Geochemistry, Geophysics, Geosystems* 12: Q08012. http://dx.doi.org/10.1029/2011GC003697.

Valet JP, Tauxe L, and Clement BM (1989) Equatorial and mid-latitude records of the last geomagnetic reversal from the Atlantic Ocean. *Earth and Planetary Science Letters* 94: 371–384.

Valet JP, Tric E, Herrero-Bervera E, Meynadier L, and Lockwood JP (1998) Absolute paleointensity from Hawaiian lavas younger than 35 ka. *Earth and Planetary Science Letters* 161: 19–32.

van Vreumingen M (1993a) The magnetization intensity of some artificial suspensions while flocculating in a magnetic field. *Geophysical Journal International* 114: 601–606.

van Vreumingen M (1993b) The influence of salinity and flocculation upon the acquisition of remanent magnetization in some artificial sediments. *Geophysical Journal International* 114: 607–614.

van Zijl JSU, Graham KWT, and Hales AL (1962a) The paleomagnetism of the Stormberg Lavas 1. *Geophysical Journal of the Royal Astronomical Society* 7: 23–39.

van Zijl JSU, Graham KWT, and Hales AL (1962b) The paleomagnetism of the Stormberg Lavas, 2. The behavior of the Earth's magnetic field during a reversal. *Geophysical Journal of the Royal Astronomical Society* 7: 169–182.

Verosub KL (1977) Depositional and postdepositional processes in the magnetization of sediments. *Reviews of Geophysics and Space Physics* 15: 129–143.

Verosub KL, Herrerobervera E, and Roberts AP (1996) Relative geomagnetic paleointensity across the Jaramillo Subchron and the Matuyama/Brunhes boundary. *Geophysical Research Letters* 23(5): 467–470.

Walton D (2004) Avoiding mineral alteration during microwave magnetization. *Geophysical Research Letters* 31: L03606. http://dx.doi.org/10.1029/2003GL019011.

Walton D (2005) Isolating viscous overprints with microwaves. *EOS Transactions, AGU Fall Meeting Supplement* 86, GP12A-05.

Walton D, Share J, Rolph TC, and Shaw J (1993) Microwave magnetisation. *Geophysical Research Letters* 20: 109–111.

Wang H and Kent D (2013) A paleointensity technique for multidomain igneous rocks. *Geochemistry, Geophysics, Geosystems* 14. http://dx.doi.org/10.1002/ggge.20248.

Wang R and Lovlie R (2010) Subaerial and subaqueous deposition of loess: Experimental assessment of detrital remanent magnetization in Chinese loess. *Earth and Planetary Science Letters* 298: 394–404.

Weeks RJ, Laj C, Endignoux L, et al. (1995) Normalised natural remanent magnetisation intensity during the last 240000 years in piston cores from the central North Atlantic Ocean: Geomagnetic field intensity or environmental signal? *Physics of the Earth and Planetary Interiors* 87: 213–229.

Westphal M and Munschy M (1994) Saw-tooth pattern of the Earth's magnetic field tested by magnetic anomalies over oceanic spreading ridges. *Comptes Rendus de l'Academie des Sciences Series IIA Earth and Planetary Science* 329: 565–571.

Williams T, Thouveny N, and Creer KM (1998) A normalised intensity record from Lac du Bouchet: Geomagnetic palaeointensity for the last 300 kyr? *Earth and Planetary Science Letters* 156(1–2): 33–46.

Wilson R (1961) Paleomagnetism in Northern Ireland, 1. The thermoremanent magnetization of natural magnetic moments in rocks. *Geophysical Journal of the Royal Astronomical Society* 5: 45–58.

Winterwerp J and van Kesteren W (2004) *Introduction to the Physics of Cohesive Sediment in the Marine Environment. Developments in Sedimentology*, vol. 56. Amsterdam: Elsevier.

Wollin G, Ericson D, and Ryan WBF (1971) Variations in magnetic intensity and climatic changes. *Nature* 232: 549–550.

Worm H (1997) A link between geomagnetic reversals and events and glaciations. *Earth and Planetary Science Letters* 147: 55–67.

Xu S and Dunlop DJ (1994) Theory of partial thermoremanent magnetization in multidomain grains: 2. Effect of microcoercivity distribution and comparison with experiment. *Journal of Geophysical Research* 99: 9025–9033.

Xuan C and Channell JET (2008a) Origin of orbital periods in the sedimentary relative paleointensity records. *Physics of the Earth and Planetary Interiors* 169: 140–151.

Xuan C and Channell JET (2008b) Testing the relationship between timing of geomagnetic reversals/excursions and phase of orbital cycles using circular statistics and Monte Carlo simulations. *Earth and Planetary Science Letters* 268: 245–254.

Yamamoto Y and Shaw J (2008) Development of the microwave LTD-DHT Shaw method for absolute paleointensity determination. *Physics of the Earth and Planetary Interiors* 170: 15–23.

Yamamoto Y and Tsunakawa H (2005) Geomagnetic field intensity during the last 5 Myr: LTD-DHT Shaw palaeointensities from volcanic rocks of the Society Islands, French Polynesia. *Geophysical Journal International* 162(1): 79–114.

Yamamoto Y, Tsunakawa H, and Shibuya H (2003) Palaeointensity study of the Hawaiian 1960 lava: Implications for possible causes of erroneously high intensities. *Geophysical Journal International* 153(1): 263–276.

Yamazaki T (1999) Relative paleointensity of the geomagnetic field during Brunhes Chron recorded in North Pacific deep-sea sediment cores: Orbital influence? *Earth and Planetary Science Letters* 169(1–2): 23–35.

Yamazaki T and Ikehara M (2012) Origin of magnetic mineral concentration variation in the Southern Ocean. *Paleoceanography* 27: PA2206. http://dx.doi.org/10.1029/2011PA002271.

Yamazaki T and Ioka N (1994) Long-term secular variation of the geomagnetic field during the last 200 kyr recorded in sediment cores from the western equatorial Pacific. *Earth and Planetary Science Letters* 128: 527–544.

Yamazaki T, Ioka N, and Eguchi N (1995) Relative paleointensity of the geomagnetic field during the Brunhes Chron. *Earth and Planetary Science Letters* 136: 525–540.

Yamazaki T and Kanamatsu T (2007) A relative paleointensity record of the geomagnetic field since 1.6 Ma from the North Pacific. *Earth, Planets and Space* 59: 785–794.

Yamazaki T and Oda H (2002) Orbital influence on Earth's magnetic field: 100,000-year periodicity in inclination. *Science* 295(5564): 2435–2438.

Yamazaki T and Oda H (2005) A geomagnetic paleointensity stack between 0.8 and 3.0 Ma from equatorial Pacific sediment cores. *Geochemistry, Geophysics, Geosystems* 6. http://dx.doi.org/10.203-/2005GC001001.

Yamazaki T, Yamamoto Y, Acton G, Guidry E, and Richter C (2013) Rock-magnetic artifacts on long-term relative paleointensity variations in sediments. *Geochemistry, Geophysics, Geosystems* 14: 29–43.

Yokoyama Y and Yamazaki T (2000) Geomagnetic paleointensity variation with a 100 kyr quasi-period. *Earth and Planetary Science Letters* 181(1–2): 7–14.

Yokoyama Y, Yamazaki T, and Oda H (2007) Geomagnetic 100-kyr variation extracted from paleointensity records of the equatorial and North Pacific sediments. *Earth, Planets and Space* 59: 795–805.

Yokoyama Y, Yamazaki T, and Oda H (2010) Geomagnetic 100-kyr variation excited by a change in the Earths orbital eccentricity. *Geophysical Research Letters* 37: L11302. http://dx.doi.org/10.1029/2010GL042898.

Yoshida S and Katsura I (1985) Characterization of fine magnetic grains in sediments by the suspension method. *Geophysical Journal of the Royal Astronomical Society* 82: 301–317.

Yu Y and Tauxe L (2005) On the use of magnetic transient hysteresis in paleomagnetism for granulometry. *Geochemistry, Geophysics, Geosystems* 6: Q01H14. http://dx.doi.org/10.1029/2004GC000839.

Yu Y and Tauxe L (2006) Acquisition of viscous remanent magnetization. *Physics of the Earth and Planetary Interiors* 159: 32–42.

Yu Y, Tauxe L, and Genevey A (2004) Toward an optimal geomagnetic field intensity determination technique. *Geochemistry, Geophysics, Geosystems* 5(2): Q02H07. http://dx.doi.org/10.1029/2003GC000630.

Zhao X and Roberts AP (2010) How does Chinese loess become magnetized? *Earth and Planetary Science Letters* 292: 112–122.

TGP2: 00107

Zhu R, Laj C, and Mazaud A (1994) The Matuyama-Brunhes and upper Jaramillo transitions recorded in a loess section at Weinan, north-central China. *Earth and Planetary Science Letters* 125: 143–158.

Zhu RX, Lo CH, Shi RP, Shi GH, Pan YX, and Shao J (2004) Palaeointensities determined from the middle Cretaceous basalt in Liaoning Province, northeastern China. *Physics of the Earth and Planetary Interiors* 142(1–2): 49–59.

Zhu RX, Pan YX, Shaw J, Li DM, and Li Q (2001) Geomagnetic palaeointensity just prior to the Cretaceous normal superchron. *Physics of the Earth and Planetary Interiors* 128(1–4): 207–222.

Ziegler L, Constable C, Johnson CL, and Tauxe L (2011) PADM2M: A penalized maximum likelihood model of the 0–2 Ma paleomagnetic axial dipole moment. *Geophysical Journal International* 184: 1069–1089.